



Negative Ion Chemistry
of
Boron and Carbon Compounds

A
Thesis presented for the degree of
Doctor of Philosophy

in
The University of Adelaide

by
Graeme Currie B.Sc.(Hons)

Department of Organic Chemistry
1988

awarded 6-4-89

CONTENTS

Summary	I
Statement	V
Acknowledgements	VI
Chapter 1 Introduction	1
1.1 General	2
1.2 The production of negative ions.	2
1.3 An introduction to negative ion chemical ionization	3
1.3.1 Proton transfer	4
1.3.2 Charge exchange	6
1.3.3 Nucleophilic addition	6
1.3.4 Nucleophilic displacement	7
1.4 Sensitivity of negative ion chemical ionization	7
1.5 Magnetic sector analyser	8
1.6 Electric sector analyser	10
1.7 An introduction to collisional activation mass spectroscopy	12
1.7.1 Charge inversion of negative ions	14
1.8 An introduction to mass analysed kinetic energy spectroscopy	15
1.9 An introduction to isotope effects	19
Chapter 2 Collision induced dissociations of enolate anions	25
2.1 Introduction	25
2.2 Collision induced dissociations of the 3-ethylpentan-2-one enolate ion	28
2.2.1 Fragmentation of the tertiary carbanion	31

2.2.2 Fragmentation of the Primary anion	37
2.3 Collision induced dissociations of the 3,3-dimethylheptan-4-one enolate ion	40
2.3.1 The losses of H ₂ , Me• and Et•	43
2.3.2 The loss of ethene	44
2.3.3 The losses of C ₃ H ₈ , C ₄ H ₈ and C ₅ H ₁₂ .	45
2.3.4 The loss of methane	47
Chapter 3 Collision induced dissociations of substituted benzyl negative ions	49
3.1 An introduction to benzyl negative ions	49
3.2 Collision induced dissociations of the 3-phenylpentane anion	51
3.3 Collision induced dissociations of the anions derived from diphenylmethane and triphenylmethane	59
Chapter 4 Collision induced dissociations of some organoborates and [M-H ⁺] ⁻ ions derived from organoboranes	68
4.1 Introduction	68
4.2 Collision induced dissociations of the [M-H ⁺] ⁻ derived from trimethylborane	71
4.3 The structure of non-decomposing boron adducts	77
4.4 Collision induced dissociations of simple alkoxide organoborate adducts	81
4.5 Collision induced dissociations of negative borate ions formed from bifunctional alkoxide ions and trimethylborane	83
4.5.1 The losses of CH ₄ and Me ₃ B, and the formation of XCH ₂ CH ₂ O ⁻ , Me ₂ \bar{B} CH ₂ and C ₃ H ₄ OX ⁻	91

4.5.2 The losses of XH and XMe, and the formation of X ⁻ and Me ₃ B ⁻ X (X= F, HO, MeO, MeS and Me ₂ N)	93
4.6 Gas phase reactions of enolate negative ions with trimethylborane	99
4.6.1 Simple enolate anions	99
4.6.2 Enolates from alkyl acetates	105
Chapter 5 Conclusion	109
Chapter 6 Experimental	111

Abstract

Reaction of HO^- with MeCOCHEt_2 produces two enolate ions, $\text{MeCO}\bar{\text{C}}\text{Et}_2$ and $\bar{\text{C}}\text{H}_2\text{COCHEt}_2$. The primary carbanion competitively eliminates C_2H_4 and C_4H_8 , and forms C_2HO^- . The elimination of C_2H_4 is a stepwise reaction proceeding through a six membered transition state; the first step (deprotonation) is rate determining. The loss of C_4H_8 is a rearrangement reaction $\bar{\text{C}}\text{H}_2\text{COCHEt}_2 \longrightarrow \bar{\text{C}}\text{H}_2\text{COMe} + \text{EtCH}=\text{CH}_2$. The tertiary carbanion competitively eliminates H_2 , CH_4 , and C_3H_8 . The losses of CH_4 and C_3H_8 are stepwise processes occurring through six and five membered transition states, respectively. A double isotope fractionation experiment (D, ^{13}C) shows that both steps of the CH_4 elimination are rate determining.

The mechanisms of the formation of the major product ions produced by collisional activation of the enolate negative ion of 3,3-dimethylheptan-4-one have been studied by deuterium labelling. H_2 loss involves 1,2 elimination from the 6 and 7 positions. Methane elimination is complex involving three competitive rearrangement processes. Ethene loss produces the most abundant fragment ion and occurs by elimination of the C1-C2 ethyl group with concomitant proton transfer from the 1 position. In the case of the enolate ion from $\text{CD}_3\text{CH}_2\text{CMe}_2\text{COPr}$, the expected elimination of $\text{C}_2\text{H}_2\text{D}_2$ competes with loss of C_2H_4 from positions 6 and 7. Other decompositions are as follows: loss of C_3H_8 involves the methyl and ethyl substituents at positions 7, 1 and

2 respectively; loss of C_4H_8 occurs by two processes, (i) successive losses of two C_2H_4 units (from the 1,2 and 6,7 positions), and (ii) loss of CH_2CMe_2 (from the 2 and 3 positions); and loss of C_5H_{12} produces $Et-C\equiv C-O^-$

The major collision induced dissociations of $Ph\bar{C}Et_2$ involve the losses of H^\bullet , H_2 and CH_4 . Loss of H^\bullet occurs from the phenyl ring, H_2 is eliminated principally by the process $Ph\bar{C}Et_2 \rightarrow PhC(Et)=CH\bar{C}H_2 + H_2$, while methane is lost by the stepwise process $Ph\bar{C}Et_2 \rightarrow \{Me^-[Ph(Et)C=CH_2]\} \rightarrow (C_6H_4)^-C(Et)=CH_2 + CH_4$, in which the second step (deprotonation) is rate determining. The characteristic fragmentation of both $Ph_2\bar{C}H$ and $Ph_3\bar{C}$ is loss of C_4H_4 . This loss occurs without atom randomization and Dewar benzene structures are proposed as intermediates. The ion $Ph_3\bar{C}$ also loses C_6H_6 ; this is a slow process which is preceded or accompanied by both intra- and inter-ring hydrogen scrambling.

Trimethylborane may react with HO^- in the gas phase to produce two non decomposing ions, $Me_2\bar{B}O$ and $Me_2\bar{B}CH_2$. These ions lose H^\bullet , H_2 and CH_4 on collisional activation; it is suggested that the loss of CH_4 occurs through the intermediacy of ion complexes. The structure of the ions $Me_2\bar{B}O$ and $Me_2\bar{B}CH_2$ together with the ions from their collisional activation spectra have been investigated with the aid of *ab initio* calculations. The calculations confirm the stability of the proposed precursor and product ions, but indicate that the trismethyleneborane anion is unstable with respect to the isomeric methylene cycloborapropene anion.

The adducts formed between the reaction of organoboranes and simple alkoxides (RO^-) have been shown to have a tetrahedral geometry. On collisional activation these ions undergo a number of fragmentations including the loss of CH_4 , ROCH_3 and ROH ; these processes are believed to occur through the intermediacy of ion complexes. A hydride transfer reaction from the α centre of the alkoxide to give the borohydride anion occurs; this type of reaction has not been observed before in gas phase boron chemistry. The reaction between alkoxides of the type $\text{XCH}_2\text{CH}_2\text{O}^-$ (where $\text{X} = \text{MeO}, \text{MeS}, \text{HO}, \text{F}$ or Me_2N) and trimethylborane also form stable non decomposing adducts. On collisional activation these adducts undergo a number of standard reactions including the loss of CH_4 , and the formation of $\text{Me}_2\bar{\text{B}}\text{CH}_2$, $\text{Me}_3\bar{\text{B}}\text{H}$ and $\text{XCH}_2\text{CH}_2\text{O}^-$. These adducts also undergo a number of fragmentations not observed before in gas phase boron chemistry, e.g. the loss of XH , XMe and the formation of X^- . Alkoxides of the type $\text{XCH}_2\text{CH}_2\text{O}^-$ may produce two adducts with Me_3B viz: $\text{Me}_3\bar{\text{B}}\text{OCH}_2\text{CH}_2\text{X}$ or $\text{Me}_3\bar{\text{B}}^+\text{XCH}_2\text{CH}_2\text{O}^-$. The latter adduct is believed to be the precursor for a number of unique fragmentations e.g. the formation of $\text{Me}_2\bar{\text{B}}\text{CH}_2$ through a six centred transition state and the formation of $\text{Me}_3\bar{\text{B}}\text{X}$. The loss of XH , XMe and the formation of X^- are believed to occur through remote fragmentation processes

Simple enolate anions are binucleophilic in nature and should form two isomeric adducts on reaction with boranes, e.g. the acetaldehyde enolate anion may form two adducts $\text{Me}_3\bar{\text{B}}\text{CH}_2\text{CHO}$ or $\text{Me}_3\bar{\text{B}}\text{OCHCH}_2$. *Ab initio* calculations indicate that both adducts exist in a stable state energy

minimum. On collisional activation the adducts decompose via a number of pathways; the adducts lose CH_4 , Me_3B and form the ion $\text{Me}_2\bar{\text{B}}\text{CH}_2$. These fragmentations have been explained in terms of ion complexes and may occur from either adduct. The adduct formed from the acetaldehyde enolate anion and Me_3B undergoes an interesting hydride transfer reaction to form $\text{Me}_3\bar{\text{B}}\text{H}$. Ester enolate anions may form three isomeric adducts on reaction with trimethylborane; these adducts undergo a number of standard reactions e.g. the loss of CH_4 , and Me_3B , and the formation of $\text{Me}_2\bar{\text{B}}\text{CH}_2$. In addition the adducts also lose ketene and form the ion HC_2O^- , some mechanisms have been proposed for these processes but the formation of the isomeric precursor ions prevents us from distinguishing between the different mechanisms.

STATEMENT

This thesis contains no material which has been accepted for the award of any other degree or diploma in any university, and to the best of my knowledge and belief, the thesis contains no material previously published or written by another person except where due reference is made in the text.

Graeme Currie

Acknowledgements

I would like to thank Professor J. Bowie for his advice, encouragement and patience. I would like to thank Tom Blumenthal for the maintenance of the ZAB mass spectrometer, his instructions on its use, and for his courage in letting me use it without supervision. I am indebted to Dr. J. C. Sheldon for some *ab initio* results, and to Dr. M. B. Stringer for some labelled compounds. I would like to thank all my friends and family who put up with me, supported me and thoughtfully pointed out the new grey hairs. A special thankyou to Vicky Burgess for her support and friendship.

CHAPTER 1

INTRODUCTION

1.1 General

The first precision measurements of ionic masses and abundances were reported in 1918 and 1919 by Aston¹ and Dempster² respectively. Since then, steady improvements have been made in the performance of mass analysers³, and new forms of both analysers (e.g. the quadrupole), and ionization techniques have been developed. Mass spectrometry is now a well established technique, and is used routinely as an analytical technique and in mechanistic studies. The acceptance of negative ion mass spectrometry as a viable analytical technique was delayed by over a decade in comparison to positive ion mass spectrometry. This delay in the use of negative ions could be attributed to a number of factors associated with low sensitivity, irreproducibility, and inadequate equipment. For example, at electron energies normally employed to give positive ion mass spectra, it was originally proposed that the formation of negative ions by electron impact was in general a factor of 10^3 less than that for positive ions⁴. The strong dependence of negative ion spectra on both electron energies and source temperature often led to marked changes in the total ion current and variations in ion abundances^{5,6}. In addition, modification to the electron multiplier electronics⁷ had to be made if negative ions were to be detected at all.

A resurgence of interest in negative ions came with the development of simple and convenient means to produce large populations of negative ions⁸⁻¹². In 1971, von Ardenne¹³ carried out pioneering work in the production of negative ions using reagent gases in a chemical ionization source to moderate initially energetic electrons. Other techniques were developed to produce negative ions including negative ion fast atom bombardment^{14,15} and

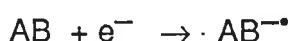
negative ion chemical ionization. In conjunction with these ionization techniques, the use of collisional activation spectroscopy, and new scanning techniques (e.g. linked scans) together with results from ion cyclotron resonance, flowing afterglow and related techniques are contributing to a growing body of information on the thermodynamics, kinetics and mechanisms of negative ion reactions⁷⁹⁻⁸¹.

In this thesis, the collision induced fragmentations of some organic and organoboron negative ions are reported. Studies in this area of negative ion chemistry may be applied, i) to determine the identities of unknown compounds, and ii) to obtain fundamental information about ion behaviour.

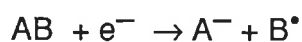
1.2 The Production of Negative Ions.

Primary negative ions are normally formed by electron impact and may be produced by three general processes, depending on the energy of the electron and the nature of the molecule. These three processes are generally classified as follows:

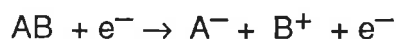
(i) Resonance Capture:



This process involves the capture of low energy electrons in the range 0 - 10 eV by molecules with a positive electron affinity. It may become an important process as the pressure is increased and in the presence of a non reactive gas such as nitrogen¹⁶.

(ii) Dissociative Resonance Capture:

This is an important process if the electron energy is less than 15 eV and provided the molecular anion ($AB^{\bullet-}$) is prone to fragment.

(iii) Ion Pair Formation:

This differs from the above two processes in that it is not a resonant process, and occurs with electrons having a wide range of energies above 10 eV.

(iv) Secondary-Electron Capture:

Electron energies in the range 0 - 5 eV and 40 - 70 eV have been used to yield negative ion in electronic ground states, formed by processes (i) and (ii). The 40 -70 eV range often gives the higher yield of negative ions^{17,18}, for in this range anions are formed by capture of secondary electrons originating at metal surfaces or from gas phase positive ionization^{18,19}.

1.3 An Introduction to Negative Ion Chemical Ionization.

The technique of chemical ionization was first introduced by Munson and Field²⁰ in 1966. Negative ion chemical ionization (NICI) consists of the formation of negative ions by a series of ion/molecule reactions rather than the more conventional electron impact.

Negative ion chemical ionization (NICI)^{21,22} is normally carried out in a high pressure source capable of operating at pressures in the range 10^{-3} to 10^{-1} Torr. In the ion source, *reagent ions* are produced by electron impact on a

reagent gas (which is at a large partial pressure with respect to the sample). The reagent ions then act upon the sample molecules via ion/molecule reactions to produce negative ions.

These ion-molecule reactions may be conveniently subdivided into four major categories, viz.

1. Proton transfer
2. Charge Exchange
3. Nucleophilic addition
4. Nucleophilic displacement

1.3.1 Proton Transfer.

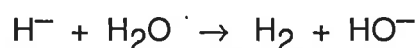
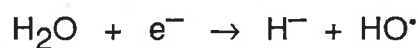


The tendency for a reagent ion R^- to deprotonate a sample molecule AH is determined by a knowledge of the gas phase proton affinities²³ of the anions R^- and A^- . Reaction 1.1 will be exothermic provided the proton affinity of the ion R^- is greater than that of the ion A^- .

Proton transfer reactions are an important class of reactions in NICI as many organic molecules contain acidic hydrogens and the consequent production of $[M-H^+]^-$ negative ions provides molecular weight information.

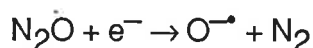
There are many types of reagent gases that have been developed to produce specific reagent ions that act as Bronsted bases. In this thesis the reagent ion HO^- has been used extensively; it is conveniently prepared by using H_2O as the reagent gas^{24,25}. *Scheme 1.1* illustrates the mechanism by which HO^- is formed from H_2O . It should be noted that H^- and $O^{\bullet-}$ (from O_2 impurities) are also present, and these may also contribute to negative ion

production.



Scheme 1.1

Other examples of commonly used "Bronsted base" type reagent ions are: NH_2^- which may be produced from NH_3 ^{26,27}; MeO^- may be produced from $\text{MeOH}/\text{N}_2\text{O}$ ²⁸ or MeONO ²⁹. The HO^- ion may also be produced from a mixture of N_2O and CH_4 or H_2 ³⁰. A general method for producing Bronsted bases as reagent ions has been described³¹; this uses a mixture of CH_4 , 1% MeONO and 5% HX , where HX may be Me_2CO , C_2H_4 , RSH , ROH , MeNO_2 etc.. The methane in these reactions acts as a buffer gas to produce the low energy electrons which initiate the sequence. The ion $\text{O}^{\bullet-}$ has also been used as a NCI reagent, it has a high proton affinity and may produce $[\text{M}-\text{H}^+]^-$ ions from organic molecules^{32,33}: it may be conveniently prepared by using N_2O as the reagent gas³⁴, i.e.



The anion radical ($\text{O}^{\bullet-}$) is also a key intermediate in the production of many other reagent ions e.g. HO^- from $\text{N}_2\text{O}/\text{CH}_4$, $\text{N}_2\text{O}/\text{C}_4\text{H}_{10}$, or $\text{N}_2\text{O}/\text{H}_2$, and MeO^- from $\text{MeOH}/\text{N}_2\text{O}$ ²⁸.

1.3.2 Charge Exchange



The charge exchange reaction shown in *Equation 1.2* will occur if the electron affinity³⁵ of A is greater than that of the reagent R.

The low electron affinity of $O_2^{\bullet-}$ (10 kcal mol⁻¹) means that it readily ionizes samples with higher electron affinities by the process of charge exchange³⁶. The ion $O_2^{\bullet-}$ may be produced from oxygen when the filament in the ion source is replaced by a Townsend discharge³⁷, it may also be produced from N_2 containing a small amount of O_2 ³⁸.

1.3.3 Nucleophilic addition



Stable addition complexes may be produced by the addition of reagent ions to sample molecules as in *equation 1.3*, particularly when the reagent ion has a low proton affinity and is unlikely to react as a Bronsted base.

The Cl^- ion is commonly used to form negative ion addition complexes. Various aliphatic chloro compounds have been used to produce chloride ions under electron impact conditions, e.g. dichloromethane^{39,40} and dichlorodifluoromethane⁴¹. The Cl^- reagent ion system has been used to produce (M + Cl^-) complexes of a range of organic compounds including polycyclic insecticides⁴², organophosphorus pesticides⁴³, alkaloids⁴⁴ and oligosaccharides⁴⁵. The ion $O_2^{\bullet-}$ has also been used to give ion attachment spectra^{46,47}; $O_2^{\bullet-}$ has a much higher proton affinity than Cl^- and may also react as a Bronsted base, however with compounds of lower acidity (e.g. alcohols), nucleophilic addition is the predominant process.

1.3.4 Nucleophilic Displacement



Nucleophilic displacement reactions (e.g. the reaction illustrated in *equation 1.4*) have been studied extensively in condensed phase chemistry. The absence of solvent in the gas phase can have a marked difference on the reactivity of nucleophiles. Nucleophilic reactions in the gas phase generally occur provided, i) the reaction is exothermic or thermoneutral, and ii) there are no facile proton transfers occurring (for a review on gas phase nucleophile reactions see ref. 48). The application of nucleophilic displacements to analytical NCI mass spectrometry is limited, as they provide no molecular weight information and minimal structural information.

Although the ions HO^- and $\text{O}_2^{-\bullet}$ generally react by proton transfer, there have been some reports of them acting as nucleophiles^{49,50}, for example reactions of aliphatic esters (RCOOR') with HO^- or $\text{O}_2^{-\bullet}$ may form the carboxylate anion (RCO_2^-)⁵⁰.

1.4 Sensitivity of Chemical Ionization

The sensitivity of an NCI technique is dependent on the rate constant for ion formation in that system. Absolute sensitivities are difficult to estimate due to unknown and variable source extraction efficiencies and mass spectrometer transmissions.

The fastest ion/molecule reactions proceed with rate constants of 1 to $4 \times 10^{-9} \text{cm}^3 \text{ molecule}^{-1} \text{s}^{-1}$, this corresponds to a reaction occurring at every collision between reactants, and applies to both positive and negative chemical ionization. NCI is therefore comparable in efficiency to positive ion CI.

The rate constants for electron capture reactions depend upon the structure

of the molecule being studied. However, under favourable conditions the electron capture sensitivity may be orders of magnitude greater than that observed for the formation of positive ions by chemical ionization^{51,52}.

1.5 Magnetic Sector Analyser.

The separation of ions by mass may be carried out with a mass spectrometer containing a magnetic sector, this principle is illustrated in *Figure 1.1*.

Ions produced in an ion source are accelerated through a potential voltage difference (V). The gain in kinetic energy of an ion is dependent on the charge z , the mass m , and the accelerating voltage V , as defined by *equation 1.5*.

$$zeV = \frac{1}{2}mv^2 \quad (1.5)$$

(e is the charge of an electron).

For an ion to reach the detector of the mass spectrometer, the ion must traverse a path of radius of curvature r , through a magnetic field of strength B . The magnetic sector influences the ions in a direction vertical to their flight path, and hence the ions are forced to traverse a circular flight path, the radius of which is defined by the balance of angular momentum and centrifugal force caused by the field; see *equation 1.6*

$$mv^2/r = Bzev \quad (1.6)$$

$$mv = Bzer \quad (1.7)$$

$$m/z = B^2r^2e/2V \quad (1.8)$$

Rearrangement of *equation 1.6* gives *equation 1.7*, this demonstrates that the radius of the flight path is proportional to the momentum of the ion (i.e. the magnetic sector is a momentum analyser, not a mass analyser as is commonly assumed). Combining *equations 1.6* and *1.7* gives *equation 1.8*. It can be seen from *equation 1.8* that ions of different m/z ratios can be made to traverse the magnetic sector and reach the collector by varying B and V . In addition, the magnetic sector has a focusing effect, i.e. ions of the same mass, kinetic energy and charge are focused at one point as in an optical system.

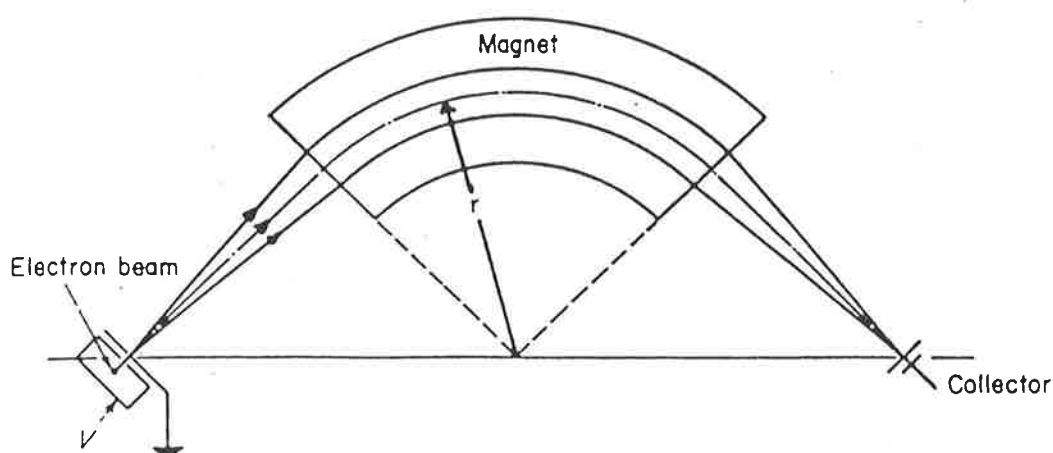


Figure 1.1 Schematic diagram of a single focusing magnetic sector analyser.

In practice, variation of the accelerating voltage causes defocusing and a loss of sensitivity, therefore ions are generally scanned by varying the magnetic field.

1.6 Electric sector analyser.

Since a magnetic sector is a momentum analyser, ions of the same mass and different kinetic energies are not focused at a single point. This means that ions formed with a spread of kinetic energy will reduce the resolution of the mass spectrometer. The addition of an electrostatic sector to a mass spectrometer allows the selection of ions with a defined kinetic energy and hence increases the resolution.

An ion entering an electrostatic field will experience a force on it perpendicular to the direction of its travel, forcing the ion to travel in a circular path of radius R . The formula for the motion of such an ion is given by *Equation 1.9*, where E is the electrostatic field strength.

$$mv^2/R = eE \quad (1.9)$$

This equation shows that the radius of the flight path of an ion is dependant on charge but not mass. Thus in an electrostatic field, separation of ions by their charge is possible.

If a narrow slit were placed in the image plane of an electrostatic sector, this could be used to transmit a narrow band of energies, however this would lead to a drastic loss in sensitivity (although resolution would be improved). This loss in sensitivity may be overcome by using a combination of electrostatic sector and magnetic sector in a Nier-Johnson geometry. This geometry allows all ions to be focused at a single point according to their mass and their energy rather than being transmitted along a plane. *Figure 1.2* illustrates the ion optics of a double focusing mass spectrometer of Nier-Johnson geometry.

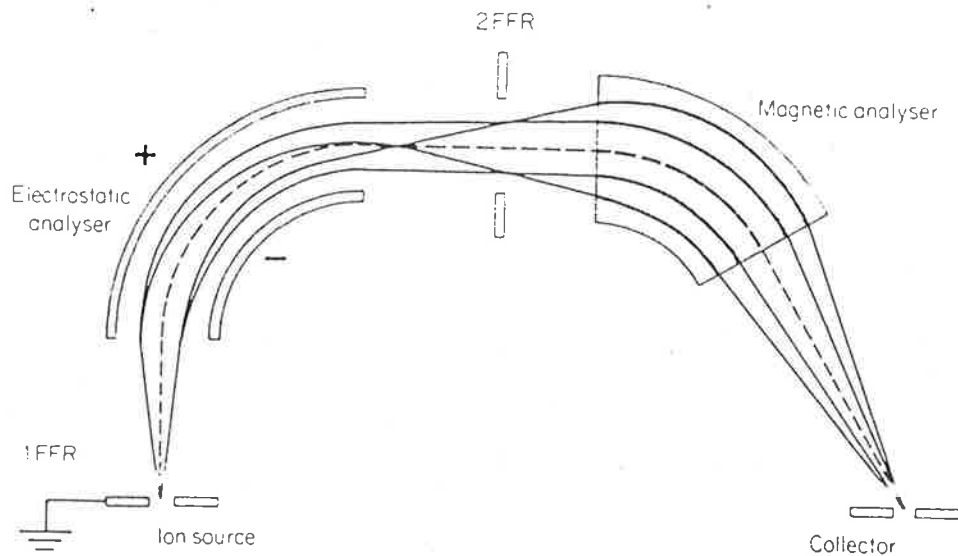


Figure 1.2 A schematic diagram of a double focusing magnetic and electric sector instrument of Nier-Johnson geometry.

In *figure 1.2* the ion following the optical axis has mass m and velocity v . A second ion of mass m may have a velocity $v(1 + \beta)$ (where β represents the spread in speed of ions produced in the source), and an angular divergence α from the optical axis when it leaves the ion source. In a Nier-Johnson geometry mass spectrometer this second ion would traverse a different pathway through the mass spectrometer compared to the ion following the optical axis, but ultimately this ion and others with different velocities produced in the source would be focused at the same point. A well designed double focusing instrument can give good resolution even when α and β are large.

1.7 An Introduction to Collisional Activation Mass Spectroscopy.

Negative ions may be produced from organic molecules using the technique of HO^-/NICl . This *soft ionization* technique often gives molecular weight information, but since the $[\text{M}-\text{H}^+]^-$ ions are in general formed from thermal ion molecule reactions, fragmentations are not common. Collisional activation (CA)⁵³⁻⁵⁵ of the ion may be used to force the ion to decompose thus providing valuable structural information.

Ions produced in the ion source of a mass spectrometer are then generally accelerated to a high translational energy (in the case of the VG ZAB 2HF mass spectrometer up to 8 keV). If an inert gas (e.g. helium) is introduced into a field free region of the mass spectrometer, this may result in a collision between the accelerated ion and an inert atom or molecule. If such an ion impinges upon a neutral atom, some translational energy of the ion may be converted into internal energy. Internal energies of up to 25 eV have been reported^{56,57}. This increase in internal energy, i) intensifies any existing fragmentations, and ii) may allow the ion to overcome activation barriers for decompositions otherwise inaccessible. This in turn may lead to an increase in the amount of structural information available.

The collision process leads to energy transfer to the electrons associated with the ion with little momentum transfer. This electronic excitation is rapidly converted into vibrational energy and spread statistically over the whole ion in accordance with the Quasi-Equilibrium Theory⁵⁸. For this reason there are often strong similarities between a CA mass spectrum and the corresponding electron impact mass spectrum.

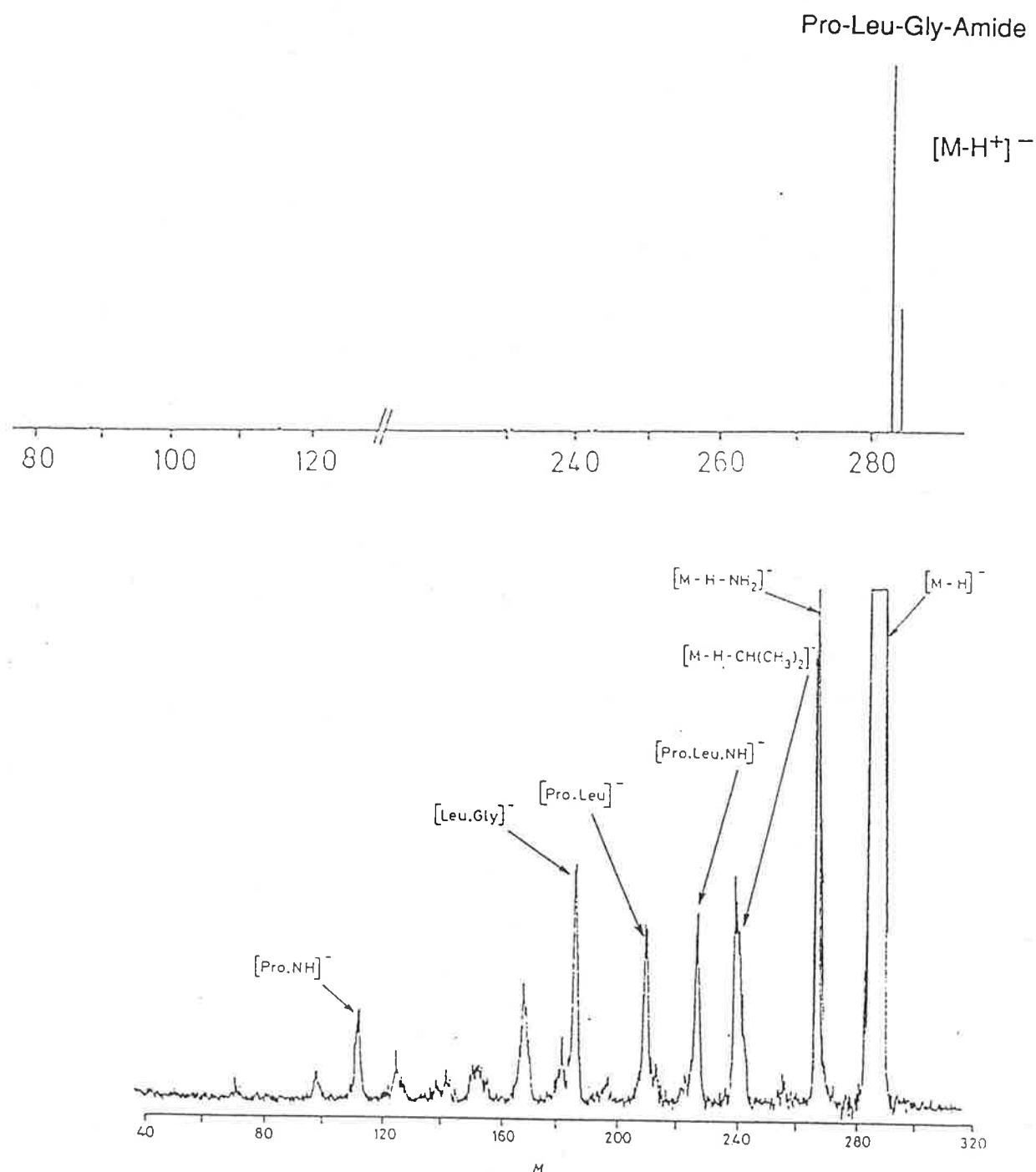


Figure 1.3 Top: The HO^- negative ion chemical ionization mass spectrum of pro-leu-gly amide. Bottom: Collision activated mass analysed ion kinetic energy spectrum of the $(M-H^+)^-$ ion of pro-leu-gly amide⁵⁹. The collision gas was argon, the $(M-H^+)^-$ ion was produced by HO^- negative ion chemical ionization.

Many commercial mass spectrometers are now available with inbuilt "collision cells" for the purpose of producing collisional activation spectra. A

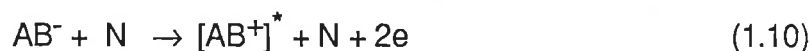
collision cell normally has narrow ion entrance and exit slits, is ideally located at the focus point within a field free region, and is differentially pumped.

The collisional activation technique may be applied to any polyatomic negative ion: *Figure 1.3* illustrates the added structural information that may be obtained from a C A mass spectrum of a particular ion.

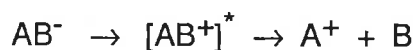
1.7.1 Charge Inversion of negative ions

During a collision of an accelerated ion with a neutral molecule in a field free region, some ions will obtain sufficient energy to undergo processes that will alter the nature of the charge associated with them. This work was pioneered in the early 1970's by Cooks and Beynon⁶⁰.

A non decomposing negative ion may be converted into a positive ion by a collision with a neutral atom or molecule in a field free region (c.f. collisional activation spectra) via the process illustrated in *equation 1.10*.



The energy required for this process (if AB^- and AB^+ are in ground states), equals the sum of the electron affinity (EA) and the ionization energy (IA) of AB. If a peak corresponding to AB^+ is present, the difference in translational energy between AB^- and AB^+ may be measured to estimate the electron affinity of AB. Generally AB^+ is only a transient species, as it has a large amount of excess energy and only the fragmentations of this ion are observed. The minimum energy of the reaction



is given by

$$\Delta E = \Delta EA_{AB} + IE_{AB} + D$$

where D is the bond dissociation energy. Measurement of the difference in ion

translational energies of AB^- and AB^+ can be used to estimate D and hence provide valuable information⁶¹ concerning the mechanism of the reaction under study.

Since the electric sector in this technique will be analysing positive ions while the source and magnetic sector are transmitting negative ions, the polarity of the electric sector is reversed hence the spectra recorded are called +E spectra. This technique produces a positive ion spectrum of an initially non decomposing negative ion and may be used to provide information concerning both the negative ion and its precursor neutral^{62,63}.

1.8 An Introduction to Mass Analysed Ion Kinetic Energy Spectroscopy

Ions often fragment to produce a variety of daughter ions. The elucidation of these decomposition pathways may be aided by the study of metastable ions^{60,64,65}.

Ions produced in the ion source of a mass spectrometer may be formed with a wide range of energies. Ions formed with a large amount of energy often undergo one or more decompositions while still in the ion source. Some ions which are formed do not decompose in the ion source yet have too much energy to enable them to pass through the mass spectrometer intact. These ions dissociate in transit after acceleration and are called "metastable ions".

Consider an ion m_1^+ undergoing a "metastable" decomposition (i.e. a decomposition occurring after acceleration) as in *equation 1.11*.



At a first approximation the products may be assumed to continue in the same direction and speed as m_1^+ . As a consequence of the ion m_2^+ having a

reduced mass and the velocity of the parent ion m_1^+ , the ion m_2^+ will pass through the mass spectrometer at quite different focusing conditions compared to an ion of the same mass and charge that was formed in the ion source. The "metastable" ion m_2^+ therefore appears at an apparent mass m^* which is defined by *Equation 1.12*.

$$m^* = m_2^2/m_1 \quad (1.12)$$

where m_1 is the mass of the parent ion and

m_2 is the mass of the fragment ion.

Observation of a metastable ion, when used in conjunction with *equation 1.12* may be used to determine the fragmentation pathways (i.e. $m_1^+ \rightarrow m_2^+$).

Following a "metastable" decomposition, the velocity of m_2^+ does not exactly match that of m_1^+ . During the decomposition of the metastable ion, some of the internal energy of m_1^+ released as a result of the decomposition, manifests itself as kinetic energy. This kinetic energy may appear with any velocity, and can oppose or supplement either wholly or partially the original velocity. This leads to a "spread" in the velocities of the ions. Under conditions of good energy resolution this energy spread can be a sensitive probe for mechanistic studies. For example cleavage reactions often give Gaussian shape metastable peaks and low kinetic energy release T (small T value = narrow peaks). An example of a metastable peak for a negative ion cleavage reaction is illustrated in *figure 1.4(a)* for the loss of an acetyl radical from the molecular anion of *p*-nitrophenyl acetate. Rearrangement reactions often yield metastable peaks of various shapes including Gaussian, flat-topped or dish-shaped; these peaks are often very wide indicating considerable kinetic

energy release. An example of a dish shaped metastable peak is illustrated in *figure 1.4 (b)* this is due to the loss of NO^\bullet from the molecular anion of *p*-nitrobenzoic acid⁸. Composite metastable peaks may also be observed; these indicate the occurrence of more than one mechanism for the decomposition. *Figure 1.5* illustrates a composite peak for the loss of NO^\bullet from the molecular anion of *m*-nitrobenzoic acid⁶⁶.

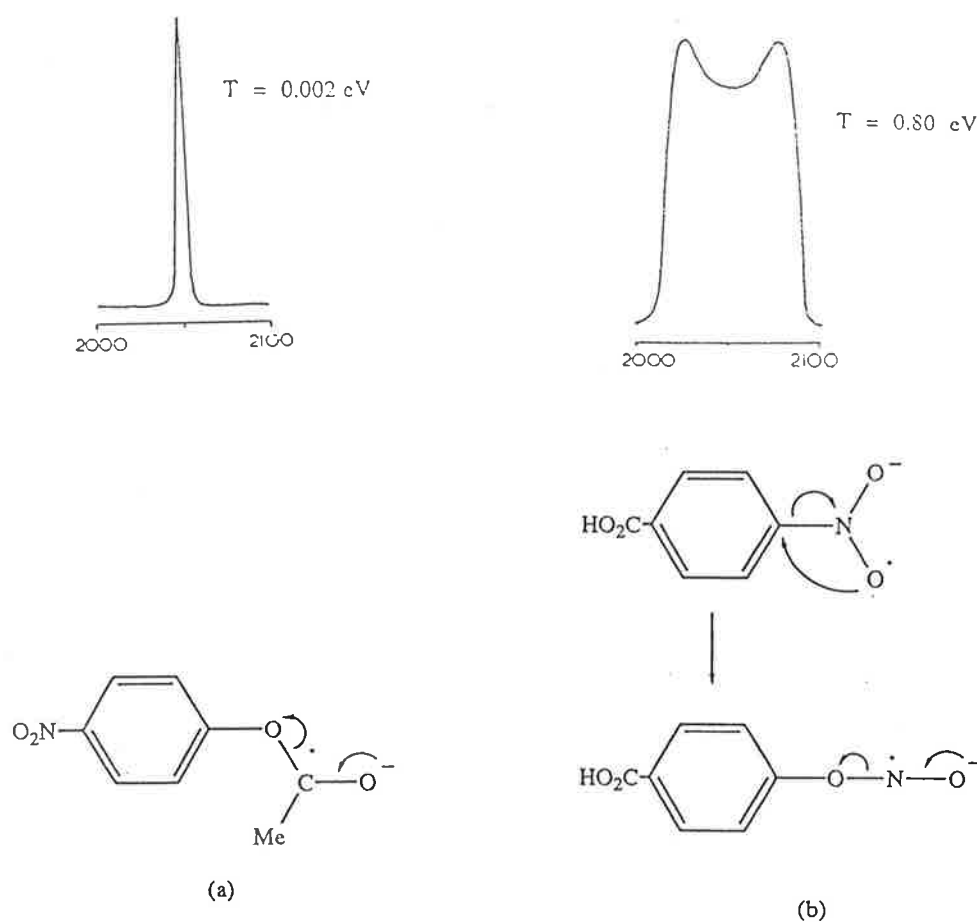


Figure 1.4: Metastable peaks for, a) the loss of an acetyl radical from the *p*-nitrophenylacetate molecular negative ion, and b) the loss of NO^\bullet from the *p*-nitrobenzoic acid molecular negative ion.

Metastable peaks in a normal spectrum, while important, are generally diffuse and weak. This may be overcome by using special metastable scanning

techniques. There are a variety of ways in which to record metastable ion spectra, for example ion kinetic energy spectra⁶⁷, mass analysed ion kinetic energy spectra⁶⁸ and various linked scan techniques^{69,70}. The MIKE technique is described further in this thesis.

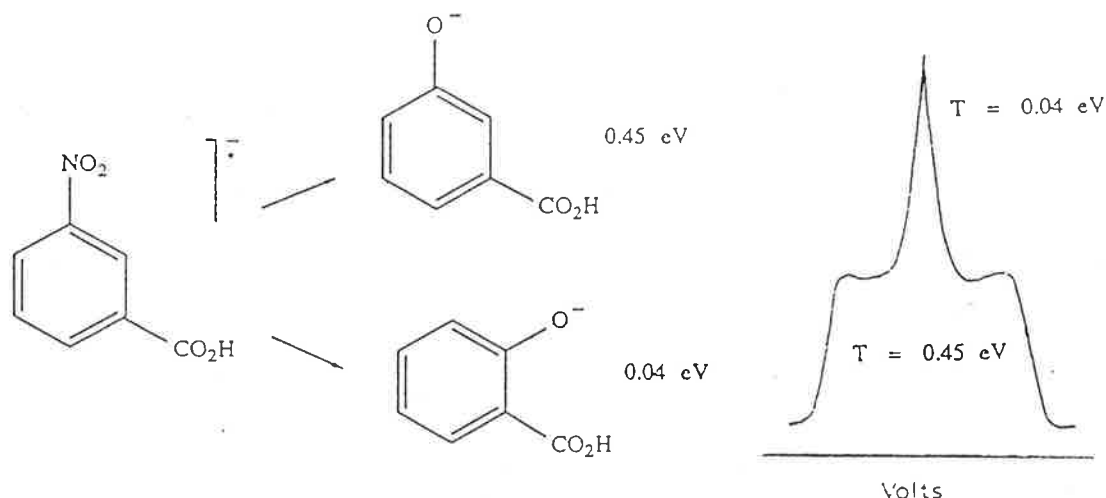


Figure 1.5. Composite metastable peak for the loss of NO^\bullet from the *m*-nitrobenzoic acid parent ion.

The studies reported in this thesis have been largely confined to the use of mass analysed ion kinetic energy spectroscopy (MIKES). A MIKE spectrum is best recorded with a reverse geometry instrument, i.e. a mass spectrometer where the magnetic sector precedes the electric sector. Such an instrument is illustrated in *Figure 1.6*.

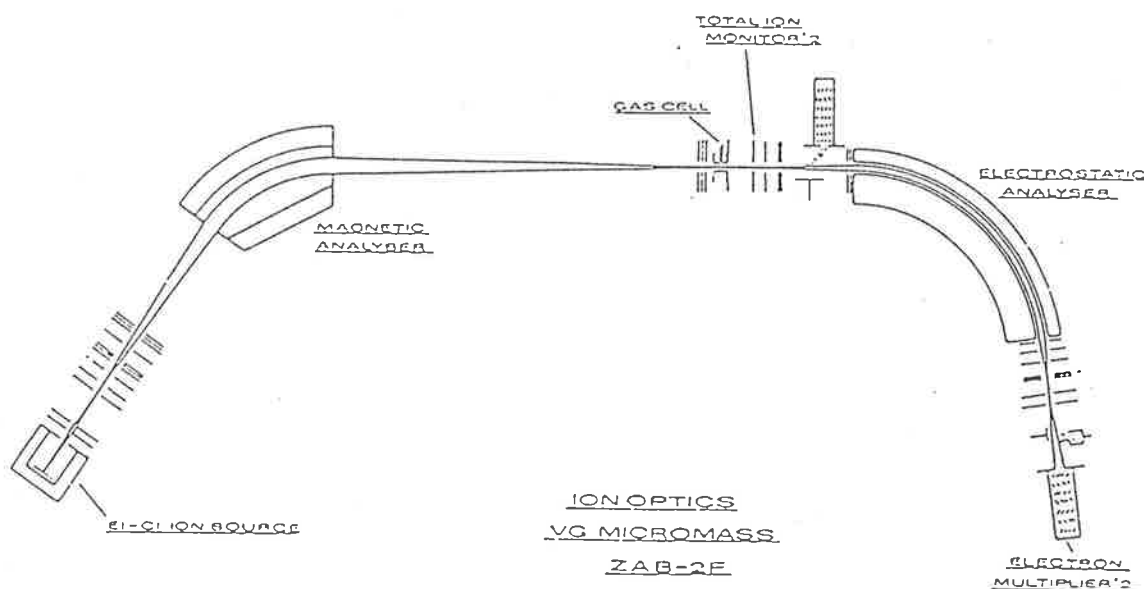


Figure 1.6. A schematic diagram of the VG ZAB-2HF mass spectrometer, a reverse geometry instrument.

To determine a MIKE spectrum, the magnetic sector is set to transmit only the ion under study to pass, and the electric sector is scanned. This results in a spectrum of all "metastable" ions produced from the decomposition of the selected ion in the second field free region. This technique is often coupled to that of collisional activation in order to increase the number of observable decompositions.

1.9 An Introduction to Isotope Effects

Isotope effects⁷¹⁻⁷³ can be an invaluable tool in the understanding of the intrinsic details of reactions. In brief, the substitution of an atom for a heavier

isotope may lead to a change in the rate of the reaction. Comparison of the individual rates may give valuable information about the kinetics and transition states, or thermodynamics of the reaction.

The classical treatment of isotope effects assumes that the origin of the isotope effect lies in the difference in zero point energy (ZPE) of a molecular species caused by isotopic substitution. *Equation 1.13* shows the zero point energy relationship.

$$\xi_0 = \frac{h}{2\pi} \cdot \sqrt{(f/m^*)} \quad (1.13)$$

where ξ is the zero point energy

m^* is the effective mass and

f is the force constant.

The force constant is a measure of the stiffness of a chemical bond and a measure of how the potential energy changes with displacement of the constituent atoms around the internuclear bond distance. When an atom is replaced by one of its isotopes, the Born-Oppenheimer approximation⁷⁴ specifies that the potential energy of a system does not change, and as a consequence force constants are unaffected by isotopic substitution. This means that ZPE change on isotopic substitution is due to changes in effective mass. Consider the diatomic system A - H where $m_A \gg m_H$. The effective mass may be calculated as

$$m^* = \frac{m_A m_H}{m_A + m_H}$$

therefore $1/m^* = 1/m_A + 1/m_H$

but since $m_A \gg m_H \Rightarrow 1/m^* \approx 1/m_H$

The ZPE difference for substitution of a deuterium for a hydrogen may be represented thus

$$\begin{aligned}\Delta\xi_0 &= \xi_0^{\text{H}} - \xi_0^{\text{D}} \\ &= (h\nu f)/4\pi \cdot [1/\sqrt{m_{\text{H}}} - 1/\sqrt{m_{\text{D}}}] \\ &= (h\nu f)/4\pi [1 - 1/\sqrt{2}]\end{aligned}$$

This expression is important in that it shows the relationship between ZPE and the force constant, $\Delta\xi_0 \propto \sqrt{f}$. Thus the force constant controls the size of the difference in ZPE between A-H and A-D.

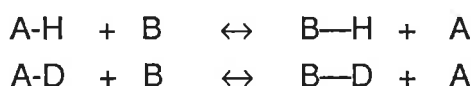
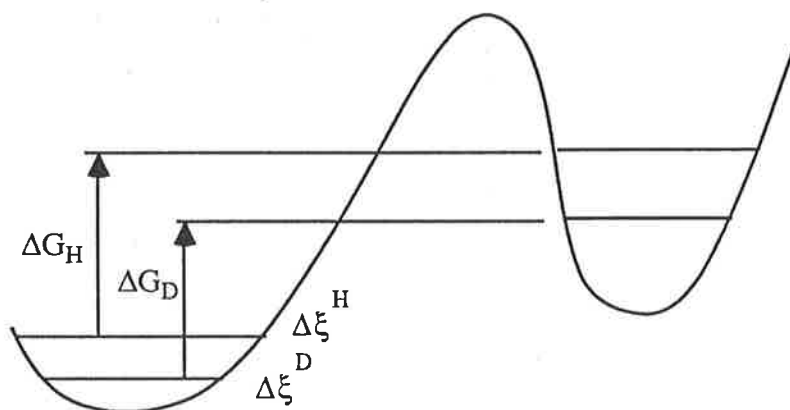
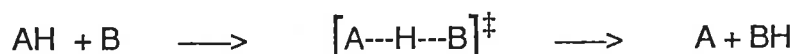


Figure 1.7 A potential energy diagram for an equilibrium process.

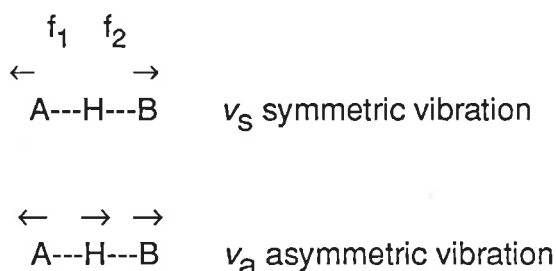
The two major types of isotope effects are equilibrium and kinetic. *Figure 1.7* shows a simple potential energy diagram for a diatomic equilibrium process. Since the force constants for the "reactants" and "products" are different, the differences in ZPE for the two isotopic species are also different. Therefore the Gibb's free energy (ΔG) for the two isotopic reactions are different, and this will result in a difference in the equilibrium constants for the two isotopic reactions.

Thus the equilibrium isotope effect value reflects differences in the force constants of both the reactants and products.

The other major type of isotope effect is the kinetic isotope effect. Consider the generalized reaction:



The deuterium kinetic isotope effect for this process is again a function of the difference in force constants and the difference in ZPE in both the reactants and transition state. The difference in ZPE in the transition state arises from the various degrees of freedom (of which there are $3N-5$). In this example there are therefore 4 degrees of freedom, two bending modes and two stretching vibrations. We are concerned with the stretching vibration.



The asymmetric vibration is along the reaction coordinate and therefore there is no restoring force (i.e. the reaction proceeds directly to products). The asymmetric vibration is therefore isotopically insensitive (i.e. introduction of say D for H will not produce a change in ZPE). The symmetric vibration is however isotopically sensitive provided $f_1 \neq f_2$. If $f_1 = f_2$ then there is no "motion" of the central atom, and on isotopic substitution there is no change in ZPE. The kinetic isotope effect may be determined from the different rates of the two reactions under consideration. The value of the isotope effect depends on the structure of the transition state. When $f_1 > f_2$ then the kinetic isotope effect (K.I.E.) approaches the value 1 and the transition state is said to be "reactant like"⁷⁸

(figure 1.8). When $f_1 = f_2$ then the K.I.E. approaches a maximum value and the transition state is said to be "symmetrical", when $f_1 < f_2$ the K.I.E. approaches the equilibrium isotope effect value and the transition state is said to be "product like".

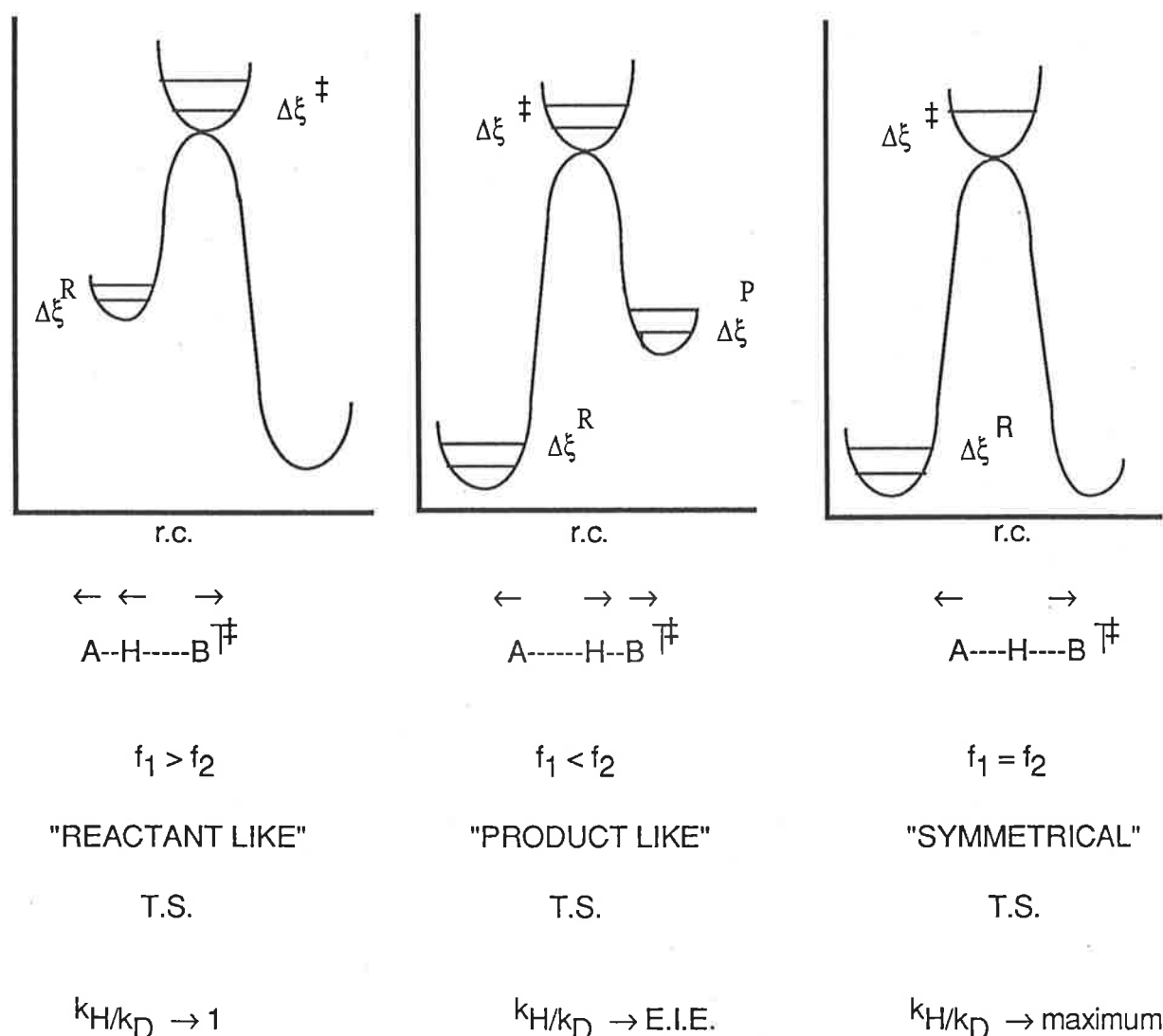


Figure 1.8: Potential energy curves showing relationship between kinetic isotope effects and transition state structures.

The above treatment illustrated in *figure 1.8* is a summary of the *classical* isotope effect theory, when species undergoing reactions have Maxwell Boltzman distributions⁷⁵ (i.e. in most condensed phase reactions). It must be stressed that

Maxwell-Boltzmann conditions are not always achieved in ion reactions in the gas phase. Thus the simple classical isotope effect theory does not always predict the correct isotope effect value in gas phase reactions. This has been discussed in a recent review by Derrick⁷⁶, and in the particular case of the McLafferty rearrangement⁷⁷. Nevertheless, we contend that the basic concepts of the classical isotope effect theory still pertain in gas phase ion chemistry, and we use these concepts in *qualitative fashion* throughout this thesis.

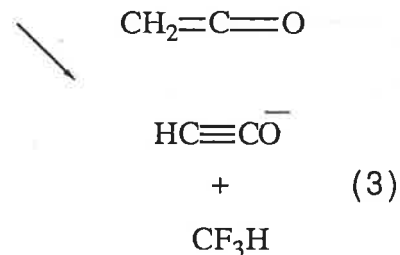
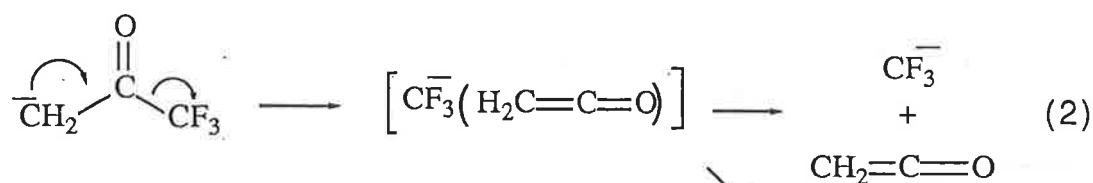
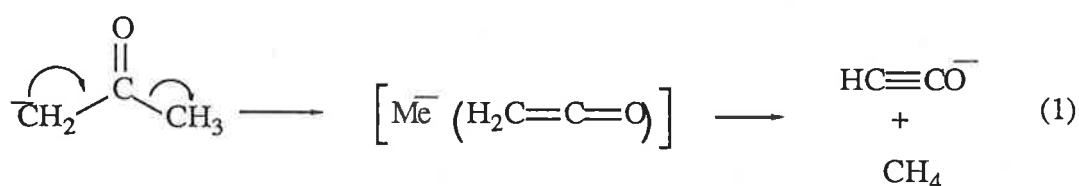
CHAPTER 2

COLLISION INDUCED DISSOCIATIONS OF ENOLATE

ANIONS

2.1 Introduction

Enolate ions may be produced by the reaction of HO^- on alkyl ketones in a chemical ionization source⁸². Brauman^{83,84} has studied the multi photon (laser induced) dissociations of simple ketone enolate ions in an ion cyclotron resonance spectrometer. The ion $^-\text{CH}_2\text{COME}$ eliminates methane, while $^-\text{CH}_2\text{COCF}_3$ eliminates CF_3H and also forms $^-\text{CF}_3$. *Equations (1) to (3)* are proposed as possible mechanisms for these reactions.

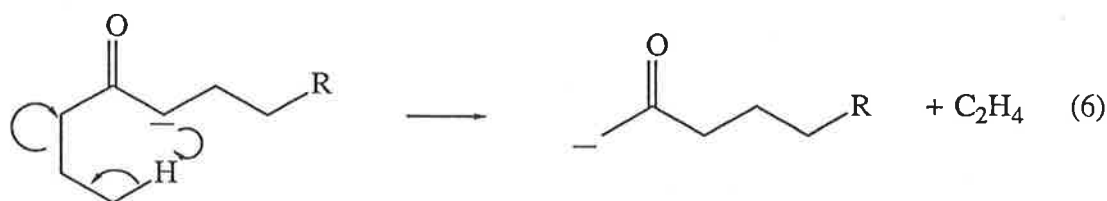


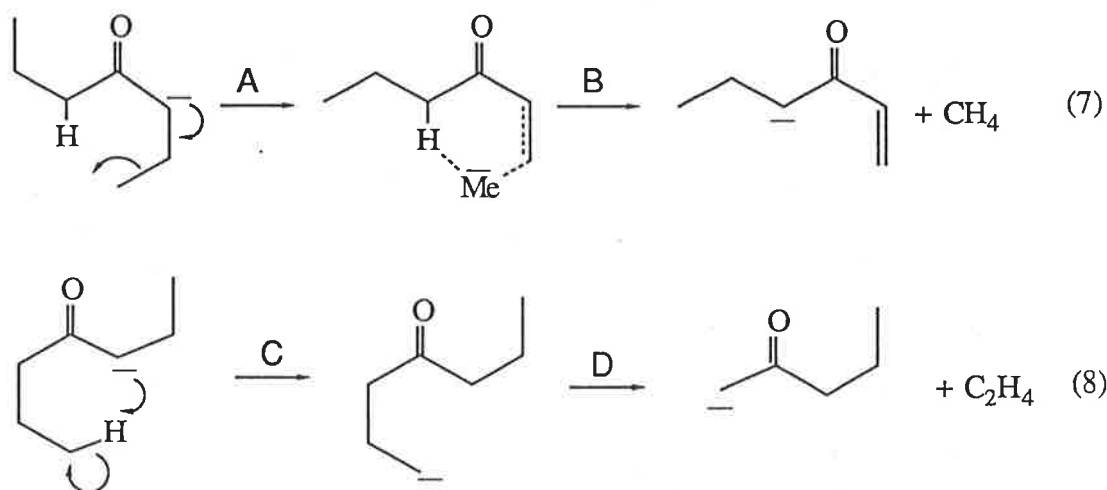
The intermediacy of ion complexes such as those in *equations (1), (2) and (3)* is an important mechanistic question, but is a matter of conjecture. The question arises as to whether such reactions are concerted or stepwise, and if they are

intermediacy of anionic intermediates rather than radical anion intermediates. Hayes and colleagues⁸⁷ have studied the collisionally activated loss of methane and dihydrogen from alkoxides using isotope effects and *ab initio* calculations. They concluded that the loss of methane and dihydrogen from alkoxides do indeed occur via a stepwise mechanism and involve the intermediacy of solvated hydride and methyl anions. Raftery and Bowie⁸⁸ have studied the collision induced dissociations of cyclohexanone enolate negative ions and observed the loss of H₂ from the 3,4 and 3,6 positions and rationalized this in terms of a solvated ion complex intermediate.

A number of reactions described in this thesis are thus rationalized in terms of the intermediacy of ion complexes .

Hunt and colleagues^{89,28} have studied the collisional activation spectra of a variety of $[M-H^+]^-$ ions derived from ketones. They have suggested that the rearrangement peaks observed may be explained by the γ -hydrogen rearrangement and olefin elimination shown in *equation 6*. The collision induced dissociations of the enolate ions of heptan-4-one⁹¹ and butyrophenone⁹² have been studied using ²H and ¹³C labelling. The suggested mechanisms for the two major reactions of the heptan-4-one enolate ion are shown in *equations (7) and (8) (Scheme 2.1)*.





Scheme 2.1

2.2 Collision Induced Dissociations of the 3-Ethylpentan-2-one Enolate Ion

In earlier studies, heptan-4-one was chosen for study since only one carbanion may be initially formed due to the symmetry of the molecule. This thesis extends that work to a consideration of 3-ethylpentan-2-one. 3-Ethylpentan-2-one was chosen for study for two reasons: i) it may form both a primary and tertiary carbanion by deprotonation and both should fragment differently, and ii) since the neutral molecule is symmetrical with two identical side chains, this allows the determination of intramolecular isotope effects which may be used as probes for reaction mechanisms.

The labelled compounds used in this study are listed in *Table 2.1*, water was used to produce HO^- as the reagent ion, and helium was used as the collision gas in the second field free region. Full details are given in the experimental section. The details of the C.A. mass spectra of compounds (1) - (11) are listed in *Tables 2.2* and *2.3*; a typical spectrum is shown in *figure 2.1*.

$\text{CH}_3\text{COCH}(\text{C}_2\text{H}_5)_2$	(1)	$\text{CH}_3\text{COCH}(\text{CD}_2\text{CH}_3)_2$	(7)
$\text{CH}_3\text{COCH}({}^{13}\text{CH}_2\text{CH}_3)_2^\dagger$	(2)	$\text{CH}_3\text{COCH}(\text{CD}_2\text{CH}_3)(\text{C}_2\text{H}_5)$	(8)
$\text{CH}_3\text{COCH}({}^{13}\text{CH}_2\text{CH}_3)(\text{C}_2\text{H}_5)$	(3)	$\text{CH}_3\text{COCH}(\text{CH}_2\text{CD}_3)_2$	(9)
$\text{CH}_3\text{COCH}(\text{CH}_2{}^{13}\text{CH}_3)_2$	(4)	$\text{CH}_3\text{COCH}(\text{CH}_2\text{CD}_3)(\text{C}_2\text{H}_5)$	(10)
$\text{CH}_3\text{COCH}(\text{CH}_2{}^{13}\text{CH}_3)(\text{C}_2\text{H}_5)$	(5)	$\text{CH}_3\text{COCH}(\text{CD}_2\text{CD}_3)(\text{C}_2\text{H}_5)^\dagger$	(11)
$\text{CD}_3\text{COCD}(\text{C}_2\text{H}_5)_2^\dagger$	(6)		

TABLE 2.1: Compounds used in the study of 3-ethyl-pentan-2-one.

† Indicated compounds were synthesised by Dr. M.B.Stringer (see acknowledgements).

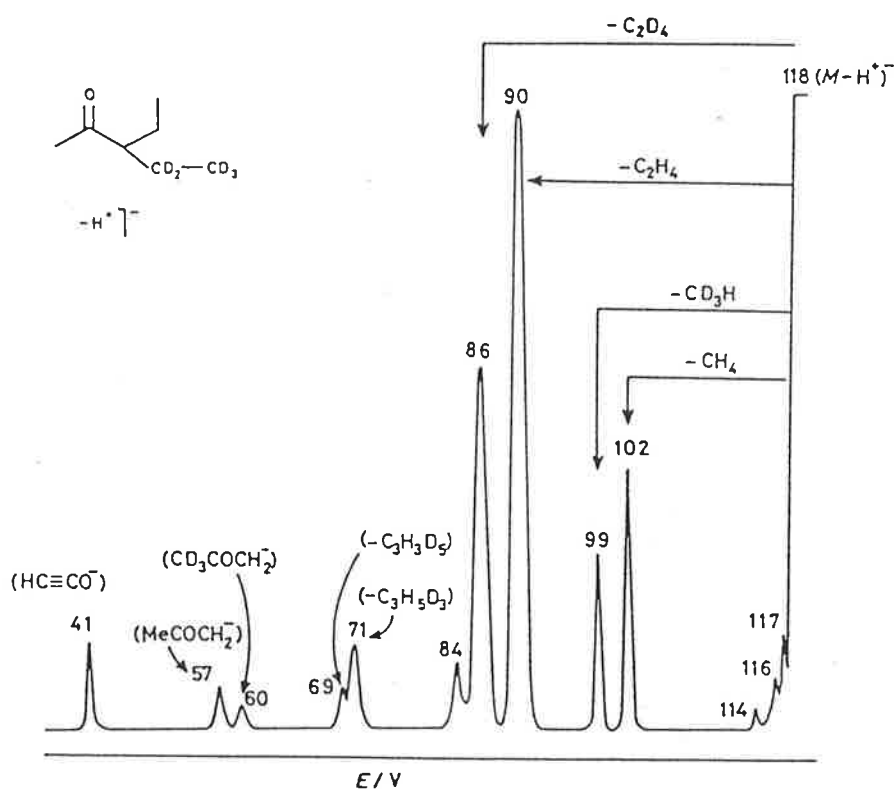


Figure 2.1: Collisional activation spectrum of the enolate ions of $\text{CH}_3\text{COCH}(\text{CD}_2\text{CD}_3)(\text{C}_2\text{H}_5)$

Table 2.2. Collisional activation mass spectra of enolate anions derived from compounds (1) - (11); losses of H•, H₂, CH₄, and C₂H₄

Compound	Loss of					Loss of					Loss of			
	H•	D•	H ₂	HD	D ₂	CH ₄	¹³ CH ₄	¹³ CH ₃ D	CD ₃ H	CH ₃ D	C ₂ H ₄	¹² C ¹³ CH ₄	C ₂ H ₂ D ₂	C ₂ D ₄
(1)	16		12			39					100			
(2)	15		11			37						100		
(3)	30		21			70					100	100		
(4)	16		14				38					100		
(5)	32		18			38	35				106	100		
(6)		17 ^a	17 ^a							22	100			
(7)	15			8		37								100
(8)	30			10	3	71					102			100
(9)	15			6					31					100
(10)	22		8	3		31			24		100		58	
(11)	26		12		3	35			25		100			57

^a Involves loss of 2 a.m.u.

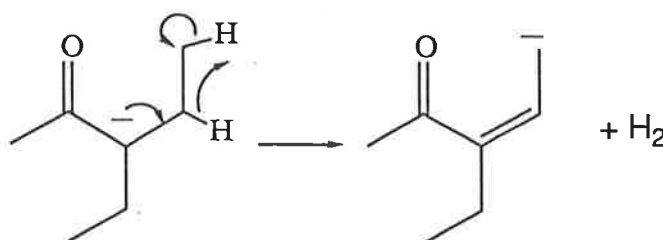
Table 2.3. Collisional activation mass spectra of enolate anions derived from compounds (1) - (11); loss of C₃H₈ and formation of C₂H₅O⁻ and HC₂O⁻

Compound	% Relative Abundance											
	Loss of						Formation of				Formation of	
	C ₃ H ₈	¹² C ¹³ CH ₈	¹² C ¹³ C ₂ H ₈	C ₃ H ₆ D ₂	C ₃ H ₃ D ₅	C ₃ H ₂ D ₆	C ₂ H ₅ O ⁻	¹² C ¹³ CH ₅ O ⁻	C ₂ H ₃ D ₂ O ⁻	C ₂ H ₂ D ₃ O ⁻	C ₂ HIO ⁻	C ₂ DO ⁻
(1)	9						3					7
(2)		8					4					7
(3)	4.07	3.99					4					8
(4)			10					4				7
(5)		10					2.05	1.92				8
(6)									4			6
(7)	11			11			3					7
(8)				6.7			6					10
(9)	8.3					8						8
(10)					10		2.0				3	10
(11)					11	7.5	3.0				1.4	10
											2.1	13

The data in *Tables 2.2* and *2.3* and *Figure 2.1* may be rationalized in terms of a number of specific processes occurring from both the primary and tertiary carbanions: the tertiary carbanion competitively eliminates H_2 , CH_4 and C_3H_8 , whereas the primary carbanion eliminates C_2H_4 and C_4H_8 , and forms HC_2O^- .

2.2.1 Fragmentation of the Tertiary Carbanion.

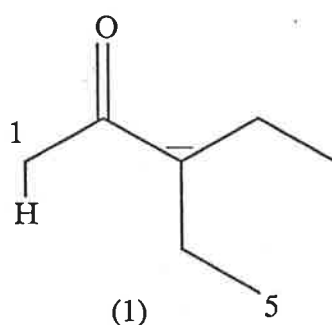
Deuterium labelling shows that the elimination of dihydrogen specifically involves loss of hydrogens from the 4- and 5- positions. This process is analogous to the stepwise 1,2 elimination of hydrogen from alkoxides^{87,93}, and a suggested mechanism is shown in *Scheme 2.2*. The loss of H^\bullet occurs from positions 1 and/or 3, and can therefore come from either enolate anion to produce $^-\text{CH}_2\text{CO}\dot{\text{C}}(\text{Et})_2$ and $^\bullet\text{CH}_2\text{CO}\bar{\text{C}}(\text{Et})_2$.



Scheme 2.2

The loss of CH_4 is specific and is analogous to the process described earlier in *equation 7* (*Scheme 2.1*). The terminal methyl from an ethyl substituent is eliminated together with a hydrogen from C-1. Deuterium and carbon-13 isotope effects were measured for this process by comparing the loss of methane and labelled methane in the appropriate spectra. Each reported value is an average of ten individual measurements. Experimentally determined isotope effects for

this process are listed alongside *formula (1)*. The isotope effect H/D at position 1 was determined in the following manner. Partial exchange of 3-ethylpentan-2-one with 0.1N NaOD/D₂O for 10 min at 20°C gave D₁ = 15, D₂=46, D₃=30 and D₄=9%. Measurement of the appropriate losses of CH₄ and CH₃D from the enolates CHD₂CO⁻Et₂ and CH₂DCO⁻Et₂ gave an average value (statistically corrected) for H/D of 2.5. The isotope effects may be interpreted in either of two ways : i) the reaction is a concerted process, or ii) the reaction is stepwise with two kinetically significant steps. These two possibilities are shown in *Scheme 2.3*.



Position 1

$$\text{H/D} = 2.5 \pm 0.3$$

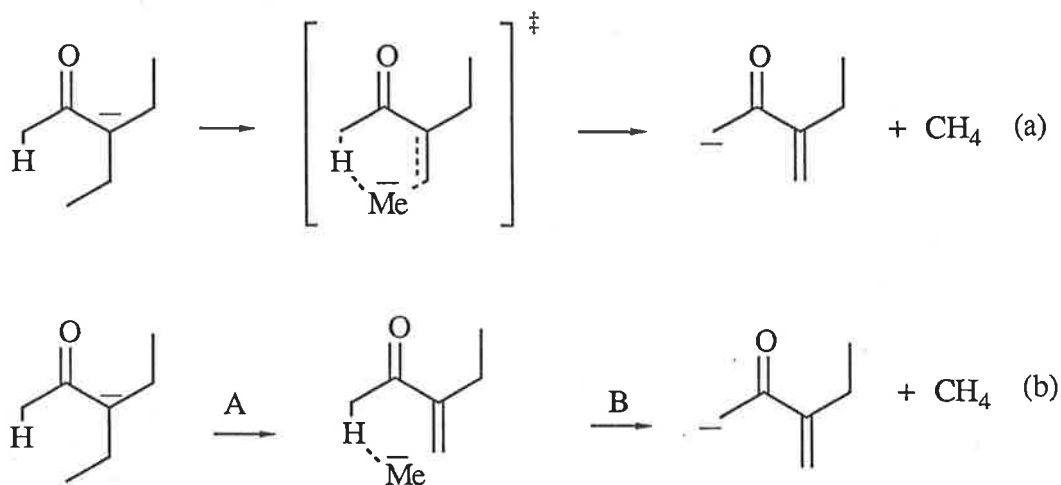
Position 5

$$\text{H/D} = 1.28 \pm 0.03$$

$$^{12}\text{C}/^{13}\text{C} = 1.09 \pm 0.01$$

In order to differentiate between these two possibilities, a double isotope fractionation experiment of the type proposed initially by Belasco, Alberty and Knowles⁹⁴ was performed. Consider the case in *figure 2.2* where the reaction is stepwise with two kinetically significant steps. The first step has a high activation barrier, is a rate determining step, and a kinetic isotope effect may be observed. The second step also has a high activation barrier. Provided the reaction intermediate has a reasonable lifetime, the second step may also be rate

determining and a kinetic isotope effect may also be observed. In the case of 3-ethylpentan-2-one the rate determining nature of step A (*Scheme 2.3*) may be, and is observed by using ^{13}C labelling at position 5. Similarly, the rate determining nature of the second step may be, and is observed by using D labelling at position 1. (*c.f. formula 1*)



Scheme 2.3

If all the hydrogen atoms on C-1 were replaced with deuteriums then the activation barrier for the second step would be increased (i.e. $\Delta E^{\ddagger}_{\text{H}} < \Delta E^{\ddagger}_{\text{D}}$). On increasing the activation barrier of the second step, the significance of the first rate determining step (step A) would diminish, and any isotope effects associated with that step should also decrease (i.e. the ^{13}C isotope effect observed for step A should decrease). Conversely in the case of a concerted reaction, the introduction of deuteriums at C-1 should have a minimal effect on the observed ^{13}C isotope effect.

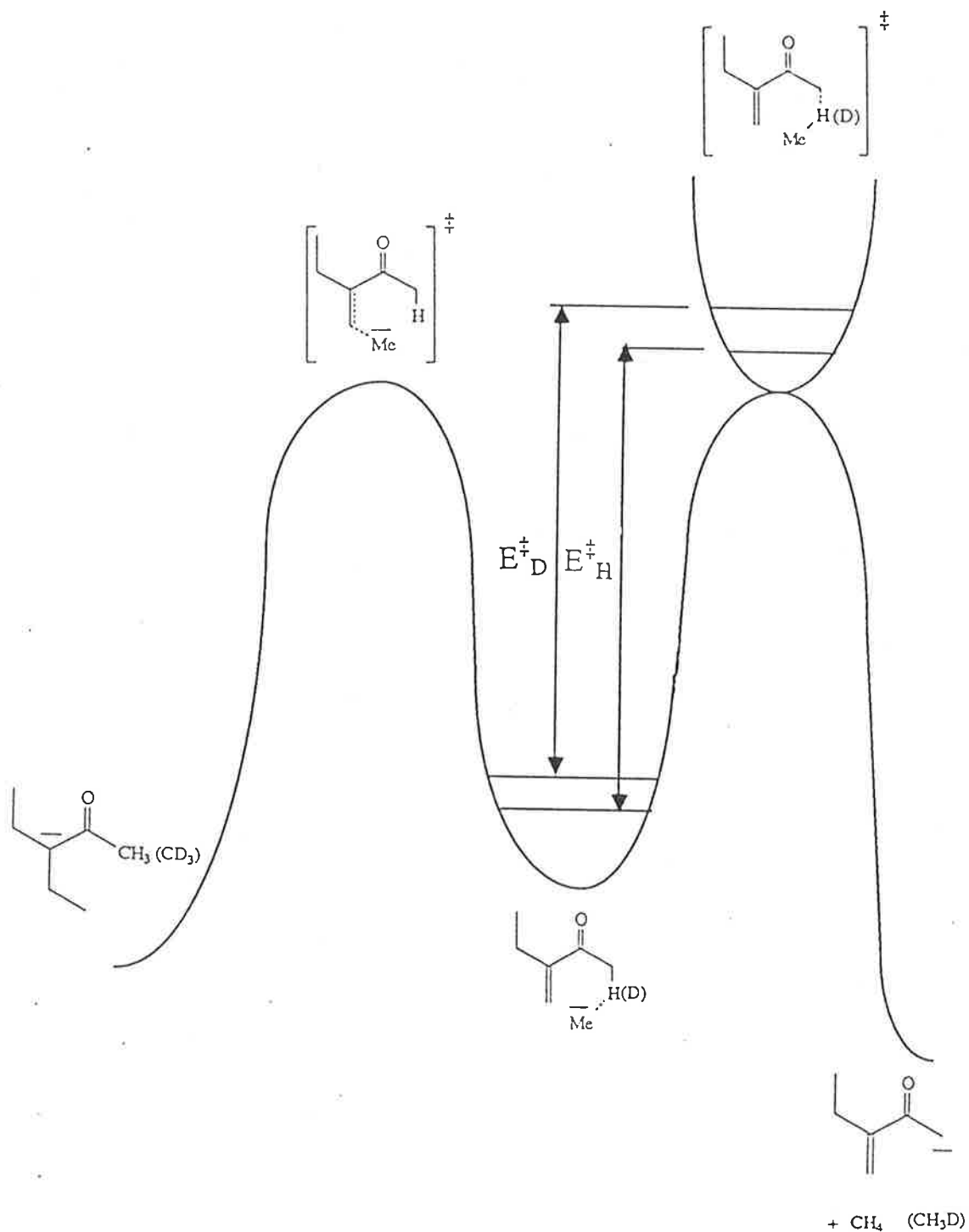
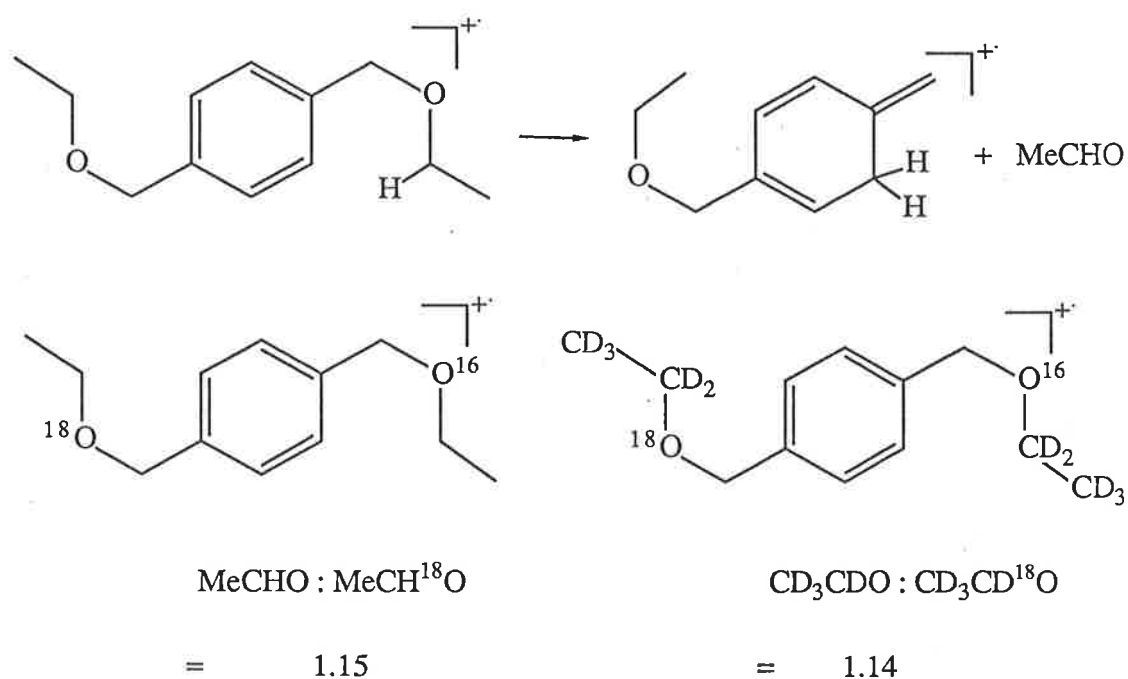


Figure 2.2. A schematic potential energy diagram for the stepwise loss of methane from 3-ethylpentan-2-one. The diagram illustrates: i) two kinetically significant steps, and ii) the increased activation energy for the second step on the introduction of deuterium at position 1 of 3-ethylpentan-2-one.

The experiment that needs to be carried out is as follows. It is already known that the losses of CH_4 and $^{13}\text{CH}_4$ from $\text{CH}_3\text{CO}^-\text{C}(\text{CH}_2^{13}\text{CH}_3)(\text{C}_2\text{H}_5)$ occur in the ratio of 1.09 : 1 (see formula 1 and *Table 2.2*), i.e. $^{12}\text{C}/^{13}\text{C} = 1.09$. If the $^{12}\text{C}/^{13}\text{C}$ isotope effect for the loss of CH_3D and $^{13}\text{CH}_3\text{D}$ from $\text{CD}_3\text{CO}^-\text{C}(\text{CH}_2^{13}\text{CH}_3)(\text{C}_2\text{H}_5)$ is considerably less than 1.09, the Knowles approach would indicate the reaction to be stepwise. If however the isotope effect is largely unchanged it is likely that the reaction is concerted.



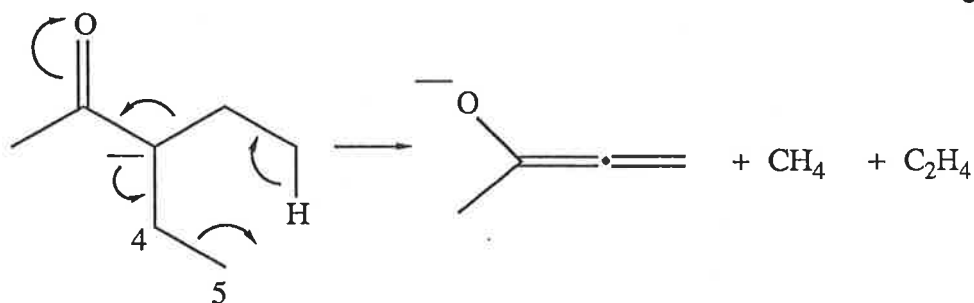
Scheme 2.4

It should be noted that Derrick *et al.*⁷⁷ have used the double isotope labelling experiment to investigate the loss of acetaldehyde from the benzyl ethyl ether molecular cation. The bis ether was used so that intramolecular isotope effects could be determined. The results are summarized in *scheme 2.4*. This reaction is considered to be concerted, but Derrick *et al* contend that in this

case the small difference observed in the $^{16}\text{O}/^{18}\text{O}$ ratios does not differentiate between, i) a stepwise reaction where the two steps are kinetically significant, and ii) a concerted reaction. Derrick *et al* argued that the increase of the activation barrier of the second step would increase the "back reaction" on the first step. This "back reaction" would be accompanied by an isotope effect and as a result a small decrease in the isotope effect for the first step would be observed. Derrick *et al* concluded that the small decrease observed from their fractionation experiment was diagnostically inconclusive, in this particular case.

In our studies of 3-ethylpentan-2-one, a ratio of exactly 1 : 1 was observed for the loss of CH_3D and $^{13}\text{CH}_3\text{D}$ from $\text{CD}_3\text{CO}\bar{\text{C}}(\text{CH}_2^{13}\text{CH}_3)(\text{C}_2\text{H}_5)$, i.e. $^{12}\text{C}/^{13}\text{C} = 1.00$. Thus the $^{12}\text{C}/^{13}\text{C}$ isotope effect has decreased from 1.09 [for $\text{CH}_3\text{CO}\bar{\text{C}}(\text{CH}_2^{13}\text{CH}_3)(\text{C}_2\text{H}_5)$] to 1.00 [for $\text{CD}_3\text{CO}\bar{\text{C}}(\text{CH}_2^{13}\text{CH}_3)(\text{C}_2\text{H}_5)$]. It is most unlikely that the total removal of the isotope effect may be accounted for by a "back reaction", and *it is proposed that the mechanism is stepwise with two kinetically significant steps (Equation b Scheme 2.3).*

The loss of C_3H_8 is a minor process but it has an interesting mechanism. Labelling data (*Table 2.3*) indicate that the fragmentation involves the loss of one methyl and one ethyl group from the two ethyl substituents. Kinetic isotope effects were determined from the spectra of (3), (5), (8) and (10) (*Tables 2.3*) and are summarized in *Scheme 2.5*. These results are consistent with either a concerted process, or a stepwise process with two rate determining steps (see *Scheme 2.5*). Insufficient data is available to distinguish between these two possibilities.

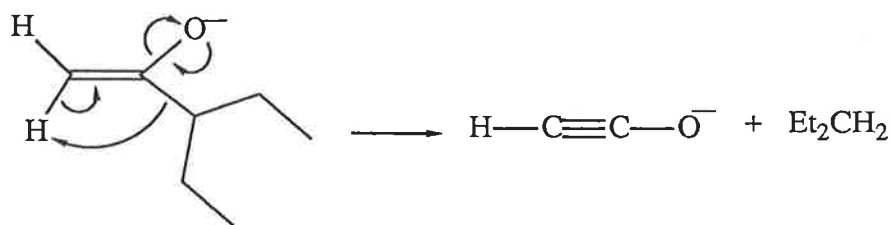


Position 4	Position 5
H/D = 1.23 ± 0.02	H/D = 1.48 ± 0.02
$^{12}\text{C}/^{13}\text{C} = 1.02 \pm 0.01$	$^{12}\text{C}/^{13}\text{C} = 1.06 \pm 0.01$

Scheme 2.5

2.2.2 Fragmentation of the Primary Anion

The formation of $\text{RC}\equiv\text{C}-\text{O}^-$ (where R = alkyl, aryl or H) is a characteristic reaction of enolate ions.^{84,91,92} The overall mechanism for this process is shown in *Scheme 2.6*, it is not known whether the reaction is stepwise or concerted. The product ion in this fragmentation (when R = H) has been shown to have the structure $\text{H}-\text{C}\equiv\text{C}-\text{O}^-$ ⁹⁵ and not the structure $^-\text{HC}=\text{C}=\text{O}$ suggested by Squires in his study of ester enolate ions⁹⁶.



Scheme 2.6

The major fragmentation of the 3-ethylpentan-2-one enolate is the loss of C_2H_4 . Data shown in *Table 2.2* shows that the fragmentation occurs with loss of an ethyl substituent along with transfer of a terminal hydrogen to C-1. It is

suggested the fragmentation is produced specifically from the primary enolate since the corresponding enolate anion (2) from 2-ethylbutanal shows no loss of C_2H_4 .

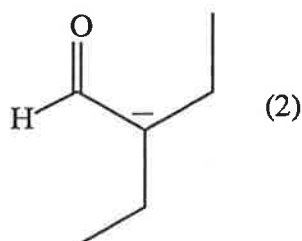
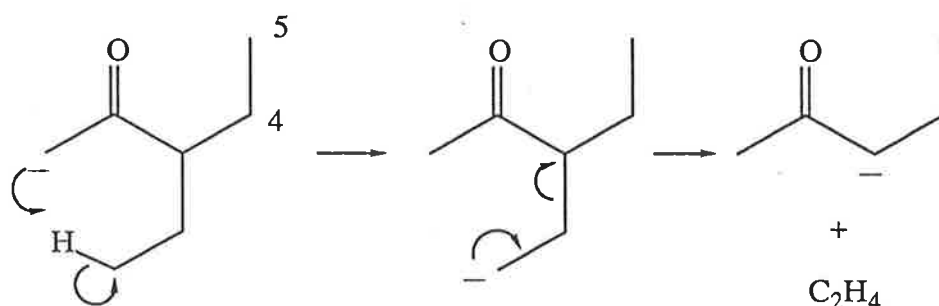


Table 2.2 lists data for the loss of C_2H_4 ; isotope effect values from compounds (3), (5), (8) and (10) are listed with Scheme 2.7. The high isotope effect for labelling at position 5 together with the low isotope effects for labelling at position 4 suggest that the reaction is stepwise with the first step being rate determining. The mechanism proposed is shown in Scheme 2.7

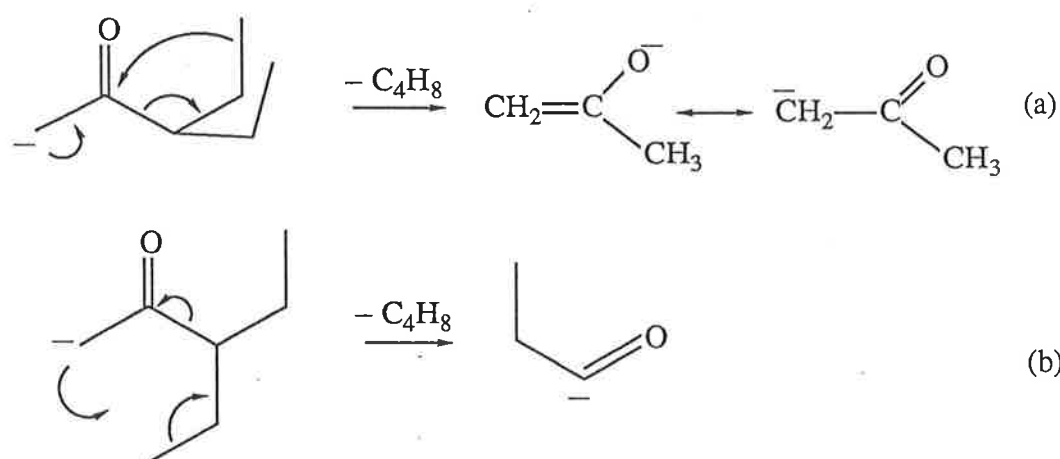


	Position 4	Position 5
H/D =	1.02 ± 0.02	1.71 ± 0.02
$^{12}C/^{13}C =$	1.00 ± 0.01	1.06 ± 0.01

Scheme 2.7

The final fragmentation involves elimination of C_4H_8 to form an anion $C_3H_5O^-$. This unusual fragmentation occurs with loss of C1 and C2 together

with their appropriate substituents. The primary $^{12}\text{C}/^{13}\text{C}$ and secondary H/D isotope effects for the methyl transfer are 1.07 ± 0.01 and 1.28 ± 0.02 respectively. The two mechanisms shown in *scheme 2.8* accord with these results. In order to distinguish between the two mechanisms, the charge reversal spectrum (see section 1.7.1) of the product ion was investigated. Ions RCOCH_2^- on collision with helium yield RCO^+ plus CH_2^{91} . The charge reversal spectrum of the ion $\text{C}_3\text{H}_5\text{O}^-$ from 3-ethylpentan-2-one shows loss of CH_2^\ddagger . In addition both the charge reversal spectrum and the CA mass spectrum are identical with those of the acetone enolate anion ‡ . It is therefore suggested this unusual rearrangement proceeds by the mechanism shown in *Scheme 2.8(a)*.



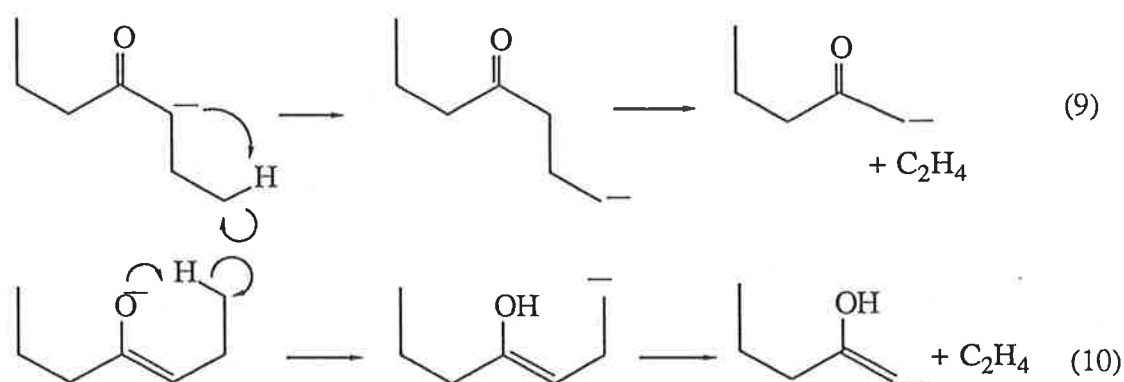
Scheme 2.8

‡ Charge Reversal spectrum of the ion $\text{C}_3\text{H}_5\text{O}^-$: m/z (%) : 43 (35), 42 (100), 41 (29), 39 (35), 29 (77), 28 (32), 27 (57), 26 (15), 15 (16), 14 (24), 13 (8).

‡ Charge Reversal spectrum of the ion $\text{CH}_2\text{COCH}_3^-$: m/z (%) : 43 (31), 42 (100), 41 (29), 39 (24), 29 (35), 28 (31), 27 (31), 26 (21), 15 (12), 14 (18), 13 (13).

2.3 Collision Induced Dissociations of the 3,3-Dimethylheptan-4-one Enolate Ion

From previous studies the evidence suggests the elimination of ethene from the heptan-4-one⁹¹ enolate ion occurs as shown in *equation 8 (page 28)*, however there is always the possibility of alternative reactions such as those shown in *equations 9 and 10*.



In order to study these possibilities the collisional activation spectra of the 3,3-dimethylheptan-4-one enolate ion and labelled derivatives have been examined. This system was chosen since it can only form one enolate ion, namely $EtCMe_2CO\bar{C}HEt \leftrightarrow EtCMe_2C(-O^-)=CHEt$. The answers to two questions were sought: i) does $EtCMe_2CO\bar{C}HEt$ eliminate C_2H_4 , and if so what is the mechanism for this reaction, and ii) since $EtCMe_2CO\bar{C}HEt$ cannot eliminate CH_4 by a process analogous to that shown in *equation 7 (page 28)* what alternative decompositions are noted?

The compounds used in this study are listed in *Table 2.4*, the collisional activation mass spectra of their $[M-H^+]^-$ and $[M-D^+]^-$ ions are recorded in

Table 2.5. A particular example is shown in Figure 2.3. The results are in accordance with previous studies in so far that neither hydrogen or carbon scrambling accompanies or precedes any decompositions in these aliphatic systems.

$ \begin{array}{c} \text{Me} \\ \\ \text{R}_1 - \text{C} - \text{C} - \text{R}_2 \\ \quad \\ \text{Me} \quad \text{O} \end{array} $	R ¹	R ²	R ¹	R ²	
	(1)	Et	Pr	(5)	MeCD ₂
(2)	Et	CD ₂ Et	(6)	CD ₃ CH ₂	Pr
(3)	Et	CH ₂ CD ₂ Me	(7)	CD ₃ CD ₂	Pr
(4)	Et	CH ₂ CH ₂ CD ₃	(8)	CD ₃ CD ₂	CD ₂ Et

Table 2.4

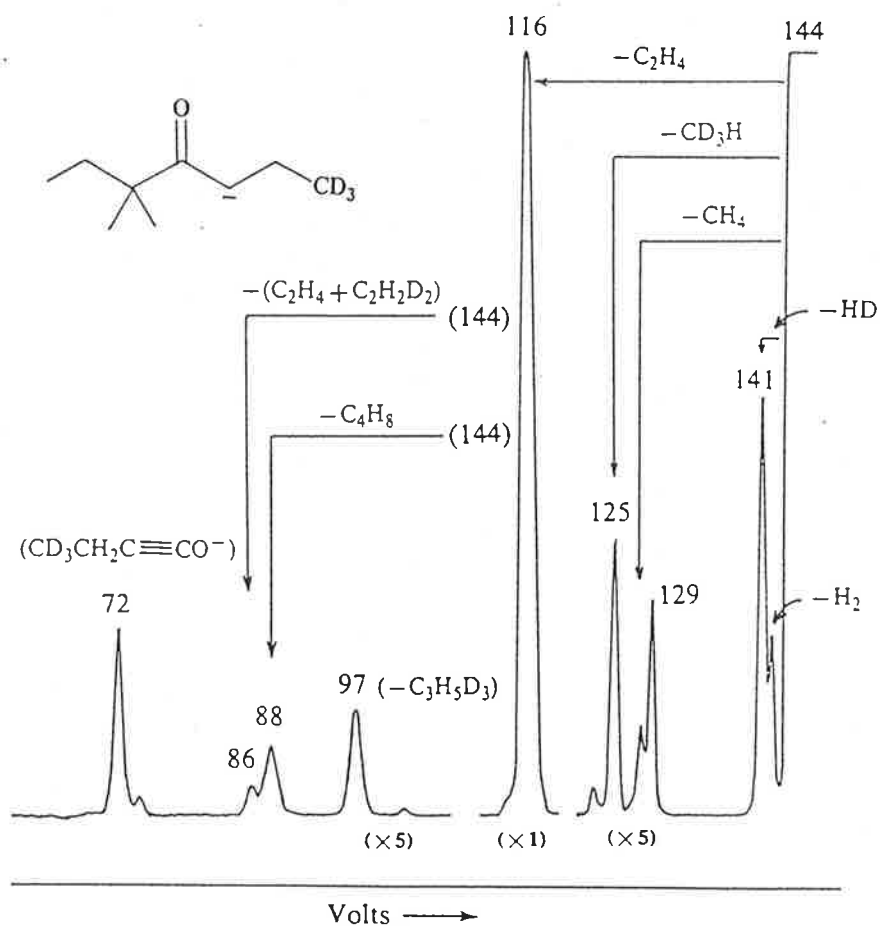


Figure 2.3: Collisional activation mass spectrum of the $[\text{M}-\text{H}^+]^-$ enolate ion derived from the compound $\text{EtCMe}_2\text{COCH}_2\text{CH}_2\text{CD}_3$.

Species Loss	Compounds						
	(1)	(2)	(3)	(5)	(6)	(7)	(8)
-H ₂	38	28		42	44	48	53
-HD			10				
-CH ₃ [•]	5	10	3	4	4	4	B
-CD ₃ [•]					2	3	B
-CH ₄	16	10	8	26	29	39	10
-CH ₃ D		13					22
-CD ₃ H					9	14	2
-CD ₄							14
-C ₂ H ₄	100	100	100	15	25	28	28
-C ₂ H ₂ D ₂				100	100		
-C ₂ D ₄						100	100
-C ₂ H ₅ [•]	A	A	A				
-C ₂ H ₃ D ₂ [•]				A			
-C ₂ H ₂ D ₃ [•]					A		
-C ₂ D ₅ [•]						18	25
-C ₃ H ₈	4	6	3		2		
-C ₃ H ₆ D ₂				3			
-C ₃ H ₃ D ₅						3	3
-C ₄ H ₈	5	7	3		3		
-C ₄ H ₆ D ₂			2	5	2	2	2
-C ₄ H ₄ D ₄						2	2
EtC ₂ O ⁻	13	9		5	5	5	6
MeCD ₂ CO ⁻			6				

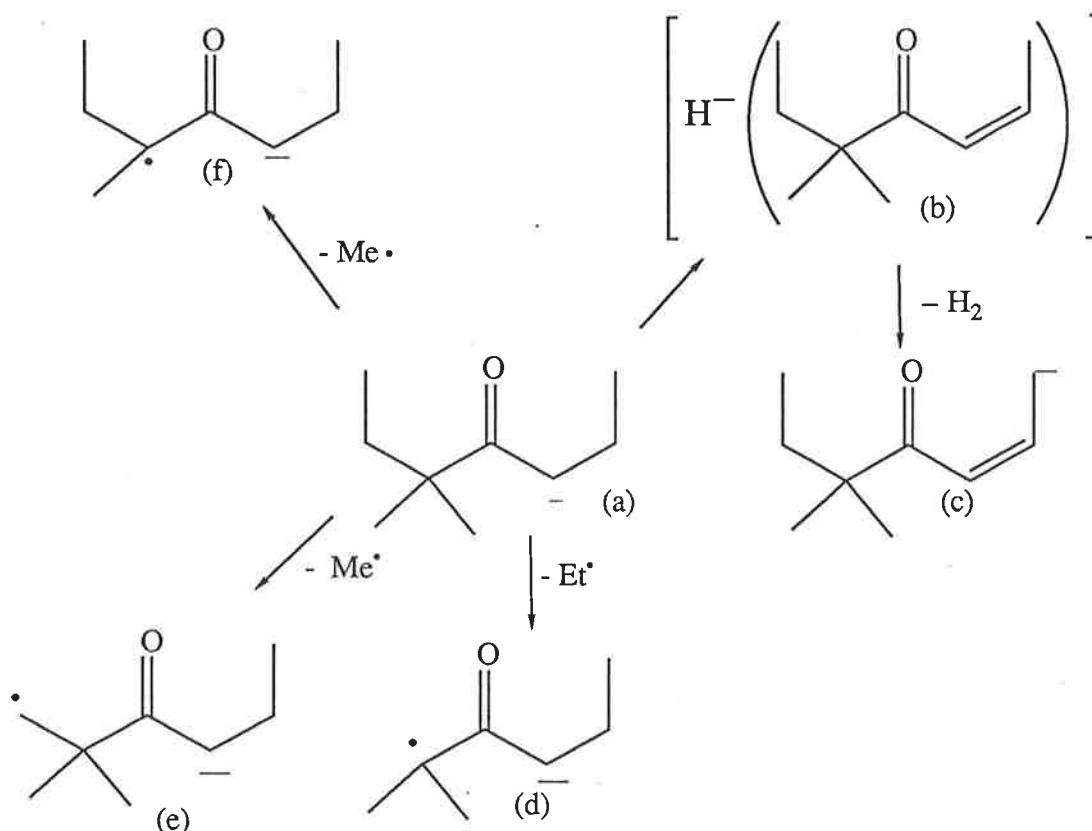
A Not Resolved. B Not resolved, but less than 5 % of base peak.

Table 2.5: Collisional activation mass spectra of enolate ions derived from the compounds (1) to (8) listed in *Table 2.4*. For the spectrum of compound (4), see *Figure 2.3*.

2.3.1 The Losses of H₂, Me[•] and Et[•]

The loss of H₂ follows a similar mechanism for that reported for 3-ethylpentan-2-one⁹⁷ and heptan-4-one⁹¹, and is also analogous to the reported stepwise loss of H₂ from alkoxides⁸⁷. The enolate ion a (*scheme 2.10*) produces a hydride ion complex b which may then undergo allylic deprotonation to form the product ion c. This loss is specific except in the one case, illustrated in *figure 2.3*. The deprotonation step for the reaction b → c is the rate determining step. This result is confirmed by comparison of the losses of H₂ from the ion derived from compound (1) (*Table 2.5*) and the loss of HD from the ion derived from compound (6) (*Table 2.5*). The ratio of this loss is 4:1. Thus the introduction of deuterium at the terminal carbon increases the activation energy of the rate determining step (ΔE^{\ddagger}_D) such that the expected loss of HD is discriminated against. The discrimination is so pronounced that a second competing process involving the loss of H₂ is observed in *Figure 2.3*. The mechanism for this latter process is unknown.

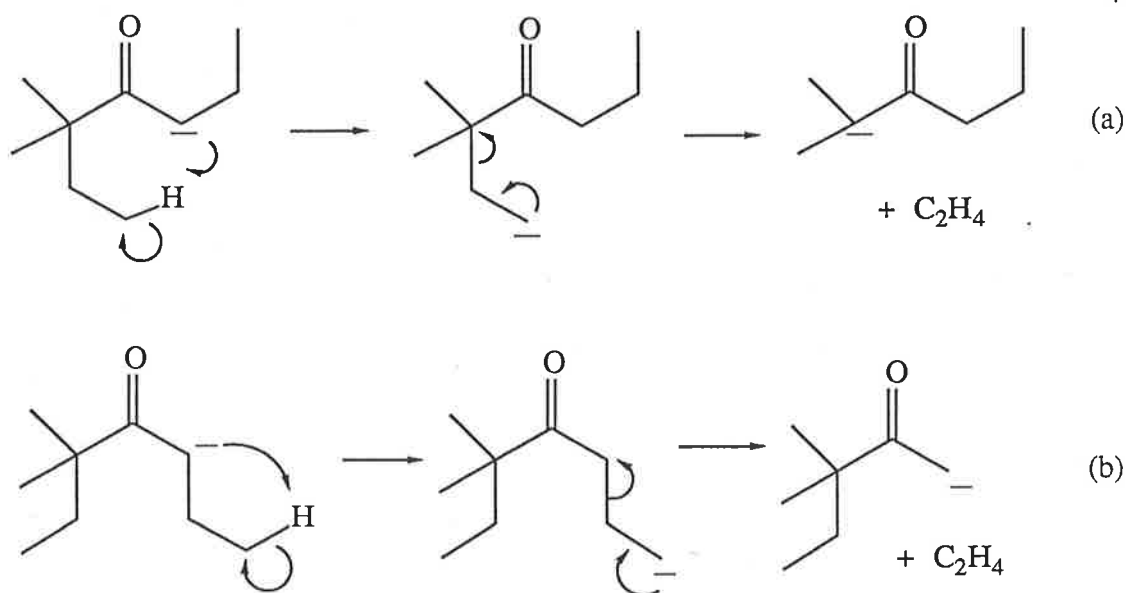
The losses of Me[•] and Et[•] are standard reactions involving a simple radical cleavage of a bond to form radical anion products^{91,97}, the mechanisms for these processes are illustrated in *Scheme 2.10* (a → d) and (a → f). There is however a second loss of Me[•] which involves loss of a C1 methyl group (*scheme 2.10* a → e), this loss seems to be unusual in that the radical product ion e is not resonance stabilized.



Scheme 2.10

2.3.2 The Loss of Ethene

The peak corresponding to loss of C_2H_4 in the CA mass spectrum of the 3,3-dimethylheptan-4-one enolate ion is the base peak of the spectrum. The peak has no fine structure, is steep sided with a round top, and is very wide having a width at half height of 89 V. This corresponds to an energy release of 0.39 eV, which suggests that the reaction has a reverse energy barrier. The value is similar to that of 0.42 eV obtained for the loss of C_2H_4 from the heptan-4-one enolate anion⁹¹, and suggests the mechanism is stepwise with the first step being rate determining (*scheme 2.11 (a)*) [c.f. *equation (6) page 27*]. This process occurs exclusively in the spectra of compounds labelled in either the 5, 6 or 7 positions [compounds (2), (3) and (4) *Table 2.5* and *Figure 2.3*].



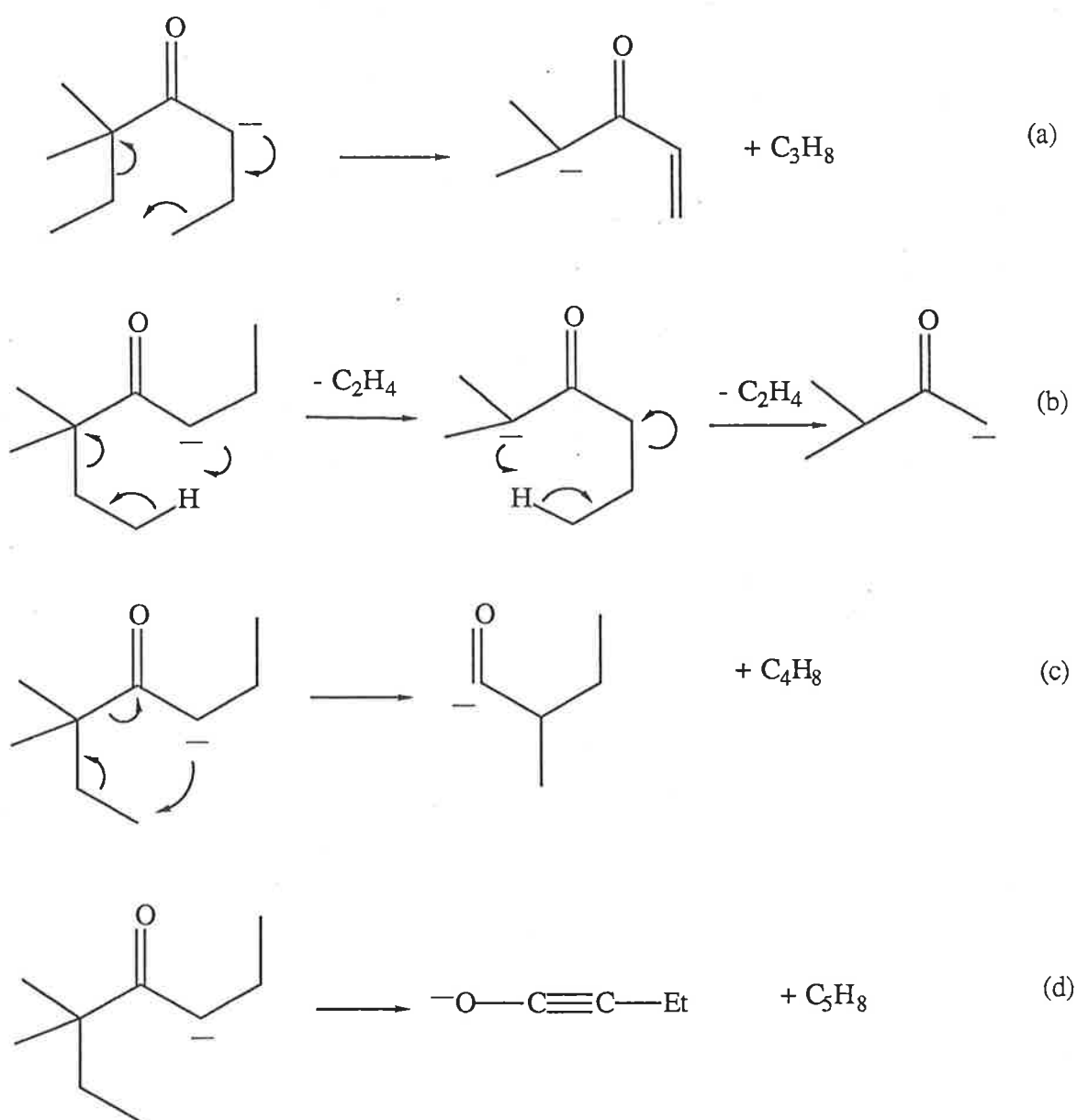
Scheme 2.11

The situation becomes more complex when deuterium is introduced at the 1 or 2 positions. For example $\text{CD}_3\text{CH}_2(\text{Me})_2\text{CO}\bar{\text{C}}\text{HEt}$ eliminates $\text{C}_2\text{H}_2\text{D}_2$ and C_2H_4 in the ratio of 100:25, with the two peaks having widths at half height of 89 and 78 eV respectively. It is suggested that this result is due to the increased activation energy for the deprotonation step, arising from the isotope effects caused by the introduction of deuterium at position (1). This increase in "activation energy" is discriminating against the loss of $\text{C}_2\text{H}_2\text{D}_2$, such that the extra energy required to overcome the barrier has led to an alternative process (*Scheme 2.11 b*) becoming viable.

2.3.3 The Losses of C_3H_8 , C_4H_8 , and C_5H_{12}

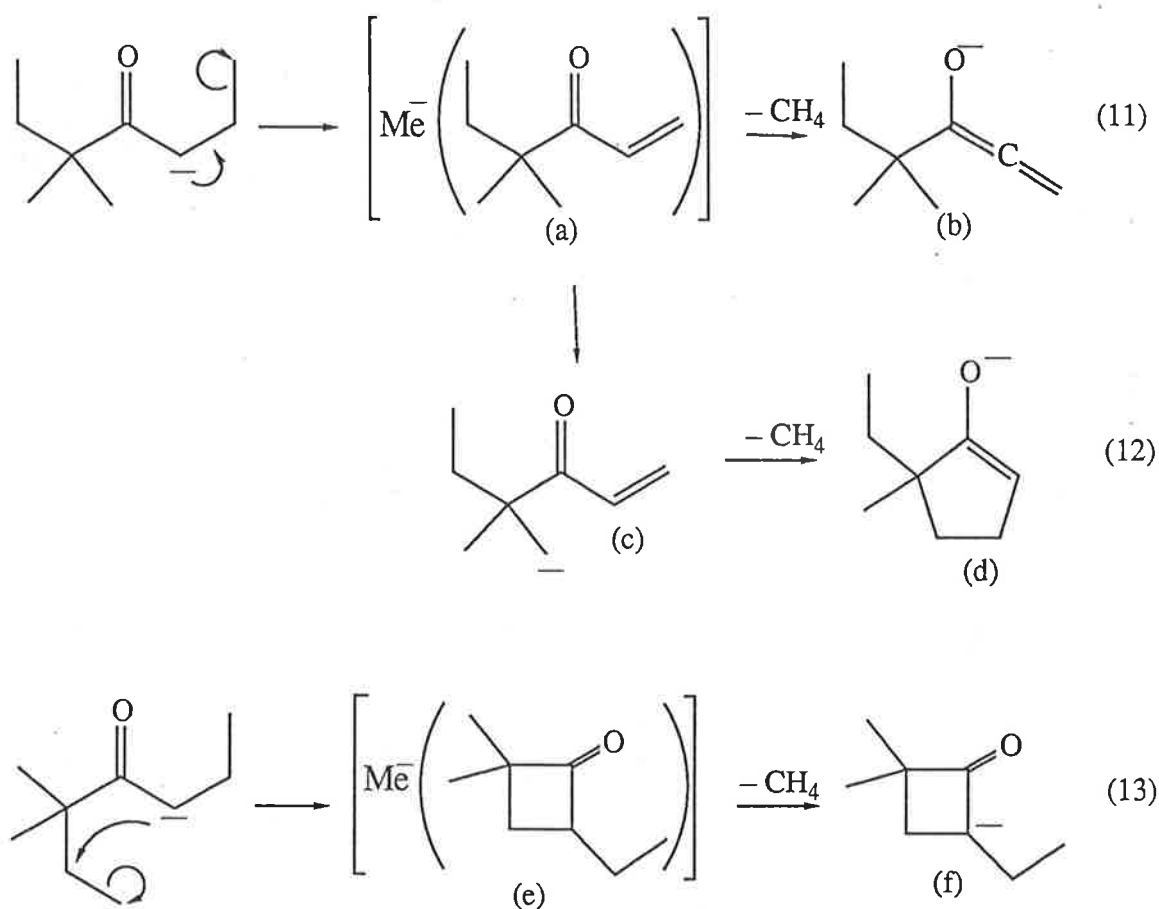
Examination of *Figure 2.3* together with the spectrum from $\text{CD}_3\text{CD}_2(\text{Me})_2\text{CCO}\bar{\text{C}}\text{HCH}_2\text{CH}_3$ (*Table 2.5*) shows that the loss of C_3H_8 involves the elimination of the C1, C2 ethyl group together with the C7 methyl group. This elimination is rationalized in *scheme 2.12(a)*, and is analogous to

processes from heptan-4-one⁹¹ and 3-ethylpentan-2-one (scheme 2.5 page 37) enolate anions. There are two distinct and competitive losses of C_4H_8 . These can be seen in Figure 2.3. One loss involves the sequential losses of two C_2H_4 units from either end of the ion, and is rationalized in scheme 2.12 (b). It is likely that both losses of C_2H_4 involve mechanisms similar to that already described for the loss of ethene (i.e. the formation of an incipient anion c.f. scheme 2.11a).



Scheme 2.12

The second loss of C_4H_8 involves migration of the methyl group at position 1 together with elimination of C2 and C3 with their associated substituents (see Table 2.5). It is not known whether the methyl group migrates to C5 or oxygen, a possible mechanism is that shown in Scheme 2.12 (c). The elimination of C_5H_{12} to produce the ion $EtC\equiv CO^-$ is a standard reaction^{91,97,98} type for enolate anions and is illustrated in Scheme 2.12 (d) (c.f. Scheme 2.6 page 37).



Scheme 2.13

2.3.4 The Loss of Methane

The inability of the 3,3-dimethylheptan-4-one ion to lose methane (and hence

excess energy) through facile six centred transition state processes [c.f. 3-ethylpentan-2-one (*scheme 2.3 b page 33*) and heptan-4-one (*equation 7 page 28*)] is due to the lack of hydrogens at C3. However, methane is lost by three alternative competing processes; the spectra of compounds (4), (6) and (8) (*Figure 2.3, Table 2.5*) illustrate the nature of these processes. The various losses of methane involve the methyl groups at position 1 and 7. The major loss involves the methyl group at position 7 (*equation 11 Scheme 2.13*) and a "solvated methyl anion complex" a is a likely intermediate in this pathway. The methyl anion of this ion complex a may then abstract the C5 vinyl proton from the neutral moiety to give the product ion b.

The second loss of methane involves the methyl group from position 7, together with one of the gem dimethyl hydrogens (*equation 12 Scheme 2.13*). It is proposed that the reaction proceeds through ion complex a to c. The product ion c which is formed from this reaction is non stabilized and may spontaneously undergo a "Michael addition" to form the more stable ion d. There is however no direct evidence for the formation of an ion of this structure. The third loss of methane (*equation 13 Scheme 2.13*) involves the methyl at C-1 together with a hydrogen at C5. The ion complex e (*Scheme 2.13*) is suggested as an intermediate for this process, with the product ion f forming when the methyl anion deprotonates α to the carbonyl group.

CHAPTER 3

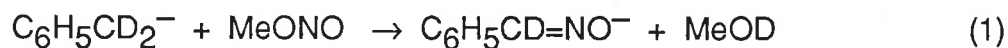
Collision Induced Dissociations of Substituted Benzyl Negative Ions.

3.1 An Introduction to Benzyl Negative Ions

In Chapter 2, the basic fragmentations of stabilized enolate ions were considered. Another system which may form "stable" carbanions by deprotonation are molecules related to toluene.

The benzyl/tropylium cation story is one of the most researched in gas phase ion chemistry^{99,100}. The tropylium cation is the more stable of the two ions, and its formation from the benzyl cation is accompanied or preceded by hydrogen and carbon randomization. Randomization reactions also occur for simpler aromatic systems, e.g. the benzene^{101,102} and pyridine radical cations¹⁰³, where H and C scrambling occur by different mechanisms¹⁰¹⁻¹⁰³, with H scrambling being the faster reaction¹⁰⁴.

The structure and reactivity of $C_7H_7^-$ species are also of interest. There are (at least) three discrete $C_7H_7^-$ ions; $PhCH_2^-$, cyclo $C_7H_7^-$ (from deprotonation of cycloheptatriene) and a third isomer formed by deprotonation of norbornadiene¹⁰⁵⁻¹⁰⁷. The three isomers may be distinguished by their exchange reactions with MeOD ($PhCH_2^-$ and cyclo $C_7H_7^-$ incorporate up to two and seven deuteriums respectively¹⁰⁵), and by their infrared photochemistry¹⁰⁶. Cyclo- $C_7H_7^-$ rearranges to $PhCH_2^-$ when HO^- is allowed to react with cycloheptatriene, and it has been suggested that the rearrangement proceeds through the intermediacy of a $[C_7H_7^- (H_2O)]$ ion complex¹⁰⁷.



Aryl H scrambling reactions are not as well known (or understood) for negative ions as they are for positive ions. The first observations were for ions $(\text{Ph})_n\text{X}^-$ ($n=3$, $\text{X} = \text{As}$ and $n = 4$, $\text{X} = \text{Si}$)^{108,109}; more recently for benzoyl enolate anions⁹² and ions PhOCHR ($\text{R} = \text{alkyl, allyl or aryl}$)¹¹⁰. However there are also cases where a loss involving an aryl hydrogen is specific, e.g. from the molecular anions of fluoroacetanilides¹¹¹, benzil monoxime¹¹² and from thiophenoxides¹¹³. Finally, the methylene hydrogens of PhCH_2^- retain their positional identity during the ion molecule reaction shown in *equation 1*¹¹⁴.

In recent years NICI mass spectrometry has become increasingly used in the determination of aromatic residues¹¹⁶⁻¹²². However little is known about the fragmentation patterns of aromatic anions. The collision induced mass spectrum of a polyatomic negative ion is often a structural fingerprint of that ion¹¹⁵. In this chapter the collision induced dissociations of the substituted benzyl systems $\text{Ph}\bar{\text{C}}(\text{Et})_2$, $\text{Ph}_2\bar{\text{C}}\text{H}$ and Ph_3C^- are reported. Two questions have been addressed:- i) what are the characteristic fragmentations of alkyl and aryl substituted benzyl negative ions, and ii) does hydrogen or carbon scrambling occur prior to or during these fragmentations?

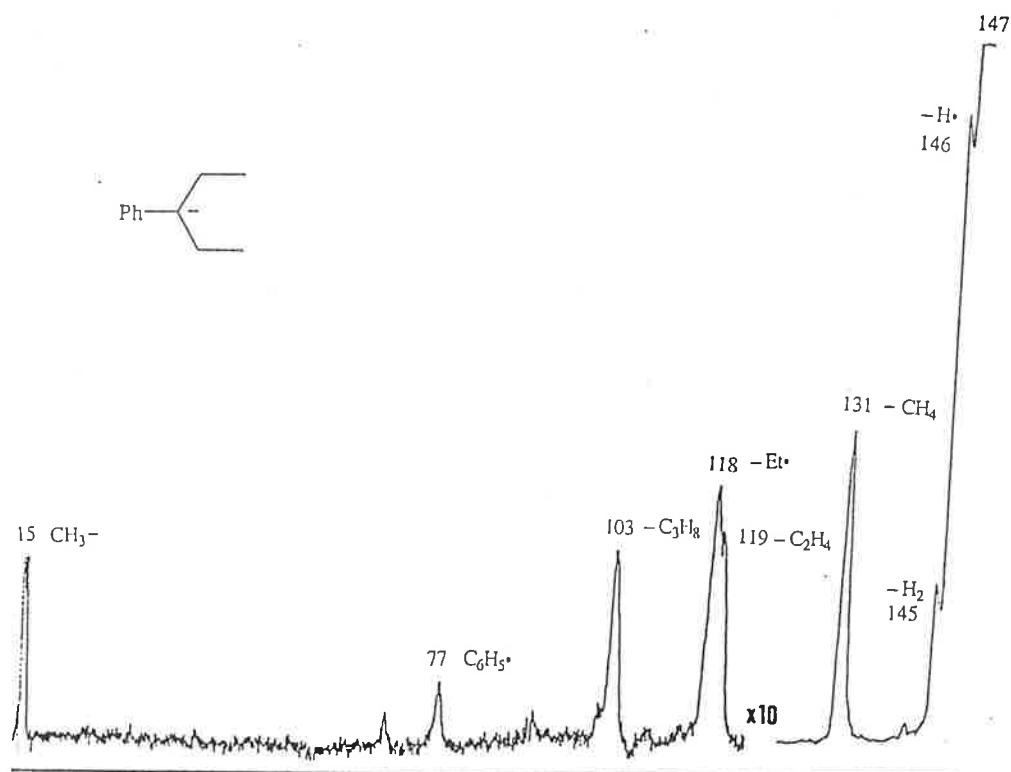


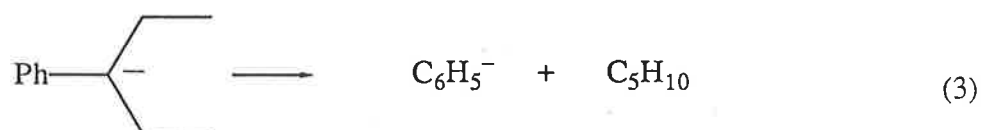
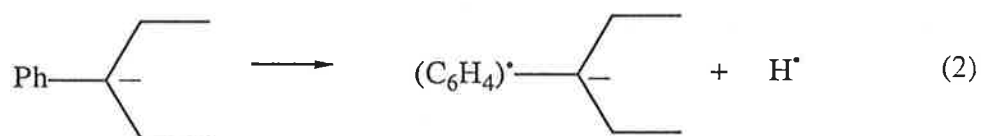
Figure 3.1: Collisional Activation Mass Spectrum of the deprotonated 3-Phenylpentane anion.

3.2 Collision Induced Dissociations of the 3-Phenylpentane Anion.

All compounds used for this study are listed in *Table 3.1*. The CA mass spectrum of the ion $\text{Ph}\bar{\text{C}}\text{Et}_2$ is shown in *Figure 3.1*; the spectra of its labelled derivatives are listed in *Table 3.2*.

The symmetrical ion $\text{Ph}\bar{\text{C}}\text{Et}_2$ was chosen for study in order that fragmentations of the side chains could be investigated with the aid of intramolecular isotope effects. The ion $\text{Ph}\bar{\text{C}}\text{Et}_2$ loses $\text{H}\cdot$, H_2 , CH_4 , ($\text{C}_2\text{H}_4 + \text{H}\cdot$), C_2H_4 , C_3H_8 and forms the ions CH_3^- and C_6H_5^- (*Figure 3.1*). With the exception of the loss of $\text{H}\cdot$ and the formation of C_6H_5^- , the majority of

fragmentations of the ion $\text{Ph}\bar{\text{C}}\text{Et}_2$ may be rationalized through the intermediacy of ion complexes.



Scheme 3.1

The major fragmentation of the 3-phenylpentane anion is the loss of a hydrogen atom from the phenyl ring, and the overall reaction is illustrated in *equation 2*. Specific deuterium labelling at the ortho and para positions of the aromatic ring shows the loss of both H^\bullet and D^\bullet from the ring (*Table 3.2*); whether this loss of H^\bullet (D^\bullet) occurs randomly from the ring or whether it is lost from a specific position following H randomization is not known. Whatever the mechanism there is a pronounced deuterium isotope effect [$\text{H}/\text{D} > 4$] operating for the process. Apart from this process and the minor formation of C_6H_5^- illustrated in *equation 3*, all other fragmentations may be rationalized as occurring through the intermediacy of ion complexes.

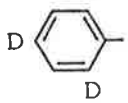
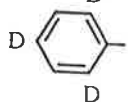
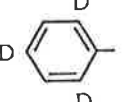
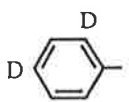
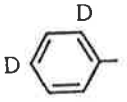
$ \begin{array}{c} R^1 \quad R^4 \\ \diagdown \quad / \\ \text{C} \\ / \quad \diagdown \\ R^2 \quad R^3 \end{array} $					
	R^1	R^2	R^3	R^4	$\dagger C$
I	Ph	H	Et	Et	12
II	Ph	H	Et	$\text{CH}_2^{13}\text{CH}_3$	12
III	Ph	H	Et	CH_2CD_3	12
IV	Ph	H	Et	CD_2CH_3	12
V	C_6D_5	H	Et	Et	12
VI		H	Et	Et	12
VII	Ph	H	H	Ph	12
VIII	Ph	H	H	Ph	13
IX	Ph	D	D	Ph	12
X	C_6D_5	H	H	Ph	12
XI		H	H	H	12
XII	Ph	H	Ph	Ph	12
XIII	Ph	H	Ph	Ph	13
XIV	C_6D_5	H	Ph	Ph	12
XV		H			12

Table 3.1

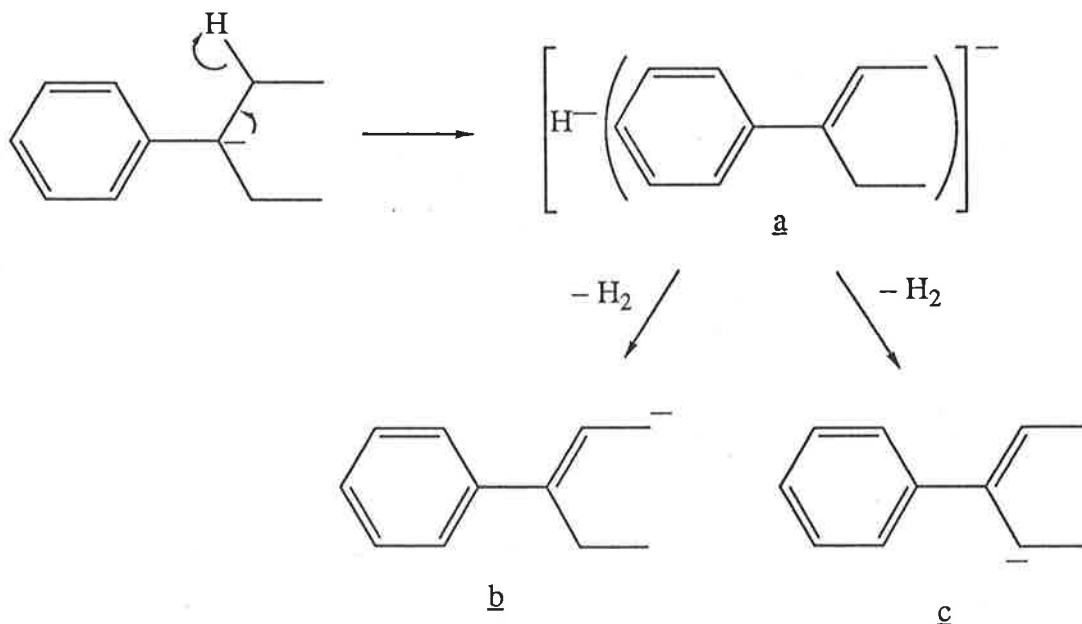
TABLE 3.2: Collisional activation mass spectra of labelled analogues of deprotonated 3-phenylpentane.

Loss	(2) Ph \bar{C} (Et)(CH ₂ ¹³ CH ₃)	(3) Ph \bar{C} (Et)(CH ₂ CD ₃)	(4) Ph \bar{C} (Et)(CD ₂ Me)	(5) C ₆ D ₅ \bar{C} Et ₂	(6) (C ₆ H ₂ D ₃) \bar{C} Et ₂
H \cdot	100	100	100		100
D \cdot		a	20 ^b	100 ^b	42 ^b
H ₂	25	a	20 ^b	100 ^b	42 ^b
HD			8		
CH ₄	29.0	28.0	51	3	45
¹³ CH ₄	28.9				
CH ₃ D		24.9		18	18
CD ₃ H		24.9			
C ₂ H ₄	a	a	a	2	2
C ₂ H ₃ D					
C ₂ H ₅ \cdot	4.0	6.1	5	8	6
¹² C ¹³ CH ₅ \cdot	3.8				
C ₂ H ₃ D ₂ \cdot			3.5		
C ₂ H ₂ D ₃ \cdot		2.7			

^a Small not resolved. ^b D \cdot = H₂ = 2 a.m.u.

Table 3.2 Continued.

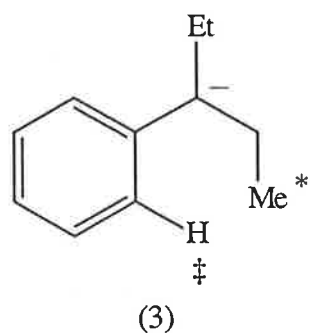
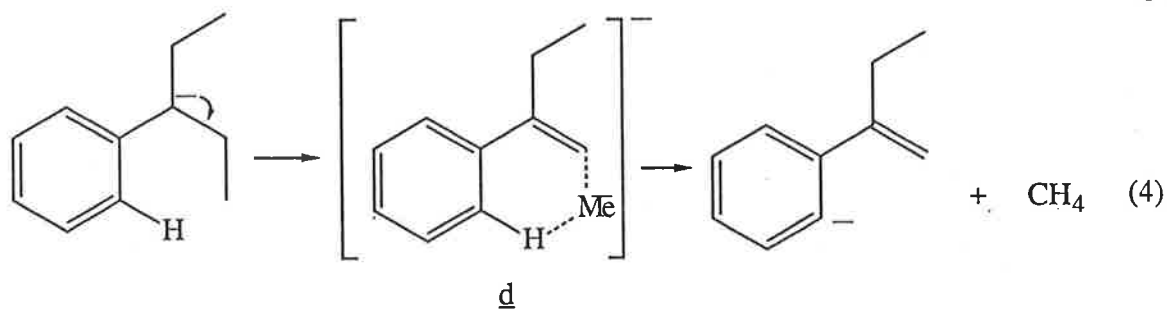
Loss	(2) Ph \bar{C} (Et)(CH ₂ ¹³ Me)	(3) Ph \bar{C} (Et)(CH ₂ CD ₃)	(4) Ph \bar{C} (Et)(CD ₂ Me)	(5) C ₆ D ₅ \bar{C} Et ₂	(6) (C ₆ H ₂ D ₃) \bar{C} Et ₂
C ₃ H ₈			2.5	3	4
¹² C ₂ ¹³ CH ₈	3			1.8	
C ₃ H ₆ D ₂					
C ₃ H ₅ D ₃		3			
Formation					
C ₆ H ₅ ⁻	1	1	2		
C ₆ D ₅ ⁻				1	
C ₆ H ₂ D ₃ ⁻					0.5
CH ₃ ⁻	1.1	1.5	1	2	3 3
CD ₃ ⁻		1.0			
¹³ CH ₃ ⁻	1.0				



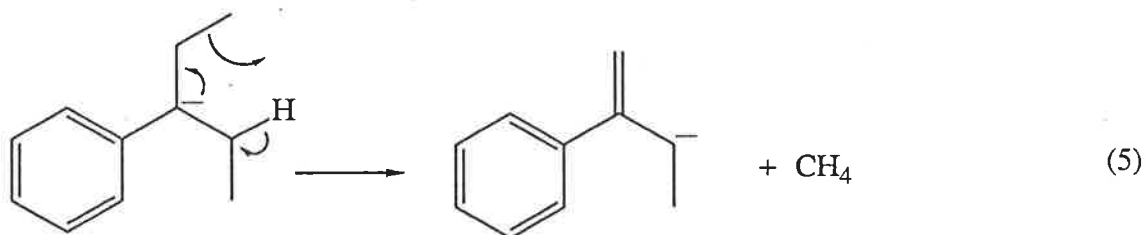
Scheme 3.2

The CA mass spectra of the ions $\text{Ph}\bar{\text{C}}(\text{Et})(\text{CH}_2\text{CD}_3)$ and $\text{Ph}\bar{\text{C}}(\text{Et})(\text{CD}_2\text{CH}_3)$ (Table 3.2) show that there are two competing 1,2 elimination reactions in operation for the loss of H_2 . These two processes may be rationalized by the intermediacy of ion complex **a** (Scheme 3.2). The hydride ion of the ion complex **a** may competitively deprotonate at two sites giving product ions **b** and **c**. Similar processes have been described before and are considered to be step-wise processes^{87,93}.

The loss of methane involves a terminal methyl group of the alkyl substituent together with a hydrogen from the aromatic ring as evidenced by the spectra of the five labelled derivatives (Table 3.2). It is suggested that the reaction proceeds through the intermediacy of ion complex **d** (equation 4 scheme 3.3). The D and ¹³C isotope effects (derived from the spectra of the ions $\text{Ph}\bar{\text{C}}(\text{Et})(\text{CH}_2\text{CD}_3)$, $\text{Ph}\bar{\text{C}}(\text{Et})(\text{CH}_2^{13}\text{CH}_3)$ and $\text{C}_6\text{D}_3\text{H}_2\bar{\text{C}}(\text{Et})_2$) for this process are listed alongside formula 3.



*	H/D	=	1.12 ± 0.01
$^{12}\text{C}/^{13}\text{C} = 1.00 \pm 0.01$			
‡	H/D	=	3.75 ± 0.2

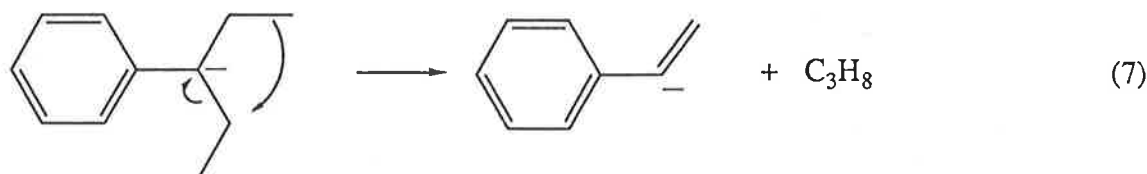
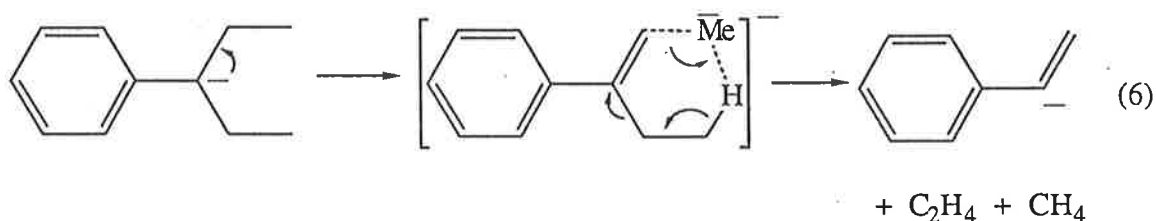


Scheme 3.3

The H/D value derived from $\text{C}_6\text{D}_3\text{H}_2\bar{\text{C}}(\text{Et})_2$ is obtained by assuming statistical randomization of H and D on the phenyl ring. These isotope effects clearly indicate that the deprotonation step of *equation 4* is rate determining, but the first step (the formation of \underline{d}) shows no ^{13}C isotope effect. Interestingly, the spectrum of $\text{C}_6\text{D}_5\bar{\text{C}}\text{Et}_2$ (*Table 3.2*) shows the loss of both CH_3D and CH_4 in the ratio of 18:3. Presumably in this case, the pronounced deuterium isotope effect operating for the deprotonation of the aromatic ring in *equation 4* discriminates against this reaction, and allows the operation of a second and minor loss of methane not observed in other spectra. It seems likely this

process would occur with the methyl anion deprotonating an allylic hydrogen (which is the most acidic hydrogen available to it); the mechanism shown in *equation 5* is proposed for this process. It is interesting to note that the loss of methane involving a six centred transition state (*equation 4*) is favoured over the methyl anion deprotonating the most acidic site (*equation 5*).

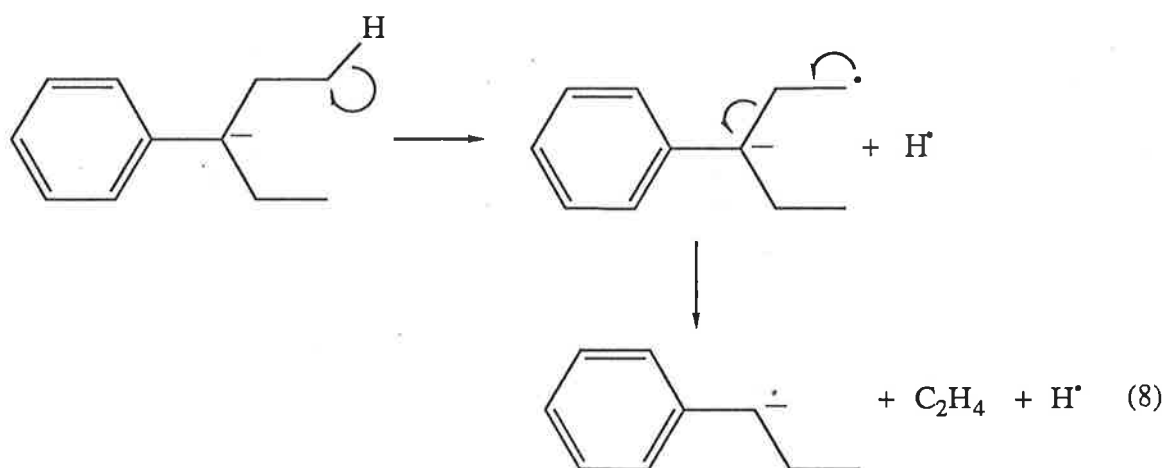
The minor loss of C_3H_8 involves the loss of a C1 methyl group from the pentane chain along with the C4, C5 ethyl group from the other end of the pentane chain. The reaction is believed to occur through a six centred elimination reaction of the type illustrated in *equation 6*, however the possibility of the alternative S_Ni reaction yielding $Ph\bar{C}=CH_2 + C_3H_8$ shown in *equation 7* cannot be discounted. The observation of the formation of Me^- anions in the spectra of 3-phenylpentane and derivatives (*Figure 3.1, Table 3.2*) is also suggestive of the formation of ion complexes in the fragmentations of these ions, since any ion complex formed is likely to dissociate to ion and neutral.



Scheme 3.4

Examination of the data in *Table 3.2* shows that the loss of C_2H_5 is unusual in that it does not involve simple loss of an ethyl radical. Isotopic labelling at the 1 and 2 positions of the pentane chain shows pronounced isotope effects; for

example the ion $\text{Ph}\bar{\text{C}}(\text{Et})(\text{CH}_2\text{CD}_3)$ loses C_2H_5 and CH_2CD_3 in the ratio 61:27, i.e. an isotope effect H/D of 2.25 is observed. It is proposed that this elimination corresponds to the loss of $\text{C}_2\text{H}_4 + \text{H}^\bullet$ (equation 8). The H/D isotope effect indicate that the first step (the loss of H^\bullet from the 1(5) position) is rate determining, the radical intermediate formed then eliminates C_2H_4 . An analogous reaction¹²³ has been observed previously for the loss of $\text{C}_2\text{H}_5^\bullet$ from $\text{Et}_2\text{CCO}_2^-$.



3.3 Collision Induced Dissociations of the Anions Derived from Diphenylmethane and Triphenylmethane

The CA mass spectrum of deprotonated diphenylmethane is shown in *Figure 3.2*; those of its labelled derivatives are listed in *Table 3.3*. The CA linked scan (E,B) spectra of the trityl anion and labelled derivatives are shown in *Figures 3.3 to 3.5*. In these cases the CA mass spectra showed unresolved peaks and linked scan spectra were required to achieve the appropriate resolution.

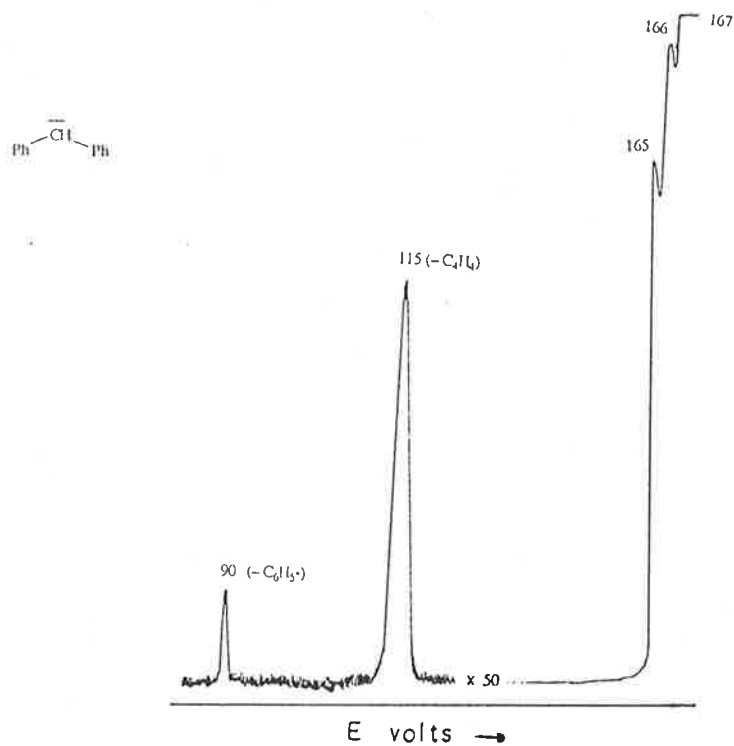


Figure 3.2: Collisional activation mass spectrum of deprotonated diphenylmethane

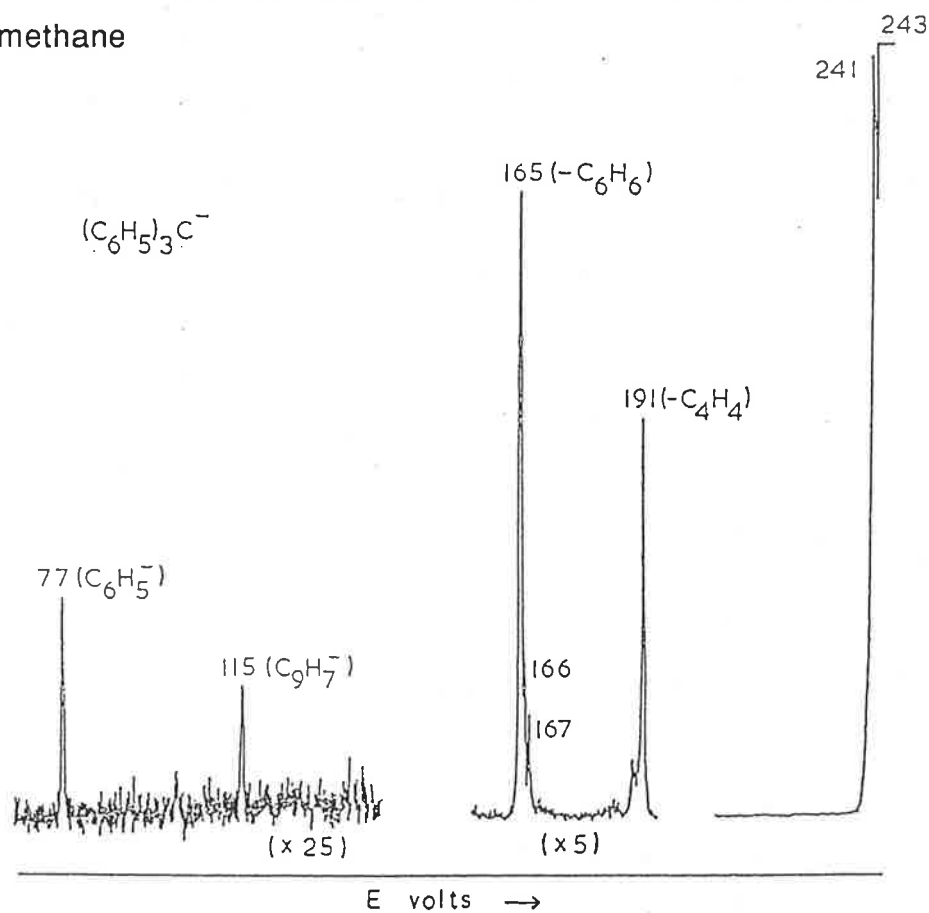


Figure 3.3: Collisional activation mass spectrum of Ph_3C^- [major peaks in the c.a. mass spectrum of $\text{Ph}_3^{13}\text{C}^-$ are m/z (loss) % 242 (H_2) 100; 192 (C_4H_4) 11; 168 (C_6H_4) 3; 167 ($\text{C}_6\text{H}_5^\bullet$) 4 ; and 166 (C_6H_6) 22].

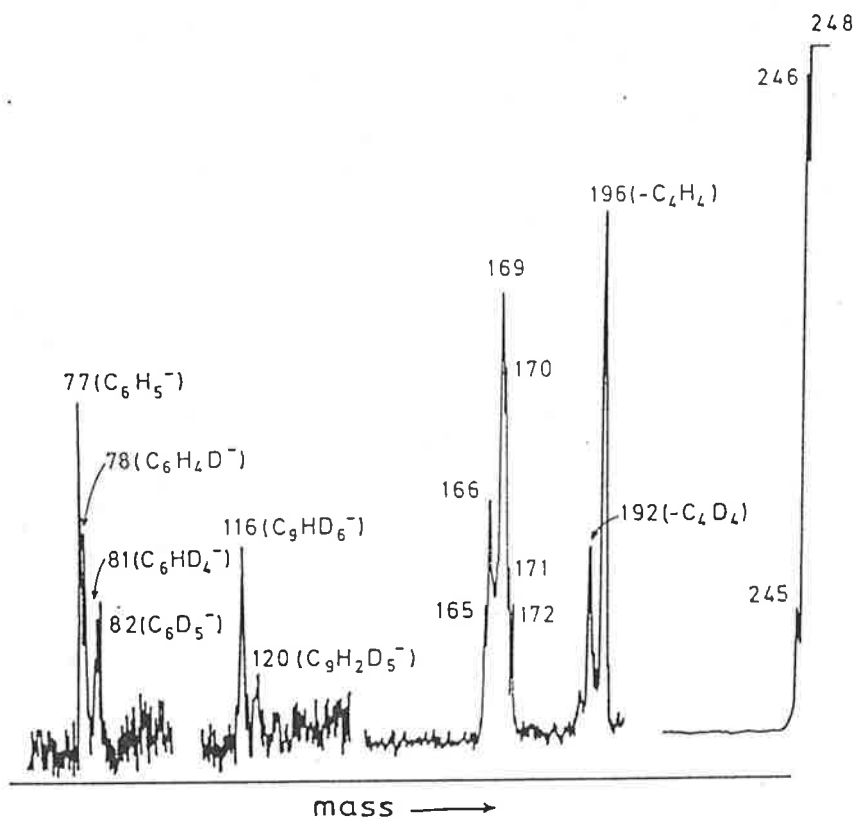


Figure 3.4: Collisional activation mass spectrum of $\text{Ph}_2(\text{C}_6\text{D}_5)\text{C}^-$

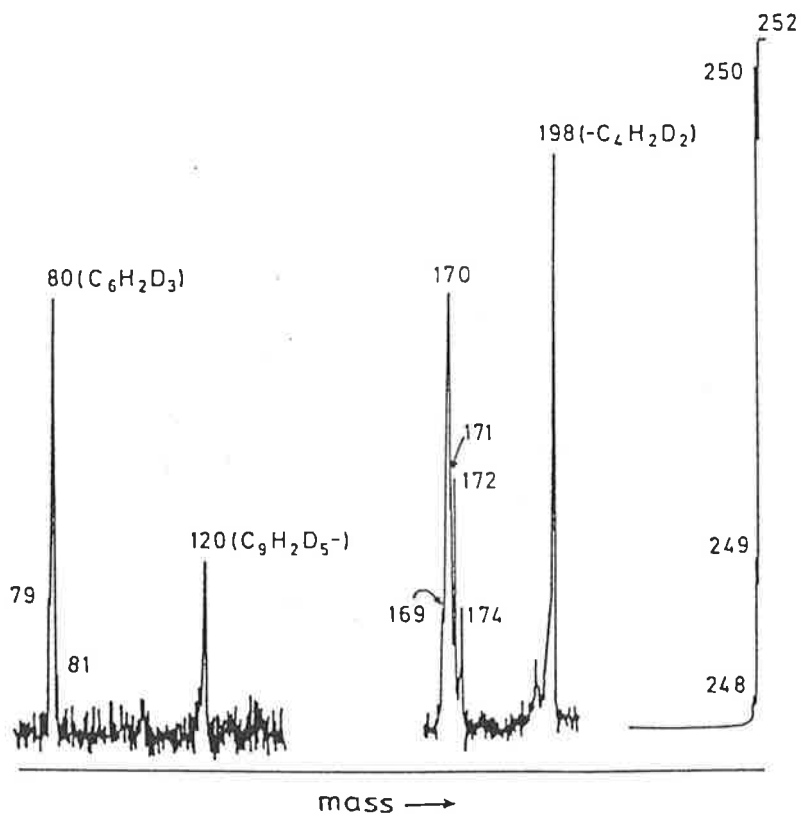


Figure 3.5: Collisional activation mass spectrum of $(\text{C}_6\text{H}_2\text{D}_3)_3\text{C}^-$

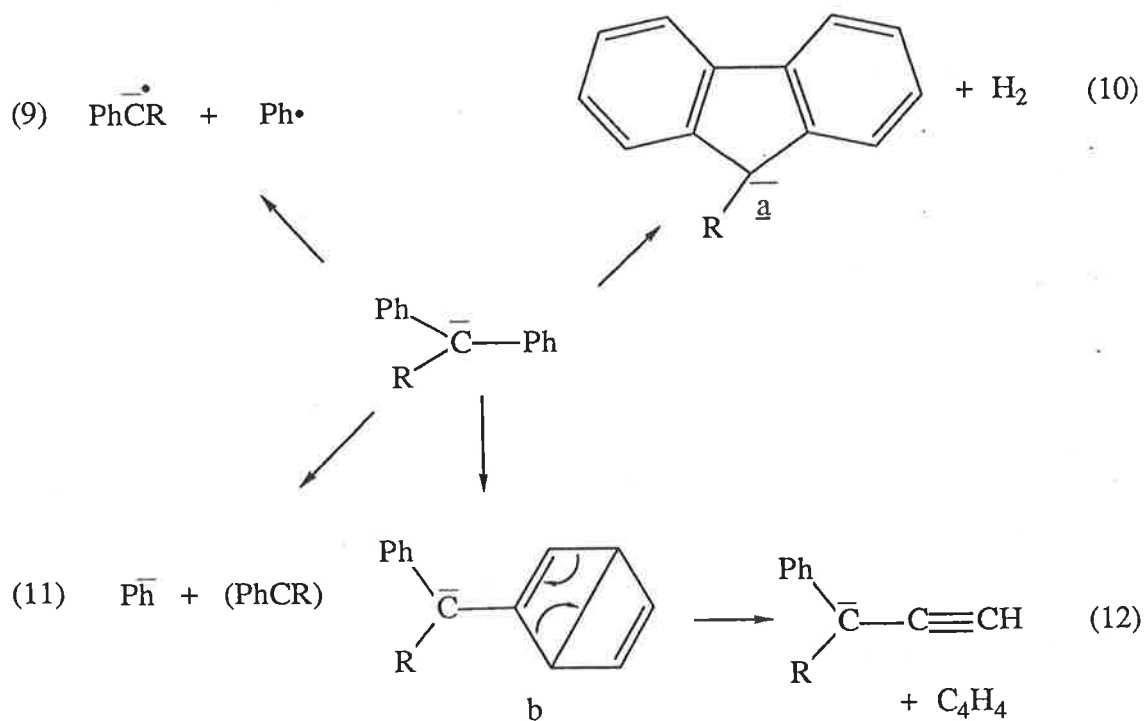
Table 3.3 Collisional Activation Mass Spectra of Ph_2CH^- and labelled derivatives.

Compound	Ion	Loss of									
		H^\bullet	D^\bullet	H_2	HD	C_4H_4	$\text{C}_4\text{H}_2\text{D}_2$	C_4D_4	$\text{C}_6\text{H}_5^\bullet$	$\text{C}_6\text{H}_2\text{D}_3^\bullet$	$\text{C}_6\text{D}_5^\bullet$
(7)	Ph_2CH^-	100		84		2			0.5		
(8)	$\text{Ph}_2^{13}\text{CH}^-$	100		80		1.5			0.2		
(9)	Ph_2CD^-	100	75 ^a	75 ^a		2			0.3		
(10)	$\text{Ph}(\text{C}_6\text{D}_5)\text{CH}^-$	100	36 ^a	36 ^a	12	1.01 ^b	0.70 ^b		0.16 ^c		0.15 ^c
(11)	$\text{Ph}(\text{C}_6\text{H}_2\text{D}_3)\text{CH}^-$	100	17 ^a	17 ^a	13	1.13 ^b	0.94 ^d		0.20 ^e	0.18 ^e	

^a Both H_2 and $\text{D}^\bullet = 2$ a.m.u. ^{b-c} An average of 10 individual scans.

Compound	Ion	Formation of		
		C_6H_5^-	$\text{C}_6\text{H}_2\text{D}_3^-$	C_6D_5^-
(7)	Ph_2CH	0.2		
(8)	$\text{Ph}_2^{13}\text{CH}^-$	0.2		
(9)	Ph_2CD^-	0.1		
(10)	$\text{Ph}(\text{C}_6\text{D}_5)\text{CH}^-$	0.05	0.05	
(11)	$\text{Ph}(\text{C}_6\text{H}_2\text{D}_3)\text{CH}^-$	0.05		0.05

The major fragmentations of $\text{Ph}_2\bar{\text{C}}\text{H}$ are losses of H^\bullet and H_2 , and for Ph_3C^- loss of H_2 . The loss of H_2 presumably occurs through similar mechanisms in both the diphenylmethane and triphenylmethane anion systems. The loss involves two separate phenyl groups, however it is preceded or accompanied by hydrogen scrambling within each phenyl group. Interpretation of the data for this process in the diphenyl methane system is complicated by the accompanying loss of D^\bullet in some spectra. Exact isotope effect measurements are not possible, however consideration of the data in *Table 3.3* and *Figures 3.3 to 3.5* shows that there is an H/D isotope effect of close to 3 operating for this process. The exact mechanism for this process is not known, but whatever the mechanism, it is likely that fluorenyl anions (*a equation 10*, $\text{R} = \text{H}$ or Ph) are product ions of these reaction. There is no direct evidence for the formation of these anions.



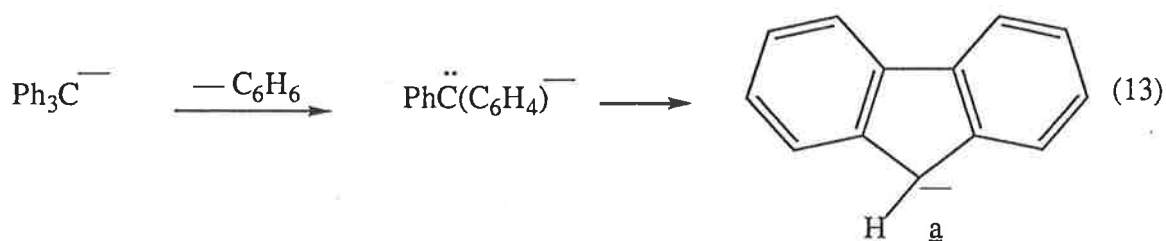
Scheme 3.5

The loss of Ph^\bullet and PhCR are minor processes and occur in both systems (i.e. from the diphenylmethane and triphenylmethane anions). These losses are simple cleavage reactions and are illustrated in *equations 9 and 11 (Scheme 3.5)*; in the case of the Ph_3C^- anion process 11 co-occurs with inter ring H transfer (see later).

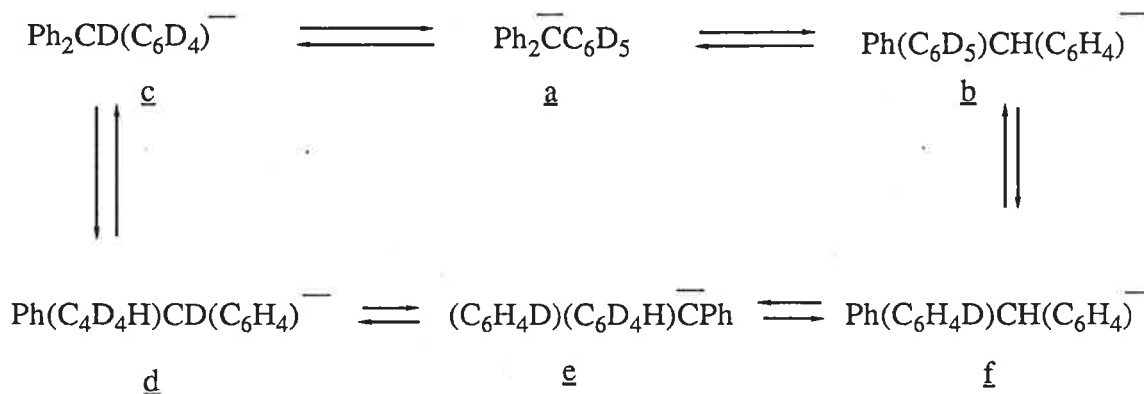
The characteristic fragmentation of $\text{Ph}_2\bar{\text{C}}\text{R}$ systems ($\text{R} = \text{H}$ or Ph) is loss of C_4H_4 . This reaction is specific; *there is neither evidence of the benzylic carbon inserting into a phenyl ring nor of intra or inter ring scrambling*. Both $\text{Ph}_2^{13}\text{CH}^-$ and $\text{Ph}_3^{13}\text{C}^-$ eliminate C_4H_4 ; *Figure 3.4* shows specific losses of C_4H_4 and C_4D_4 , while *Figure 3.5* shows specific loss of $\text{C}_4\text{H}_2\text{D}_2$. Isotope effects H/D of 1.45 and 1.42 (correction made for statistical factors where appropriate) are noted for respective losses of C_4H_4 and C_4D_4 from the ions $\text{Ph}(\text{C}_6\text{D}_5)\bar{\text{C}}\text{H}$ (*Table 3.3*) and $\text{Ph}_2(\text{C}_6\text{D}_5)\text{C}^-$ (*Figure 3.4*) respectively. It is proposed that this fragmentation occurs through a Dewar benzene intermediate b (*Scheme 3.5*, $\text{R} = \text{H}$ or Ph) and the overall reaction is illustrated in *equation 12*. Bowie and Stringer¹¹³ reported earlier the specific loss of C_4H_4 from PhS^- , but at that time offered no mechanism for the reaction because of the multitude of complex decompositions noted for the PhS^- system. It is probable that this decomposition of PhS^- is directly analogous to that shown in *equation 12*.

Other fragmentations observed for Ph_3C^- give rise to peaks at m/z 167, 166, 165, 115 and 77 (see *Figure 3.3*) which are formed respectively by losses of C_4H_4 , $\text{C}_6\text{H}_5^\bullet$, $(\text{C}_6\text{H}_4 + \text{C}_4\text{H}_4)$ and $\text{C}_{13}\text{H}_{10}$. The spectrum of $\text{Ph}_3^{13}\text{C}^-$ (see legend to *Figure 3.3*) shows that no fragmentation involves insertion of ^{13}C into

a phenyl ring to effect carbon scrambling. All of these fragmentations are interrelated: consider the loss of C_6H_6 (to form m/z 165) and the formation of $C_6H_5^-$ (m/z 77). The complex nature of these reactions can be seen in *Figures 3.4 and 3.5*.



It is proposed that the loss of C_6H_6 forms the fluorenyl anion \underline{a} and a possible simplified mechanism is suggested in *equation 13*. If $Ph_2(C_6D_5)C^-$ loses only C_6H_6 , C_6H_5D and C_6HD_5 , then peaks at m/z 170, 169 and 165 would be observed in *figure 3.4*. However peaks are observed at m/z 170, 169, 168, 166 and 165 corresponding to losses of C_6H_6 , C_6H_5D , $C_6H_4D_2$, $C_6H_2D_4$ and C_6HD_5 . In addition, *figure 3.4* shows formation of $C_6H_5^-$, $C_6H_4D^-$, $C_6HD_4^-$ and $C_6D_5^-$. There is therefore a process in which a single hydrogen (deuterium) is being transferred from one ring to another. It is suggested that this occurs by the process shown in *scheme 3.6*.

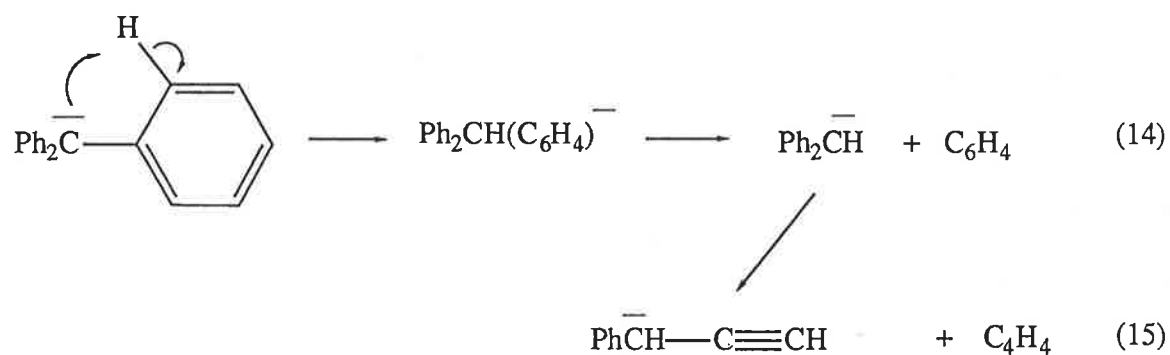


Scheme 3.6

Ion a (Scheme 3.6) may transfer an ortho H^+ or D^+ to form b and c; these ions transfer H^+ or D^+ across rings to form f and d each of which may form e. Assuming statistical elimination, a 1 : 2 ratio of a to e gives the following ratios :- $\text{C}_6\text{H}_5^- : \text{C}_6\text{H}_4\text{D}^- : \text{C}_6\text{HD}_4^- : \text{C}_6\text{D}_5^- = 100:50:50:50$, and m/z 165:166:168:169:170: = 15:20:20:100:26. Examination of Figure 3.4 shows a rough correlation with these values, but there is an appreciable deuterium isotope effect operating (e.g. see the abundances of m/z 166 and 170) making a quantitative assessment difficult. A similar treatment for $(\text{C}_6\text{H}_2\text{D}_3)_3\text{C}^-$ (Figure 3.5) will give only m/z 170 and 171 if no intra ring H/D scrambling occurs. The presence of m/z 169 (- C_6HD_5) shows that the loss of C_6H_6 from Ph_3C^- involves both intra ring H scrambling as well as specific H transfer between rings.

The minor loss of $\text{C}_6\text{H}_5^\bullet$ from Ph_3C^- yields m/z 166 (Figure 3.3), but the data in figures 3.4 and 3.5 do not indicate whether this reaction occurs following H scrambling. The loss of C_6H_4 from Ph_3C^- is likely to involve H transfer as shown in equation 14. However the positions of ring hydrogens

remain intact during the loss of C_6H_4 , as evidenced by specific losses of C_6D_4 and $C_6H_2D_2$ shown in figures 3.4 and 3.5 respectively. This indicates that the intra ring H scrambling which co-occurs with C_6H_6 loss, is concomitant with processes $\underline{d} \rightarrow \underline{e}$ (Scheme 3.3), not process $\underline{a} \rightarrow \underline{c}$.



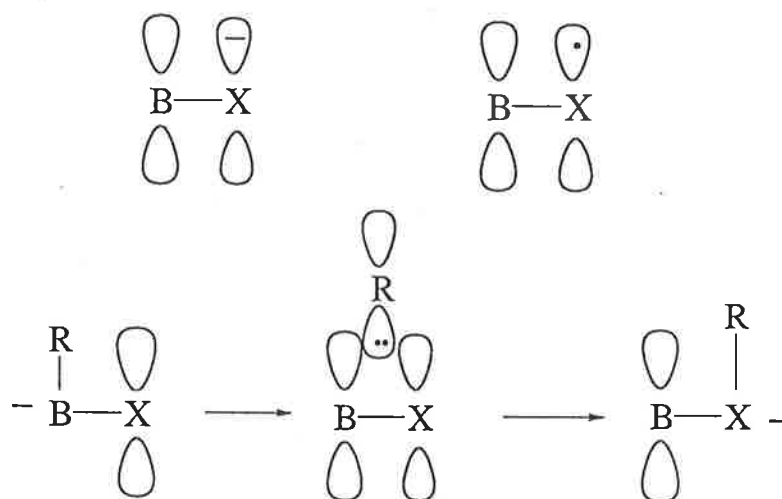
Finally, the formation of $C_9H_7^-$ (m/z 115, Figure 1) occurs by specific losses of (C_6H_4 and C_4H_4). The sequence of this consecutive process is not known; one possibility is shown in equation 15.

CHAPTER 4

Collision Induced Dissociations of some Organoborates and $[M-H^+]^-$ Ions derived from Organoboranes.

4.1 Introduction.

Organoboranes¹²⁴⁻¹²⁶ are extremely versatile and useful reagents for the synthesis of organic compounds. Surprisingly little is known about their mechanism of operation and the knowledge of their negative ion gas phase chemistry is sparse. A number of relationships exist between organoboranes compounds and organic compounds. For example, i) tricoordinate organoboranes BR_3 are isoelectronic with the corresponding carbocations R_3C^+ , and ii) the electronegativity of boron¹²⁷ has been estimated at 2.0, a value which is relatively close to that of carbon at 2.5.



Scheme 4.1

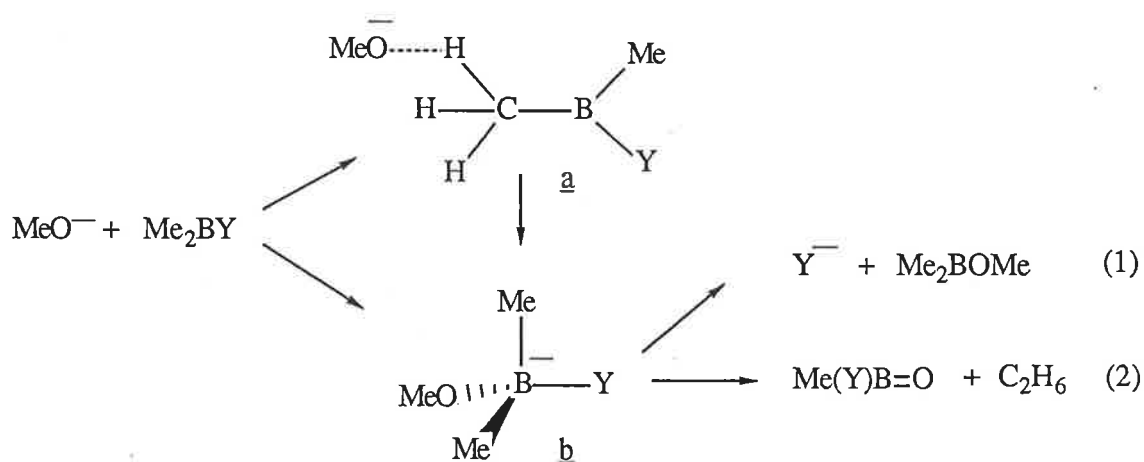
Perhaps the most useful feature of boron is the empty and readily accessible p orbital, making boranes electrophilic or Lewis acidic in nature.

This Lewis acidity leads to boranes forming complexes with neutral or negatively charged nucleophiles, and the formation of these complexes seems to be a key step in most of the ionic reactions of boranes^{124,128}. Many other compounds have vacant p orbitals and can form complexes with nucleophiles, but what makes boranes unique in nature is the ability of the boron p orbital to effectively participate in $p_{\pi}-p_{\pi}$ bonding with adjacent p or sp^n ($n = 1, 2, 3$) orbitals or with other second row elements such as C, N, O and F.

This $p_{\pi} - p_{\pi}$ overlap illustrated in *Scheme 4.1* is crucial to the reactivity of boranes in, i) allowing the stabilization of negative charges or radicals α to the boron centre, and ii) facilitating the characteristic 1,2 migrations common to organoboranes in condensed phase chemistry¹²⁹⁻¹³¹.

The majority of gas phase investigations of ions derived from organoboranes have utilized conventional electron impact, and dealt mainly with positive ions¹³²⁻¹³⁶. However, some aspects of the gas phase negative ion chemistry of boron hydrides and alkylboranes have been described. Rosen et al¹³⁷ observed the formation of negative ions from diborane (e.g. $B_2H_6^{-\bullet}$ and $B_2H_5^-$) in conventional mass spectra. Beauchamp¹³⁸⁻¹⁴⁰ has investigated the gas phase Lewis acidities of boranes by ion cyclotron resonance and observed deuterium transfer (from $DNO^{-\bullet}$), fluoride transfer (from $SF_6^{-\bullet}$ and SF_5^-) and the deprotonation of trimethylborane to form the ion $Me_2\bar{B}=CH_2$. Hayes et al^{141,142} have used ion cyclotron resonance mass spectrometry and *ab initio* calculations to investigate the reactions of alkoxides and mono solvated alkoxides with alkylboranes and alkoxyboranes. Their results suggested the mechanistic pathways shown in *Scheme 4.2*. Initial approach of the nucleophile can either, i) hydrogen bond to form ion complex a which readily

converts to tetrahedral species b over a small activation barrier, or ii) results in direct attack at the central boron to form b. Intermediate b generally lies some 200 kJ mol⁻¹ lower in energy than a, and the direct pathway to b is the more probable approach. Intermediate b decomposes principally to effect nucleophilic displacement (*equation 1*), but more complex reactions may also occur. Attempts were made by Hayes¹⁴¹ to verify the structure of the non decomposing adducts observed in the ion cyclotron resonance mass spectrometer (i.e. were they hydrogen bonded or tetrahedral adducts), however these attempts failed to produce any experimental evidence for the structure of the adducts.



Scheme 4.2

The aims of the studies reported in this chapter are as follows -

i) To investigate the characteristic collision induced dissociations of the $[\text{M}-\text{H}^+]^-$ ion derived from trimethylborane.

ii) As has been previously stated the formation of tetrahedral borates is a key step in the condensed phase reactions of nucleophiles with organo-boranes, therefore it is important to ascertain whether the adduct observed in

the ion cyclotron reaction of alkoxides with organoboranes and alkoxyboranes is indeed tetrahedral as the solution phase counterpart would suggest, or whether it is a hydrogen bonded structure.

iii) What are the characteristic fragmentation of these ions and other adducts formed from the gas phase reactions of some nucleophiles with organoboranes? In particular are the characteristic migrations common to organoborates in condensed phase chemistry observed in the gas phase?

4.2 Collision Induced Dissociations of the $[M-H^+]^-$ Ion derived from Trimethylborane

Trimethylborane may react with HO^- in a chemical ionization source to produce two stabilized ions. The HO^- ion may deprotonate the trimethylborane to produce the precursor ion shown in *equation 3* (*Scheme 4.3*), or alternatively may attack the boron atom to plausibly produce an intermediate, which decomposes to the precursor ion shown in *equation 4* (*Scheme 4.3, c.f. Scheme 4.2*). Collisional activation of these two ions show predominately loss of H_2 and CH_4 ; the overall reactions are illustrated in *equations 5-8* (*Scheme 4.3*). The collisional activation spectra derived from the product ions shown in *equations 3* and *4* are illustrated in *Figures 4.1* and *42*. The spectra of the corresponding deuterated precursors (*Table 4.1*) confirm that the major losses of H_2 and CH_4 occur to form ions of atomic composition consistent with the product ions structures shown in *equations 5-8*. The spectra also show that deuterium isotope effects are operating for the various losses of H_2 and CH_4 (see *Table 4.1*). For example the spectrum of $(CH_3)(CD_3)\bar{B}=O$ shows the loss of CH_3D and CD_3H in a ratio of 1 : 1.16, similarly the spectrum of

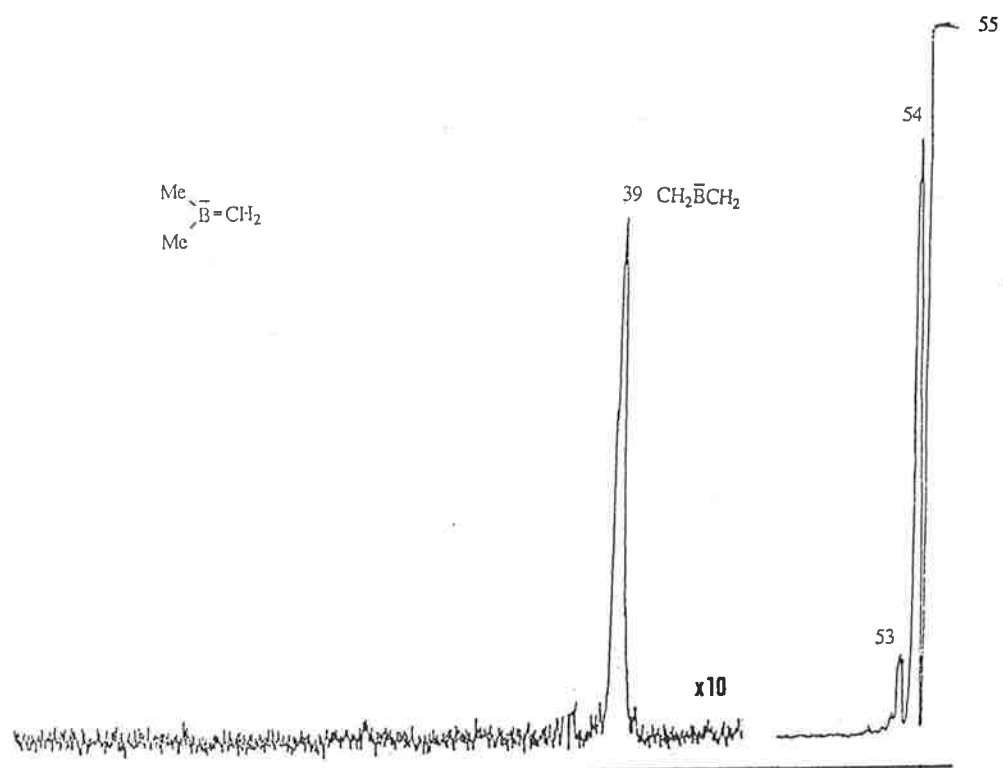


Figure 4.1 Collisional activation spectrum of the anion $\text{Me}_2\text{B}=\text{CH}_2^-$.

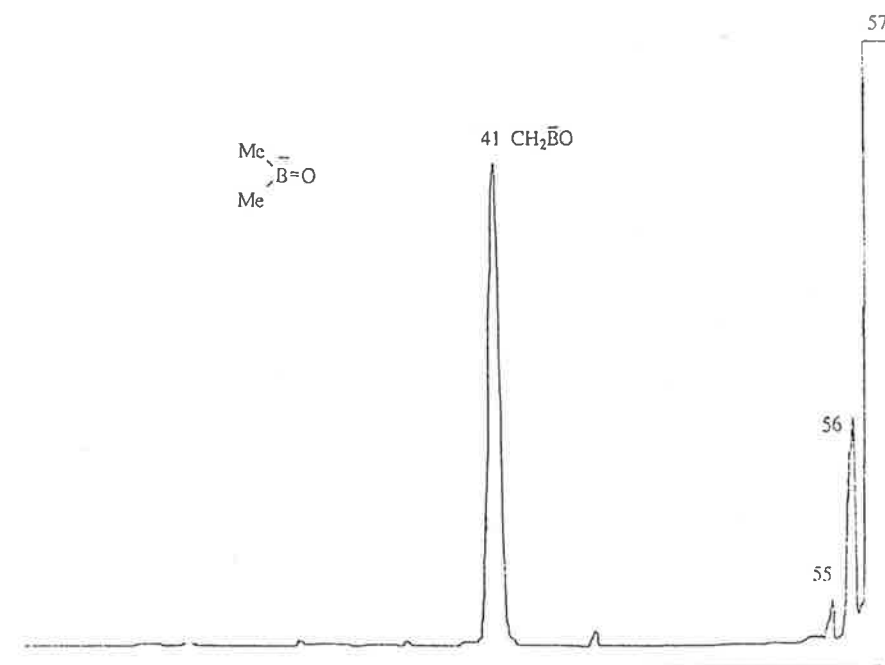
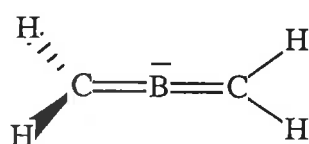


Figure 4.2 Collisional activation spectrum of the anion $\text{Me}_2\text{B}=\text{O}^-$.

Ion	H ⁺	D ⁺ /H ₂	HD	D ₂	Me ⁺	CD ₃ ⁺	CH ₄	MeD	CD ₃ H	CD ₄
Me(CD ₃) \bar{B} =CH ₂	100	89	12		1.2			1.8	4.0	
Me ₂ \bar{B} =CD ₂	100	64	14		2		9	1		
(CD ₃) ₂ \bar{B} =CH ₂	100	65	8	<1		1			1.2	3.8
Me(CD ₃) \bar{B} =O	50	29	24					25	29	

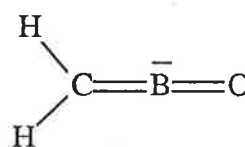
Table 4.1 Collisional Activation Mass Spectra of the (M-H⁺)⁻ or (M-D⁺)⁻ Ions Derived from Labelled Trimethylboranes

Attempts were made to confirm the structures of the product ions illustrated in *equation 5 - 8* using *ab initio* calculations[†], and the results are shown in formulae 4 to 9. Geometries were optimized using GAUSSIAN 86¹⁴⁵ at RHF/6-31+G* level ; energies were calculated using additional Moeller - Plesset correlations¹⁴⁶ (MP2) and genuine minima were confirmed by harmonic frequency analysis and by standard test of wavefunction stability by release of the RHF constraint.



$$\begin{aligned}
 E &= -103.04507 \text{ a.u.} \\
 BC &= 1.4345 \text{ \AA} \\
 CH &= 1.0820 \text{ \AA} \\
 BCH &= 122.9295^\circ
 \end{aligned}$$

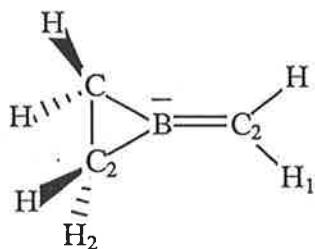
4



$$\begin{aligned}
 E &= -139.02607 \text{ a.u.} \\
 BO &= 1.23295 \text{ \AA} \\
 BC &= 1.4569 \text{ \AA} \\
 CH &= 1.0295 \text{ \AA} \\
 BCH &= 122.2031^\circ
 \end{aligned}$$

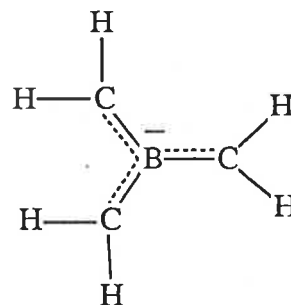
5

[†] Medium level (4-31 G) calculations on these systems were performed by the author; the final high level 6-31+G*/MP2 calculations were performed by Dr J.C. Sheldon (see acknowledgements).



E	= -142.2137 a.u.
BC ₁	= 1.4475 Å
BC ₂	= 1.5777 Å
C ₁ H ₁	= 1.0846 Å
C ₂ H ₂	= 1.0846 Å
C ₂ C	= 1.5592 Å
C ₁ BC ₂	= 123.2724°
BC ₁ H ₁	= 123.2724°
BC ₂ H ₂	= 121.6633°
H ₂ C ₂ BC ₁	= 76.2326°

6

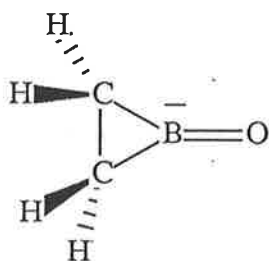


E	= -142.15996 a.u.
BC	= 1.5542 Å
CH	= 1.0860 Å
BCH	= 123.5845°

7

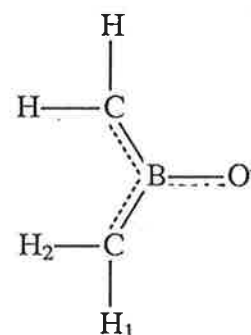
The loss of CH₄ from deprotonated trimethylborane would be expected to form an allene type structure, *ab initio* calculations show that such an ion exists in a stable state energy minimum, and the calculated structure of the bis methyleneborane ion is shown in formula 4; the calculations also show that the alternative configuration where the hydrogens are eclipsed is not stable. The corresponding loss of CH₄ from the borate ion Me₂B̄=O would be expected to give the oxa analogue [CH₂BO]⁻ which is isoelectronic with ketene, and the calculations suggest a structure 5 that reflects that resemblance. The spectrum of the deprotonated trimethylborane shows the loss of H₂ as one of the main peaks in the spectrum. The spectrum of the deuterium labelled derivative suggests that the ion could have the structure [B(CH₂)₃]⁻; if this ion exists it

must have radical character and is thus of considerable theoretical interest. *Ab initio* calculations were used in an attempt to elucidate the possible structures of this ion; the results suggest that the trimethyleneborane species $[\text{B}(\text{CH}_2)_3]^-$ does not adopt a singlet ground state in D_{3h} or lower symmetry but on modest distortion relaxes to the stable cycloborapropene ion 6. The calculations show that there is a D_{3h} structure 7, but it is a triplet state lying 141 kJ mol^{-1} above 6. The BC bond of 7 is calculated to be 1.544 \AA , a value intermediate between a single (B-C, $1.63 - 1.66 \text{ \AA}$), and a double bond (B=C, $1.43 - 1.46$). An analogous situation pertains for the oxa ion $[(\text{CH}_2)_2\text{BO}]^-$. The C_{2v} or C_2 versions of this ion do not give a stable state energy minimum, but relax to the cyclic species 8. The stable $[(\text{CH}_2)_2\text{BO}]^-$ structure is a triplet 9, 314 kJ mol^{-1} in energy above 8. Calculations of the bonding in 9 indicates CB bonds (1.519 \AA) with appreciable double bond character, whereas the BO bond (1.478 \AA) is essentially a single bond.



E	=	-142.15996 a.u.
BO	=	1.2641 Å
BC	=	1.5950 Å
CC	=	1.5807 Å
CH	=	1.0861 Å
OBC	=	150.2976°
BCH	=	124.9628°
HCBO	=	77.2241°

8

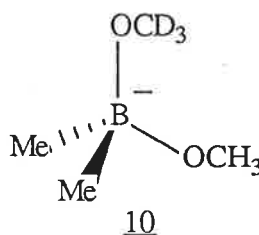


E	=	-178.04867 a.u.
BO	=	1.4784 Å
BC	=	1.5188 Å
CH ₁	=	1.0840 Å
CH ₂	=	1.0832 Å
OBC	=	118.5059°
BCH ₁	=	124.9628°
BCH ₂	=	121.2106°

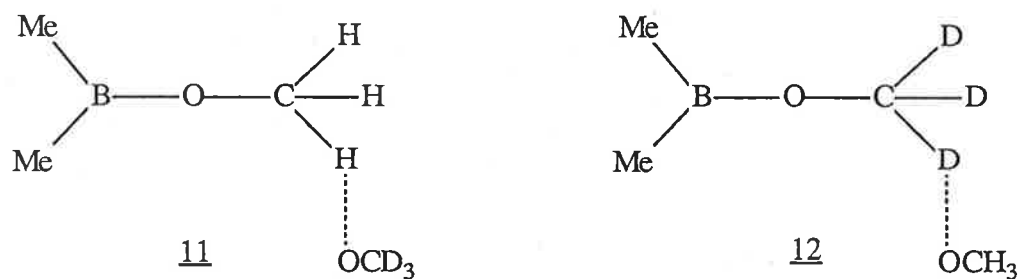
9

4.3 The Structure of Non-decomposing Boron Adducts.

Ab initio calculations¹⁴¹ suggest that two stable species, a and b (*Scheme 4.2 page 70*) may be formed when MeO^- is allowed to react with Me_2BY . These two ions should fragment differently on collisional activation. In order to determine whether the non decomposing adducts formed were hydrogen bonded or tetrahedral species a simple experiment was carried out. The reactions of Me_2BOCH_3 with CD_3O^- and Me_2BOCD_3 with CH_3O^- were carried out under identical conditions. Should the tetrahedral adduct 10 be formed then it will be identical for both reactions, i.e. a tetrahedral species with a C_2 axis of symmetry.



Thus in this case, the collisional activation spectra of the tetrahedral adducts formed by the reactions (Me_2BOCH_3 with CD_3O^-) and (Me_2BOCD_3 with CH_3O^-) should be identical. In contrast, should a hydrogen bonded species be formed, then the $\text{Me}_2\text{BOCH}_3 / \text{CD}_3\text{O}^-$ reaction should form the ion 11 and the $\text{Me}_2\text{BOCD}_3 / \text{CH}_3\text{O}^-$ reaction should form ion 12. Ions 11 and 12 should produce different collisional activation spectra; 11 will competitively form CD_3O^- and lose CD_3OH , while 12 will give MeO^- and eliminate CH_3OD .



If $\text{Me}_2\text{BOCH}_3/\text{CD}_3\text{O}^-$ gives a mixture of 10 and 11 and $\text{Me}_2\text{BOCD}_3/\text{CH}_3\text{O}^-$ gives a mixture of 10 and 12, the composite spectra of the two systems again should be different. The collisional activation spectra of the adducts ($\text{Me}_2\text{BOCH}_3/\text{CD}_3\text{O}^-$) and ($\text{Me}_2\text{BOCD}_3/\text{CH}_3\text{O}^-$) are identical within experimental error and the spectra are shown in *Figure 4.3*. In a similar way the collisional activation mass spectra of the product ions of ($\text{Me}_2\text{BOEt} / \text{C}_2\text{D}_5\text{O}^-$) and ($\text{Me}_2\text{BOC}_2\text{D}_5 / \text{C}_2\text{H}_5\text{O}^-$) ions are identical within experimental error (see *Table 4.2*). *These results are consistent with the stable adducts having tetrahedral geometry.* In this context it should be noted that the collisional activation spectra of the two corresponding silicon adducts¹⁴⁷ ($\text{Me}_3\text{SiOMe} + \text{CD}_3\text{O}^-$) and ($\text{Me}_3\text{SiOCD}_3 + \text{CH}_3\text{O}^-$) are different. Whether this is due to non equilibration of equatorial and apical substituents in a trigonal - bipyramidal intermediate or to the formation of ion complexes analogous to 11 and 12 is not known. The important observation is that the two spectra are different, whereas the spectra of the analogous boron ions are the same.

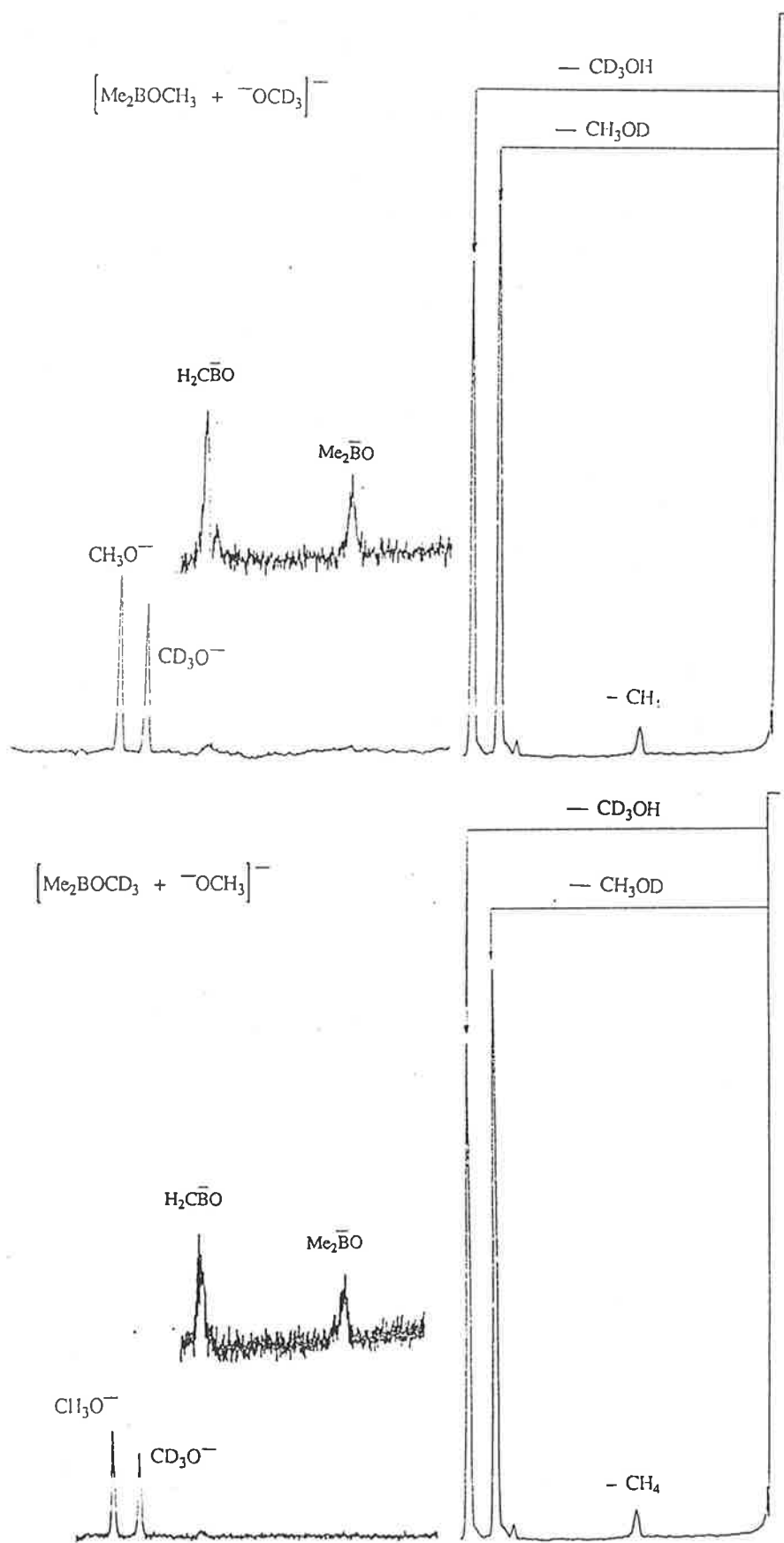


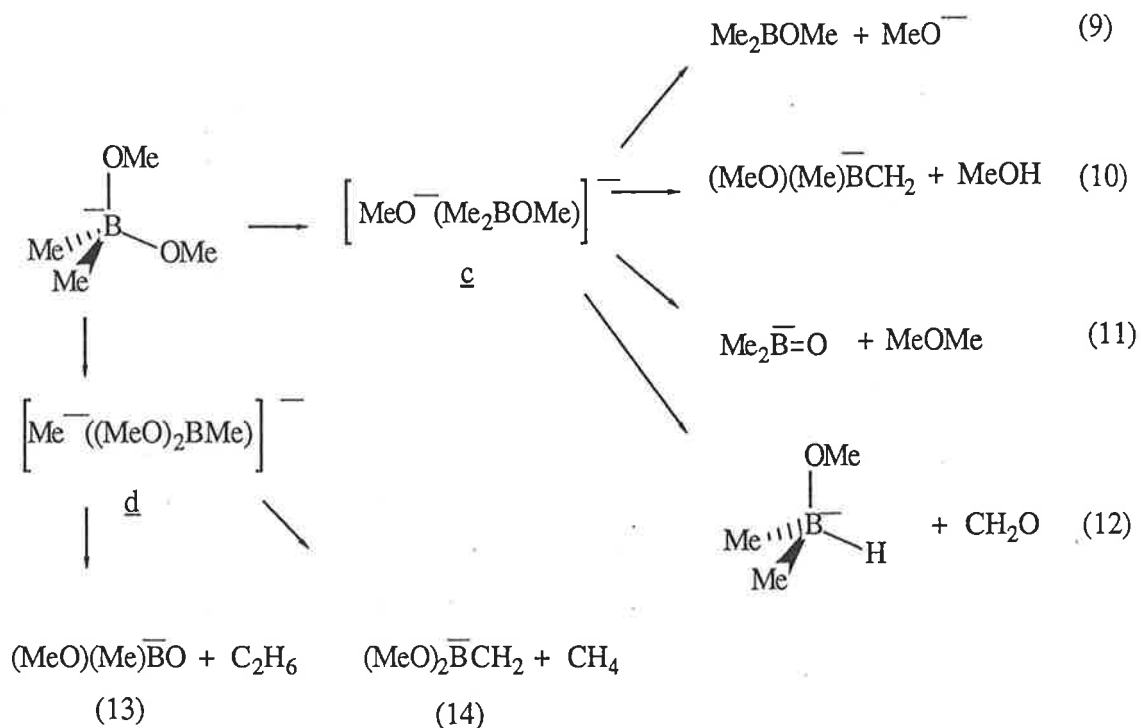
Figure 4.3 Collisional activation mass spectra of the adducts $[\text{Me}_2\text{BOCH}_3 + \text{CD}_3\text{O}^-]$ and $[\text{Me}_2\text{BOCD}_3 + \text{CH}_3\text{O}^-]$

Table 4.2 Collisional Activation Mass Spectra of Organoborane plus alkoxide Adducts.

Adduct, m/z	m/z (loss) abundance
Me ₂ BOMe + MeO ⁻ , 103	102 (H•) 4, 87 (CH ₄) 3, 73 (CH ₂ O) 4, 71 (MeOH) 100, 57 (MeOMe) 0.6, 41 (CH ₄ +MeOMe) 0.8 31 (Me ₂ BOMe) 22.
Me ₂ BOEt + EtO ⁻ , 131	130(H•) 21, 115(CH ₄) 4, 87(CH ₃ CHO)7, 85(EtOH) 100, 45(Me ₂ BOEt) 8.
Me ₂ BOEt + C ₂ D ₅ O ⁻ , 136	135(H•) 3, 120(CH ₄) 13, 92 (CH ₃ CHO)7, 90(EtOD) 100, 85(C ₂ D ₅ OH) 85, 50(Me ₂ BOEt) 18, 45(Me ₂ BOC ₂ D ₅) 13.
Me ₂ BOC ₂ D ₅ + EtO ⁻ , 136	135(H•) 3, 120(CH ₄) 8 92 (CH ₃ CHO)7, 90 (EtOD) 100, 85 (C ₂ D ₅ OH) 73, 50(Me ₂ BOEt) 9, 45(Me ₂ BOC ₂ D ₅) 13.
Et ₂ BOEt + EtO ⁻ , 159	157 (H ₂) 4, 129(C ₂ H ₆) 1, 115(MeCHO) 9, 113(EtOH) 100, 85(EtOEt) 1, 45(Et ₂ BOEt) 14.
(MeO) ₃ B + MeO ⁻ , 135	105(CH ₂ O)21, 103(MeOH) 25, 89(MeOMe) 20, 31((MeO) ₃ B) 100.
(MeO) ₃ B + MeO ⁻ , 138	115(CH ₂ O)4, 108(MeOH)11, 107(MeOD)4, 106(CD ₃ OH) 2, 92(MeOMe)8, 89(MeOCD ₃)6, 34((MeO) ₃ B)26, 31((MeO) ₂ CD ₃ OB)100.

4.4 Collision Induced Dissociation of Simple Alkoxide Organoborate Adducts.

The collisional activation mass spectra of the product ions formed between simple alkoxides and organoborates are recorded in *Table 4.2* and illustrated for a particular example in *Figure 4.3*. The general fragmentation behaviour may be illustrated by reference to the ion $\text{Me}_2\bar{\text{B}}(\text{OMe})_2$; a summary of the fragmentations of this ion are given in *Scheme 4.4*.



Scheme 4.4

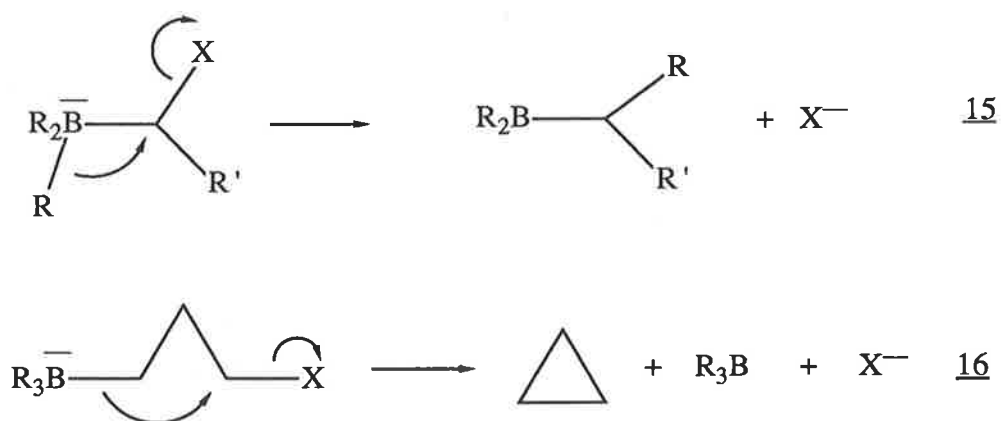
Most of the fragmentations shown in *Scheme 4.4* have analogous reactions in silicon¹⁴⁴ and phosphorus ions¹⁴³. The analogous reactions in silicon and phosphorus are considered to proceed via the intermediacy of ion complexes although in some cases radical/radical anion complexes may be involved. As a result the fragmentations of these simple alkoxide borates have been

rationalized in terms of the intermediacy of ion complexes. It is suggested that all fragmentations shown in *scheme 4.4* proceed through either ion complexes c or d. The MeO^- ion complex c is responsible for the major fragmentations; ion c may dissociate directly to form MeO^- (*equation 9*) or the MeO^- may deprotonate one of the methyl groups attached to the boron to effect elimination of MeOH (*equation 10*). Secondary deuterium isotope effects H/D of 1.23 and 1.15 are observed for MeO^- formation and MeOH loss (see *Figure 4.3*). The MeO^- ion may also effect an $\text{S}_{\text{N}}2$ reaction in which dimethyl ether is eliminated: this process is represented in *equation 11*. The hydride transfer reaction to give the borohydride anion (*equation 12*) is notable since this type of reaction has not been observed before in gas phase boron chemistry. The methoxide ion is known to be an ambident nucleophilic species in the gas phase – it may transfer a hydride ion to a number of neutrals including formaldehyde and sulphur dioxide⁹⁰. In this study the reaction becomes more pronounced as the number of methoxy groups around the boron increases; in the case of $[(\text{MeO})_4\text{B}]^-$ loss of CH_2O gives a peak of 21% abundance (*Table 4.2*).

The Me^- anion of the ion complex d may deprotonate a methyl group attached to the boron to give the product ion shown in *equation 14*. Alternatively Me^- may attack the methyl group of the methoxy substituent via an $\text{S}_{\text{N}}2$ reaction to eliminate ethane and give the product ion shown in *equation 13*.

4.5 Collision Induced Dissociations of Negative Borate Ions formed from Bifunctional Alkoxide Ions and Trimethylborane.

The occurrence of the hydride transfer reaction to trimethylboranes in the collision induced dissociation of simple alkoxide/borane adducts (see section 4.4 *page 82, 83*), together with reports of migration reactions¹²⁹⁻¹³¹ occurring in condensed phase reactions of organoborate ions (e.g. *equations 15 and 16*) has led us to consider the collisional activation spectra of adducts formed between Me_3B and some bifunctional alkoxide ions of the type $\text{^-OCH}_2\text{CH}_2\text{X}$ (where $\text{X} = \text{F}, \text{HO}, \text{MeO}, \text{MeS}$ and Me_2N).



$\text{X} = \text{halogen}, \text{N}_2, \text{OSO}_2\text{R}, \text{Me}_2\text{S}, \text{etc.}$

Scheme 4.5

The purpose of this phase of the investigation was to determine whether migrations reactions from boron occur in the gas phase. Some most unusual rearrangements do occur; some have been studied by deuterium labelling. The borate adducts $\text{Me}_3\text{B}^-\text{OCH}_2\text{CH}_2\text{X}$ (where $\text{X} = \text{F}, \text{HO}, \text{MeO}, \text{MeS}$ and Me_2N) undergo a number of standard reactions including the loss of CH_4 ,

and the formation of the ions $\text{Me}_3\bar{\text{B}}\text{H}$, ${}^-\text{OCH}_2\text{CH}_2\text{X}$, $\text{C}_2\text{H}_3\text{O}^-$, $\text{Me}_2\bar{\text{B}}=\text{CH}_2$ and $\text{C}_3\text{H}_4\text{OX}^-$. The adducts also undergo some gas phase reactions not observed before in boron chemistry such as the formation of $\text{Me}_3\bar{\text{B}}\text{X}$ and the loss of XMe and XH . The collisional activation spectra of these borate anions are recorded in *Tables 4.3, 4.4, 4.5*, and a typical spectrum is shown in *Figure 4.4*. Some of the rearrangements are studied further by recourse to the spectra of adducts $[\text{Me}_3\text{B} + {}^-\text{O}(\text{CH}_2)_n\text{X}]$ ($n=3-5$) (see *Table 4.3-4.4*).

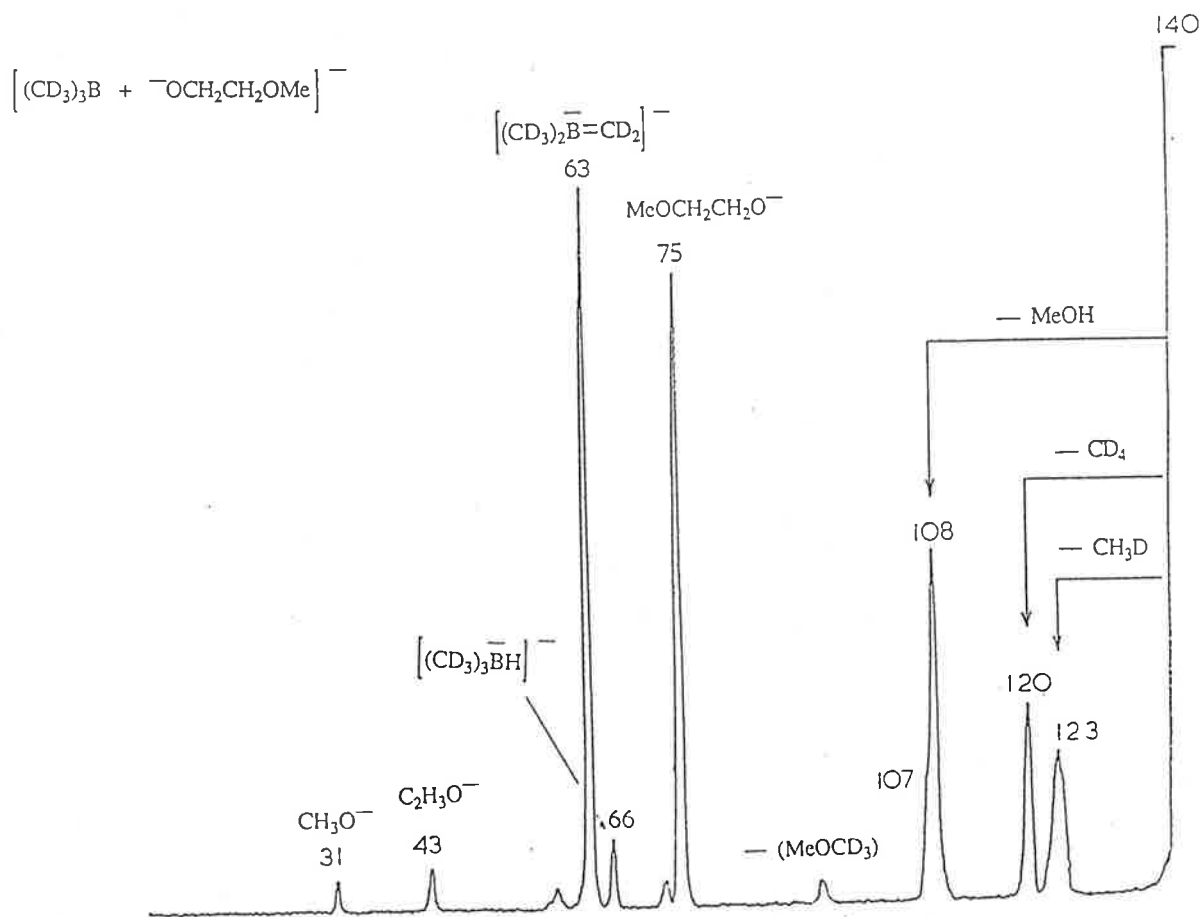


Figure 4.4: Collisional activation mass spectrum of the adduct derived from the reaction of the anion $\text{MeOCH}_2\text{CH}_2\text{O}^-$ with Me_3B .

Table 4.3: Collisional Activation Mass Spectra of the Adducts formed from the Reactions of Me_3^{11}B and $\text{MeO}(\text{CH}_2)_n\text{O}^-$ ($n = 2$ to 5) and Labelled Derivatives.

Alkoxide	Borane	Loss of										
		CH_4	CH_3D	CD_3H	CD_4	MeOH	MeOD	CD_3OH	CD_3OD	MeOMe	CD_3OMe	CD_3OCD_3
$\text{MeOCH}_2\text{CH}_2\text{O}^-$	Me_3B	52				38				2		
$\text{MeOCH}_2\text{CD}_2\text{O}^-$	Me_3B	32				6	14			4		
$\text{CD}_3\text{OCH}_2\text{CH}_2\text{O}^-$	Me_3B	26		6				18			3	
$\text{MeOCH}_2\text{CH}_2\text{O}^-$	$(\text{CD}_3)_3\text{B}$		20		27	50					3	
$\text{MeOCH}_2\text{CD}_2\text{O}^-$	$(\text{CD}_3)_3\text{B}$		21		36		30				5	
$\text{CD}_3\text{OCH}_2\text{CH}_2\text{O}^-$	$(\text{CD}_3)_3\text{B}$			11	24			19	9			1.5
$\text{MeO}(\text{CH}_2)_3\text{O}^-$	Me_3B	48				21				0.5		
$\text{MeO}(\text{CH}_2)_2\text{CD}_2\text{O}^-$	Me_3B	44					21			1		
$\text{MeO}(\text{CH}_2)_3\text{O}^-$	$(\text{CD}_3)_3\text{B}$	18	9		30		18				0.5	
$\text{MeO}(\text{CH}_2)_2\text{CD}_2\text{O}^-$	$(\text{CD}_3)_3\text{B}$	21			46		32				2	
$\text{MeO}(\text{CH}_2)_4\text{O}^-$	Me_3B	79				16				9		
$\text{MeO}(\text{CH}_2)_5\text{O}^-$	Me_3B	47				13				2		
$\text{MeOC}(\text{Me})_2\text{CH}_2\text{O}^-$	Me_3B	31				24				8		

Table 4.3: continued

Alkoxide [X(CH ₂) _n O ⁻]	Borane	Formation of									
		RO ⁻	Me ₂ B ⁻ =CH ₂	(CD ₃) ₂ B ⁻ =CD ₂	Me ₃ B ⁻ H	Me ₃ B ⁻ D	C ₂ H ₃ O ⁻	C ₂ H ₂ DO ⁻	X ⁻	[RO ⁻ -H ₂] ⁻	[RO ⁻ -HD] ⁻
MeOCH ₂ CH ₂ O ⁻	Me ₃ B	58	100		9		2		1	3	
MeOCH ₂ CD ₂ O ⁻	Me ₃ B	45	100			6		2	3		0.75
CD ₃ OCH ₂ CH ₂ O ⁻	Me ₃ B	42	100		9		2		2	2	
MeOCH ₂ CH ₂ O ⁻	(CD ₃) ₃ B	88		100	9		6		4	3	
CD ₃ OCH ₂ CH ₂ O ⁻	(CD ₃) ₃ B	82		100	9		3		3	5	
MeOCH ₂ CD ₂ O ⁻	(CD ₃) ₃ B	68		100		6		2	3		1
CH ₃ O(CH ₂) ₃ O ⁻	Me ₃ B	76	100		8		-	-	5	17	
MeO(CH ₂) ₂ CD ₂ O ⁻	Me ₃ B	78	100			6		-	6		1
CH ₃ O(CH ₂) ₃ O ⁻	(CD ₃) ₃ B	100		98				-	6	2	
MeO(CH ₂) ₂ CD ₂ O ⁻	(CD ₃) ₃ B	100		100		7		-	6		2
MeO(CH ₂) ₄ O ⁻	Me ₃ B	28	100		12			-	8	9	
MeO(CH ₂) ₅ O ⁻	Me ₃ B	16	100		13			-	7	10	
MeOC(Me) ₂ CH ₂ O ⁻	Me ₃ B	100	27		11			-	14		

Table 4.4: Collisional Activation Mass Spectra of Adducts formed by the Reactions of Me_3^{11}B with $\text{XCH}_2\text{CH}_2\text{O}^-$ ($\text{X} = \text{NMe}_2$ or SMe) and Labelled Derivatives.

Alkoxide	Borane	Loss of							
		CH_4	CH_3D	CD_3H	CD_4	XH	XD	XMe	XCD_3
$\text{Me}_2\text{NCH}_2\text{CH}_2\text{O}^-$	Me_3B	66				22		—	—
$\text{Me}_2\text{NCH}_2\text{CD}_2\text{O}^-$	Me_3B	84				6	10	—	—
$(\text{CD}_3)_2\text{NCH}_2\text{CH}_2\text{O}^-$	Me_3B	78		38		29		—	—
$\text{Me}_2\text{NCH}_2\text{CH}_2\text{O}^-$	$(\text{CD}_3)_3\text{B}$	32	16		25	24		—	—
$\text{Me}_2\text{N}(\text{CH}_2)_3\text{O}^-$	Me_3B	80				24		—	—
$\text{MeSCH}_2\text{CH}_2\text{O}^-$	Me_3B	23				47		7	
$\text{CD}_3\text{SCH}_2\text{CH}_2\text{O}^-$	Me_3B	10		8		18		2	
$\text{MeSCH}_2\text{CD}_2\text{O}^-$	Me_3B	31					30	3	
$\text{MeSCH}_2\text{CH}_2\text{O}^-$	$(\text{CD}_3)_3\text{B}$	11			5	34			a

a = 91 a.m.u. = loss of MeSCD_3 = formation of $\text{MeSCH}_2\text{CH}_2\text{O}^-$

Table 4.4: continued

Alkoxide ($X(\text{CH}_2)_n\text{O}^- \equiv \text{RO}^-$)	Borane	Formation of									
		RO^-	$[\text{RO}^-\text{H}_2]^-$	$[\text{RO}^-\text{HD}]^-$	$\text{Me}_3\bar{\text{B}}\text{H}$	$\text{Me}_3\bar{\text{B}}\text{D}$	$\text{Me}_2\bar{\text{B}}=\text{CH}_2$	$(\text{CD}_3)_2\bar{\text{B}}=\text{CD}_2$	$\text{C}_2\text{H}_3\text{O}^-$	$\text{C}_2\text{H}_2\text{DO}^-$	X^-
$\text{Me}_2\text{NCH}_2\text{CH}_2\text{O}^-$	Me_3B	72	13		8		100		1		-
$\text{Me}_2\text{NCH}_2\text{CD}_2\text{O}^-$	Me_3B	73		9		6	100			3	-
$\text{CD}_3)_2\text{NCH}_2\text{CH}_2\text{O}^-$	Me_3B	84	16		8		100		5		-
$\text{Me}_2\text{NCH}_2\text{CH}_2\text{O}^-$	$(\text{CD}_3)_3\text{B}$	100	16		8			96	5		-
$\text{Me}_2\text{N}(\text{CH}_2)_3\text{O}^-$	Me_3B	100	21		6		100		-	-	-
$\text{MeSCH}_2\text{CH}_2\text{O}^-$	Me_3B	100	-	-	22		55		9		25
$\text{CD}_3\text{SCH}_2\text{CH}_2\text{O}^-$	Me_3B	100	-	-	24		45		6		24
$\text{MeSCH}_2\text{CD}_2\text{O}^-$	Me_3B	100	-	-	1	14	45			5	19
$\text{MeSCH}_2\text{CH}_2\text{O}^-$	$(\text{CD}_3)_3\text{B}$	100	-	-	16			48	7		17

Table 4.5: Collisional Activation Mass Spectra of Adducts formed in reactions of Me_3^{11}B and $\text{XCH}_2\text{CH}_2\text{O}^-$ (X = HO or F) and Labelled Derivatives.

Alkoxide $\text{XCH}_2\text{CH}_2\text{O}^-$	Borane R_3B	Loss of									
		CH_4	CH_3D	CD_3H	CD_4	XH	XD	$\text{C}_2\text{H}_4\text{O}$	$\text{CH}_2\text{CD}_2\text{O}$	$(\text{R}_3\text{B} + \text{H}_2)$	$(\text{R}_3\text{B} + \text{HD})$
$\text{HOCH}_2\text{CH}_2\text{O}^-$	Me_3B	50				8		9		9	
$\text{DOCH}_2\text{CH}_2\text{O}^-$	Me_3B	16	28			6		11		12	
$\text{HOCH}_2\text{CH}_2\text{O}^-$	$(\text{CD}_3)_3\text{B}$			75		28	b	15		15	
$\text{FCH}_2\text{CH}_2\text{O}^-$	Me_3B	24				3		10		3	
$\text{FCH}_2\text{CD}_2\text{O}^-$	Me_3B	38				1	1		4		4
$\text{FCH}_2\text{CH}_2\text{O}^-$	$(\text{CD}_3)_3\text{B}$			6	13 ^a	6 ^a	13	8		0.5	

^a 109 a.m.u. = loss of CD_4 = loss of HF.

^b 107 a.m.u. = loss of CD_3H = loss of HOD

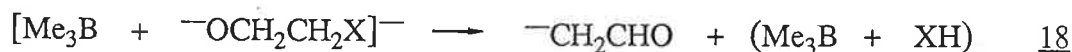
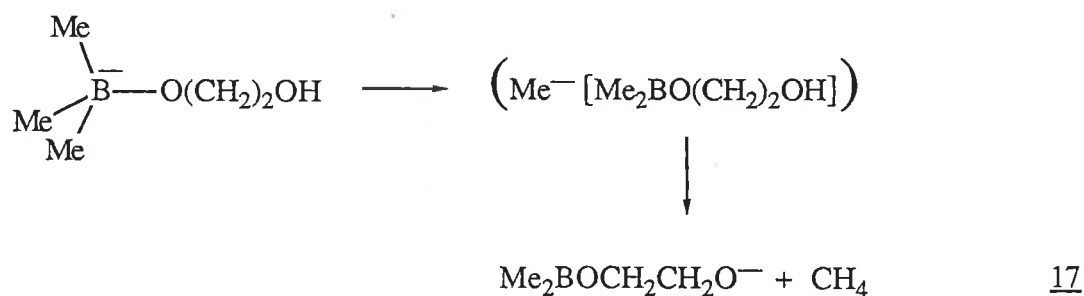
Table 4.5 continued

Alkoxide XCH ₂ CH ₂ O ⁻	Borane	Formation of								
		RO ⁻	(Me ₃) ₂ B ⁻ CH ₂	(CD ₃) ₂ B ⁻ CD ₂	Me ₃ B ⁻ H	Me ₃ B ⁻ D	HC ₂ O ⁻	DC ₂ O ⁻	C ₂ H ₃ O ⁻	C ₂ H ₂ DO ⁻
HOCH ₂ CH ₂ O ⁻	Me ₃ B	100	12		13		1		1	-
DOCH ₂ CH ₂ O ⁻	Me ₃ B	100	12		12		2		2	-
HOCH ₂ CH ₂ O ⁻	(CD ₃) ₃ B	100		28	11		0		3	-
FCH ₂ CH ₂ O ⁻	Me ₃ B	98	100		24		1		1	6
FCH ₂ CD ₂ O ⁻	Me ₃ B	82	100			19		1		4
FCH ₂ CH ₂ O ⁻	(CD ₃) ₃ B	100 ^a		100 ^a	24		1		0.5	6

^a = 63 a.m.u. = formation of FCH₂CH₂O⁻ = formation of (CD₃)₂B⁻CD₂.

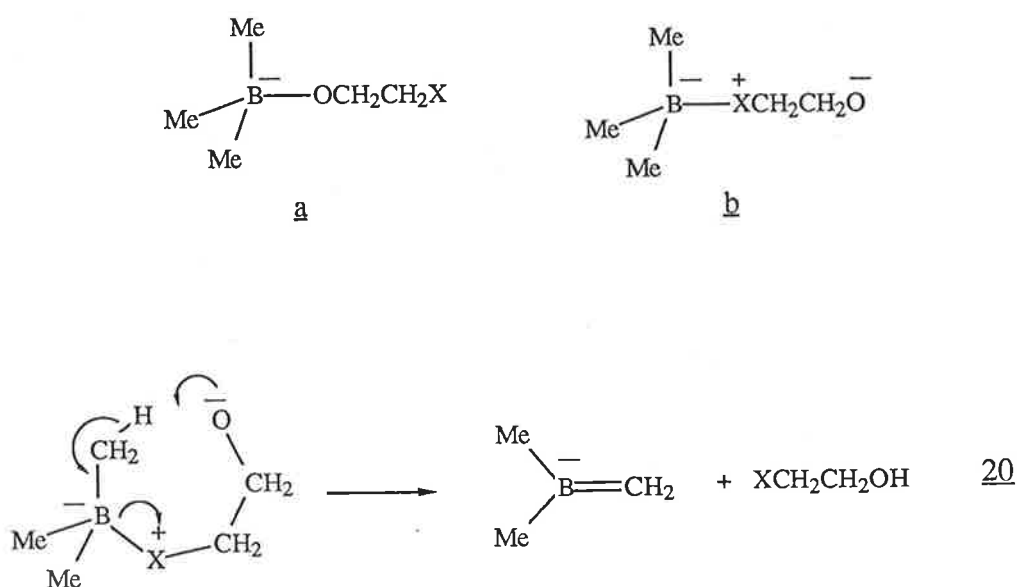
4.5.1 The losses of CH₄ and Me₃B, and the formation of XCH₂CH₂O⁻, Me₂B⁻=CH₂ and C₃H₄OX⁻.

The formation of ions XCH₂CH₂O⁻, Me₂B⁻=CH₂ and Me₃B⁻H and the loss of CH₄ are standard reactions of organoborates adducts and are observed for all species listed in *Tables 4.3 - 4.5*. The mechanisms for the formation of XCH₂CH₂O⁻ and Me₃B⁻H, and for the loss of CH₄ are analogous to those summarized in *equations 9, 12 and 14 (Scheme 4.4 page 81)*.



Scheme 4.6

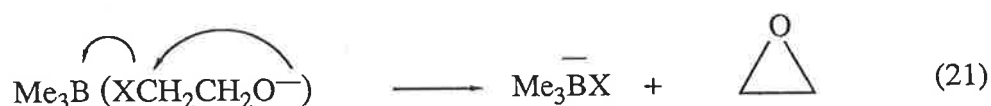
The major loss of methane from the adduct (HOCH₂CH₂O⁻ + BMe₃) does not occur by the standard mechanism. The loss involves elimination of a boron methyl group together with the hydrogen on the hydroxy substituent. The reaction is illustrated in *equation 17 (Scheme 4.6)*. The formation of C₂H₃O⁻ is a minor reaction; the formation of this ion involves loss of Me₃B, a hydrogen from C1, and the X substituent. This ion is likely to correspond to

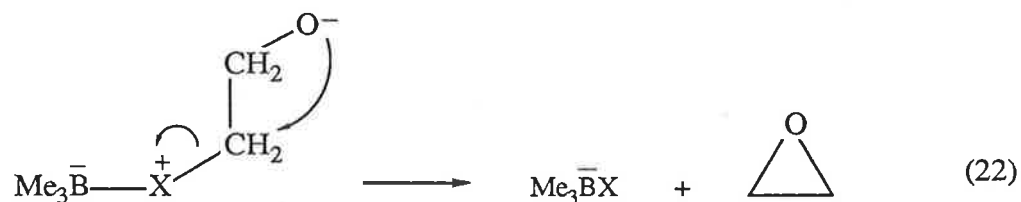


Scheme 4.7

4.5.2 The Losses of XH and XMe and Formation of X^- and $\text{Me}_3\text{B}^-\text{X}$ ($\text{X}=\text{F}, \text{HO}, \text{MeO}, \text{MeS}$ and Me_2N).

The formation of $\text{Me}_3\text{B}^-\text{X}$ is a minor reaction, but it has an interesting mechanism and occurs exclusively for the systems $\text{X} = \text{HO}$ and F). There are two possible mechanisms by which this ion may be formed; these are illustrated in *equations 21* and *22*. Since both mechanisms involve the formation of ethylene oxide and $\text{Me}_3\text{B}^-\text{X}$, it is not possible to distinguish between them.

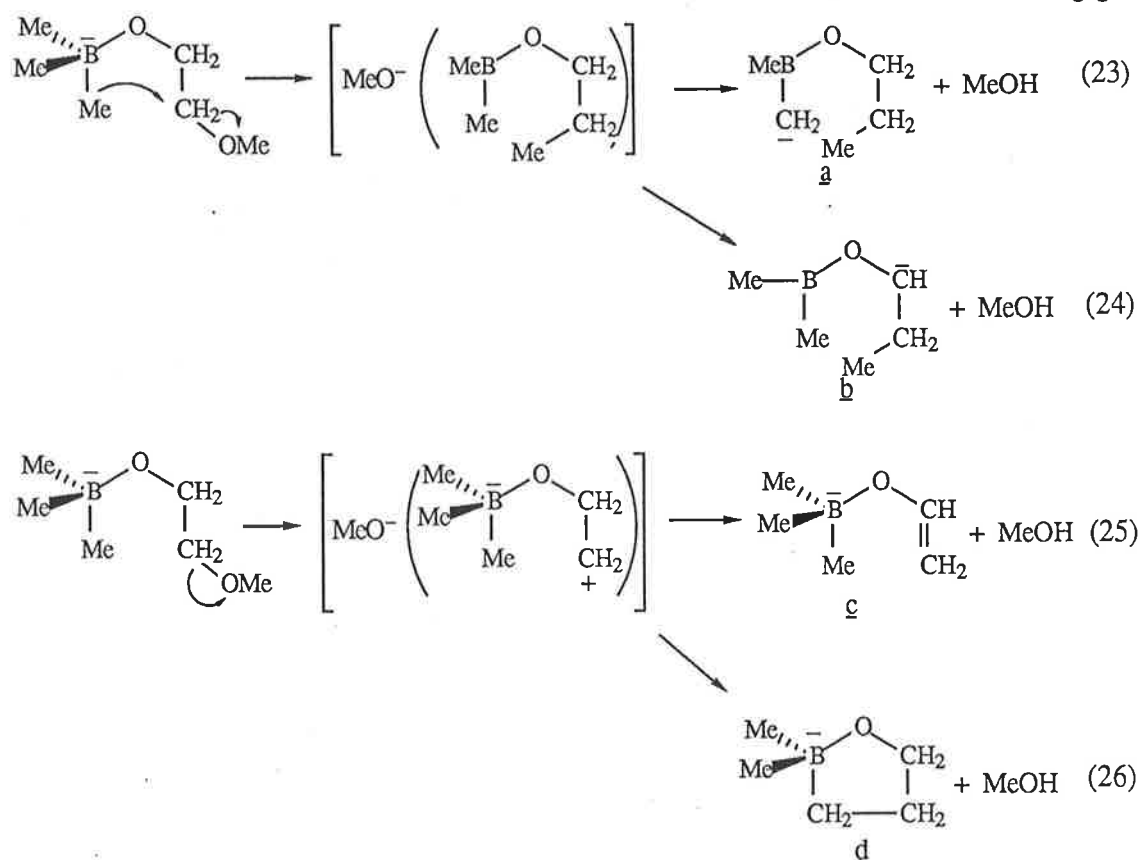




Scheme 4.8

All adducts studied (with the exception of the system where $\text{X} = \text{NMe}_2$) show the loss of XH , XMe and the formation of X^- ; for example the spectrum of $\text{Me}_3\text{B}^-\text{OCH}_2\text{CH}_2\text{OMe}$ (Figure 4.4, page 84) shows the loss of MeOH , MeOMe and the formation of MeO^- . For ease of representation and understanding, the discussion of the fragmentations and their mechanisms will be limited to $\text{X} = \text{MeO}$, although the mechanisms proposed apply to all systems unless otherwise stated.

Deuterium labelling indicates that the main loss of MeOH occurs with loss of the terminal methoxyl group and a hydrogen at C1 of the alkoxy group. However there is a minor loss of MeOH which involves the loss of a hydrogen from a boron methyl group. There are two plausible rationales for these reactions: i) where a methyl group attached to the boron migrates to C2 of the alkoxy group displacing MeO^- ; the MeO^- may then deprotonate competitively at two sites (equations 23 and 24 Scheme 4.9), and ii) a "remote" fragmentation¹⁴⁸⁻¹⁵⁰ to produce MeO^- , followed by competitive deprotonation (equations 25 and 26 Scheme 4.9).



Scheme 4.9

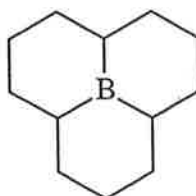
Remote fragmentations¹⁴⁸⁻¹⁵⁰ are a matter of some conjecture. They could however operate in these cases since:-

i) The ions being examined in this study carry no "formal" charge i.e. the "extra electrons" are not available for a typical "push pull" mechanism (in simple valence bond terms) since they are involved in a formal bond to the boron.

ii) As the carbon chain of the alkoxide is increased only a small decrease in the the amount of MeOH lost is observed e.g. loss of MeOH from the ion $\text{MeO}(\text{CH}_2)_2\text{O}^-\text{BMe}_3$ is 38 % of the base peak, while loss of MeOH from the ion $\text{MeO}(\text{CH}_2)_5\text{O}^-\text{BMe}_3$ is 13 % of the base peak (*Table 4.3*). In addition, substitution at the C2 of the alkoxy such that C2 becomes a tertiary centre has

little effect on the loss of MeOH, e.g. loss of MeOH from the ion $\text{MeO}(\text{CH}_2)_2\text{O}^-\text{BMe}_3$ is 38 % of the base peak, while loss of MeOH from the ion $\text{MeO}(\text{CMe}_2)\text{CH}_2\text{O}^-\text{BMe}_3$ is 24 % of the base peak (*Table 4.3*). It would be expected that a migration led reaction would be severely discriminated against by lengthening of the carbon chain and/or steric hindrance at C2 of the alkoxide group.

The migration reaction should produce the product ions a and b (*Scheme 4.9*), whereas the remote fragmentation mechanism would produce the two ions c and d.

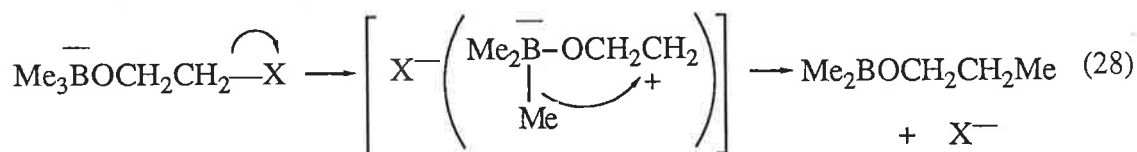
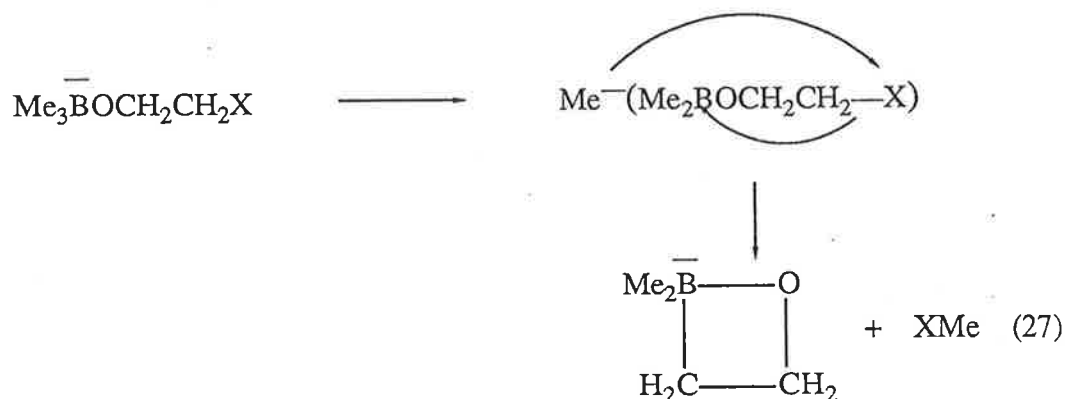


10

In order to determine conclusively that a migration led reaction was not involved in this mechanism, it was proposed to study the spectrum of an adduct formed between an alkoxide and a cyclic borane adduct (e.g. 10). The rigid structure of the cyclic borane would not allow the migration mechanism shown in *equations 23* and *24*, but should allow the remote fragmentation mechanism (*equations 25* and *26*). Unfortunately, attempts to synthesise an appropriate cyclic borane failed, and the debate as to the mechanism is unresolved.

The loss of XMe is a minor reaction and is observed for all systems except when of $X = \text{NMe}_2$ or F. The loss involves a methyl group attached to the boron together with the substituent X. The mechanism shown in *equation*

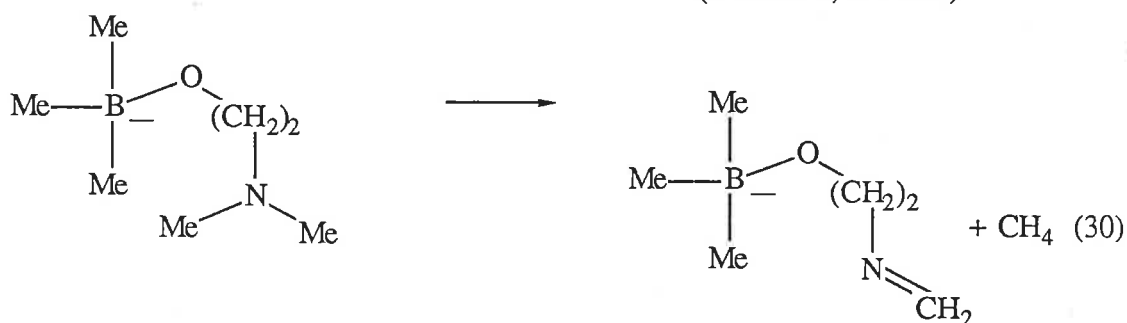
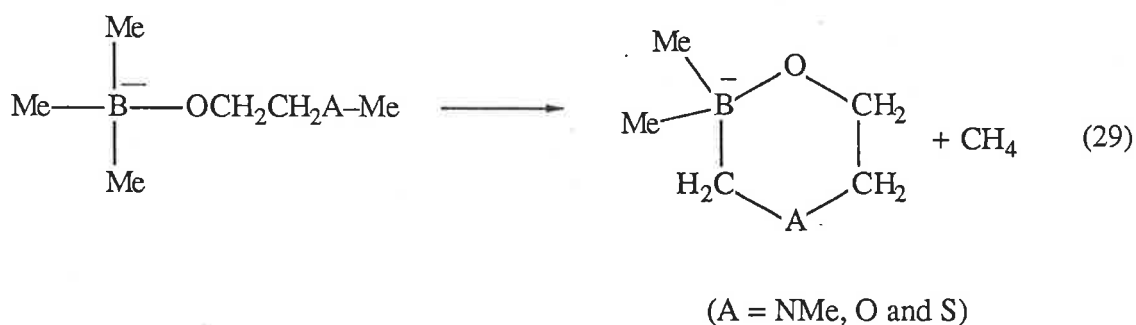
27 is suggested for this process. It is not known why $X = \text{NMe}_2$ and F substituents fail to participate in this process. The formation of X^- occurs for all systems with the exception of $X = \text{NMe}_2$. Perhaps the mechanism is of the type that occurs in condensed phase chemistry (see *equation 15 Scheme 4.5 page 83*) but this seems unlikely since extension of the carbon chain of the alkoxide does not detrimentally effect production of X^- e.g., the abundance of the peak corresponding to formation of MeO^- from adducts ($\text{MeO}(\text{CH}_2)_2\text{O}^- + \text{Me}_3\text{B}$) and ($\text{MeO}(\text{CH}_2)_5\text{O}^- + \text{Me}_3\text{B}$) are 1 and 7% respectively; a migration mechanism of the type illustrated in *equation 15 (scheme 4.5)* would be expected to discriminate against formation of X^- from longer chain alkoxides.



Scheme 4.10

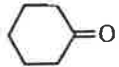
There are two other losses of methane observed in the spectra of adducts

from $(XCH_2CH_2O^-$ and Me_3B); both involve X substituents that have a methyl group (e.g $X = MeS, MeO$ and Me_2N). The first involves elimination of a methyl attached to the sulphur, nitrogen or oxygen together with a hydrogen from a boron methyl. A remote fragmentation mechanism is suggested and illustrated in *equation 29*. The other loss of methane occurs exclusively for the $X = NMe_2$ system and involves a methyl group on the amine substituent together with a hydrogen from the other methyl group on the amine substituent. A suggested mechanism for this process is shown in *equation 30*.



Scheme 4.11

Table 4.6: Collisional Activation Mass Spectra of the Adducts formed by the Reaction of Me_3^{11}B with some Enolate Anions.

Substrate	Reacting ion ≡ Nu	Loss of												
		H [•]	D [•]	CH ₄	CH ₃ D	CD ₃ H	CD ₄	CH ₂ CO	CD ₂ CO	NuH	NuD	Me ₃ B	(CD ₃) ₃ B	
(CD ₃) ₃ B	⁻ CD ₂ CHO		12				6	5	2			3		100
Me ₃ B	⁻ CD ₂ CHO	15	2	11	4					1	3		100	
Me ₃ B	⁻ CD ₂ CDO	13	2	12	4					0	4		100	
Me ₃ B	⁻ CH ₂ COMe	8		10							3		100	
Me ₃ B	Et ⁻ CHCOPr	11		9							4		100	
Me ₃ B		7		2							1		100	
Me ₃ B	⁻ CH ₂ CN	7		9							4		100	
(CD ₃) ₃ B	⁻ CH ₂ CN		4			7	3					2		100
Me ₃ B	⁻ CD ₂ CN	8	5	5							4		100	
Me ₃ B	⁻ CH ₂ SOMe	3	5	3							2		100	
Me ₃ B	⁻ CD ₂ SOCD ₃	3	2	3							1		100	

4.6 Gas Phase Reactions of Enolate Negative Ions with Trimethylborane

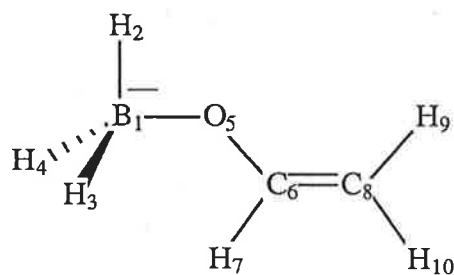
In the preceding section it was suggested that functional alkoxide ions could act as ambident nucleophiles towards boranes, i.e. the reaction between e.g. $\text{MeOCH}_2\text{CH}_2\text{O}^-$ and Me_3B could form two adducts $\text{Me}_3\bar{\text{B}}\text{OCH}_2\text{CH}_2\text{OMe}$ and $\text{Me}_3\bar{\text{B}}-\overset{+}{\text{O}}(\text{Me})\text{CH}_2\text{CH}_2\text{O}^-$. In this section we explore this possibility further by examining the ion chemistry of adducts formed by the reaction of Me_3B with enolate ions, i.e. nucleophiles which would be expected to be ambident in their reactions with boranes.

All the negative enolate ions examined in this study reacted with trimethylborane to produce collisionally stabilized adducts; the collisional activation mass spectra of these ions are shown in *Tables 4.6* and *4.8*, or *Figures 4.5* or *4.6*.

4.6.1 Simple Enolate Ions

Simple enolate anions may form two different tetrahedral adducts on reaction with trimethylborane. In order to investigate this possibility from a theoretical viewpoint, *ab initio* calculations (3-21G and 4-31G**/3-21G) have been used on the simplest model system, i.e. $\text{H}_3\text{B}/(\text{CH}_2\text{CHO})^-$. The calculations suggest that two possible tetrahedral adducts A and B (*Table 4.7*) are stable local minima; A is marginally more stable than B by only 4 kJ mol⁻¹ at the 4-31G* level.

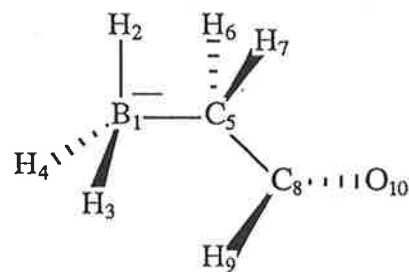
Table 4.7: Geometries and Energies of Stable Adducts from $\text{H}_3\text{B}/(\text{CH}_2\text{CHO})$ (4-31G**/3-21G).



A

-178.58412 a.u. (4-31G*)

1-2	1.22 Å	2-1-5	108.6°
1-3	1.23	3-1-5	109.9
1-4	1.24	3-1-5	109.9
1-5	1.54	1-5-6	119.0
5-6	1.30	5-6-7	115.7
6-7	1.08	5-6-8	126.0
6-8	1.33	6-8-9	121.1
8-9	1.07	6-8-10	120.4
8-10	1.07	6-5-1-2	179.8
		8-6-5-1	180.1
		7-6-5-8	180.0



B

-178.58270 a.u. (4-31G*)

1-2	1.23 Å	2-1-5	108.3°
1-3	1.24	3-1-5	109.2
1-4	1.23	4-1-5	110.2
1-5	1.69	1-5-8	110.7
5-6	1.09	5-8-9	112.4
5-7	1.09	6-5-8	112.7
5-8	1.48	7-5-8	107.6
8-9	1.10	5-8-10	128.1
8-10	1.20	8-5-1-2	177.7
		10-6-5-1	110.9
		9-8-5-10	181.8

The collisional activation mass spectrum of the adduct(s) formed between Me_3B and deprotonated acetaldehyde is shown in *Figure 4.5*. The interpretation of this spectrum is aided by those of a variety of deuterium labelled derivatives (*Table 4.6*). Fragmentations are summarized in *equations 31 to 37* (*Scheme 4.12 and 4.13*).

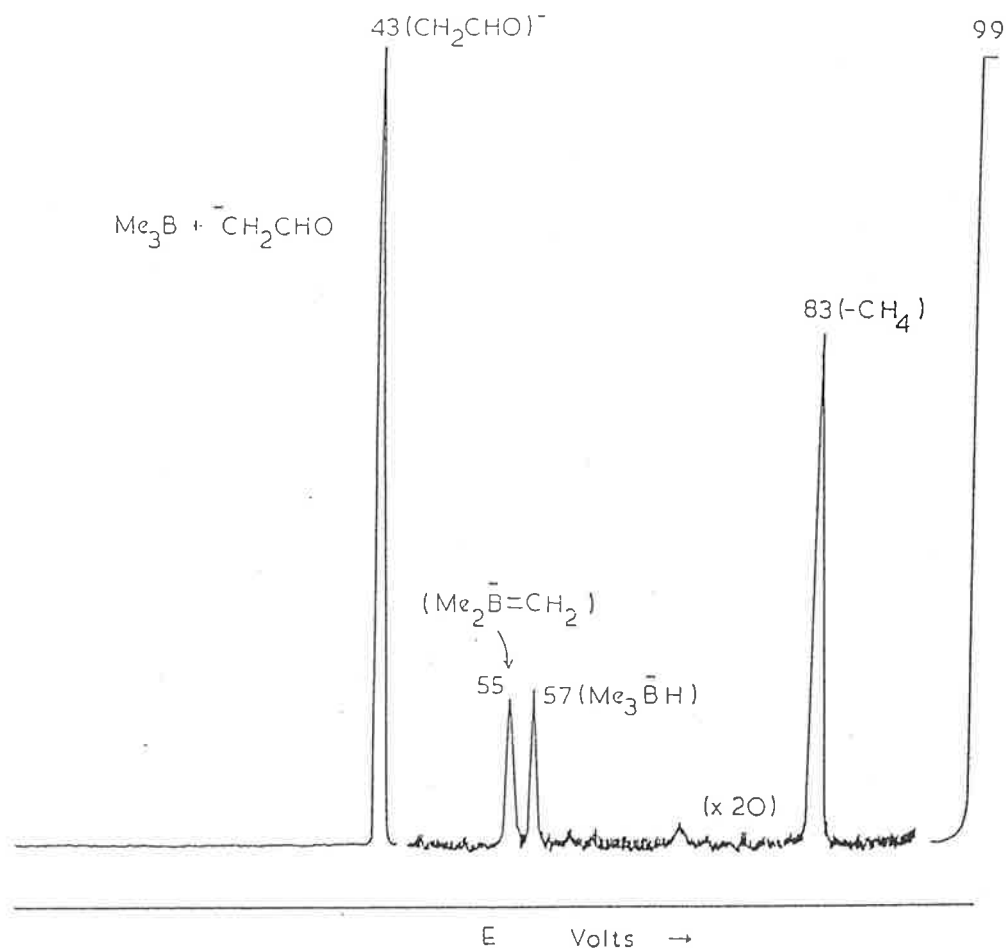
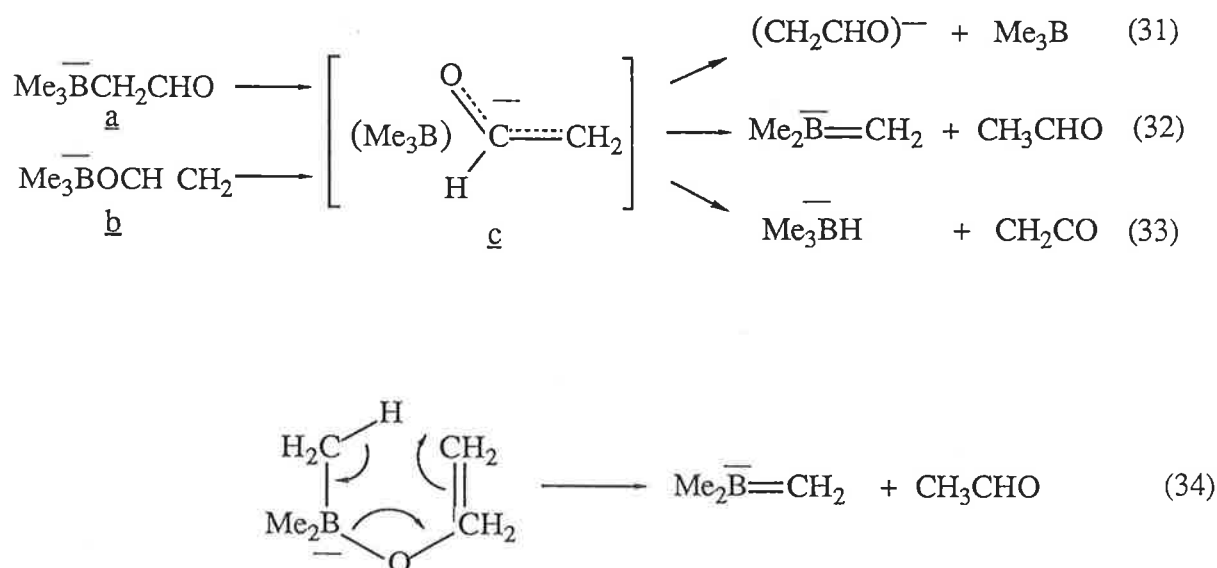


Figure 4.5: Collisional activation mass spectrum of the adduct(s) derived from the reaction of trimethylborane (^{11}B) with the acetaldehyde enolate anion.

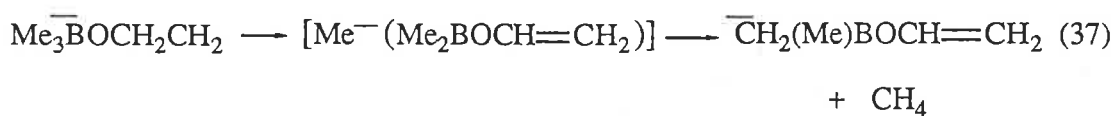
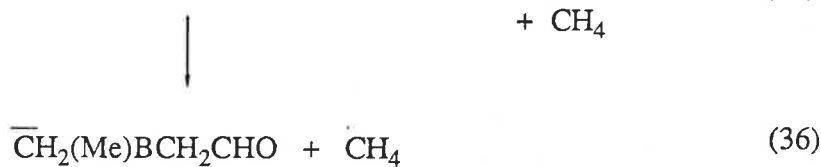
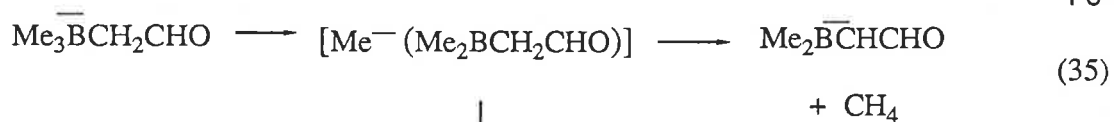
The major fragmentation of the $(\text{CH}_2\text{CHO})^-/\text{Me}_3\text{B}$ adduct is dissociation of the adduct to yield the acetaldehyde enolate ion (*equation 31*) – analogous fragmentations occur for all enolate systems. This fragmentation is represented as occurring from either of the adducts a or b through the intermediate ion complex c. Two other minor reactions may also proceed through c, viz. deprotonation to $\text{Me}_2\text{B}=\text{CH}_2^-$ (m/z 55) (*equation 32*), and the

interesting hydride ion transfer reaction to form Me_3BH^- (equation 33). The formation of $\text{Me}_2\text{B}=\text{CH}_2$ may also occur through the alternative six centred mechanism shown in equation 34, this mechanism leads to identical products as that from equation 32 and cannot be discounted. Elimination of methane is a standard reaction of Me_3B^- adducts [see section 4.4 (page 82) and 4.5.1 (page 91)]. In this case, labelling studies (Table 4.6) indicate competitive elimination of both methyl and methylene protons. These reactions are believed to proceed through ion complexes and the three reactions shown in equations 35 to 37 seems most likely, the major process being deprotonation of the methylene protons as shown in equation 35.

Fragmentations of all other species shown in Table 4.6 are directly analogous to those described in section 4.4 (pages 82 and 83).



Scheme 4.12



Scheme 4.13

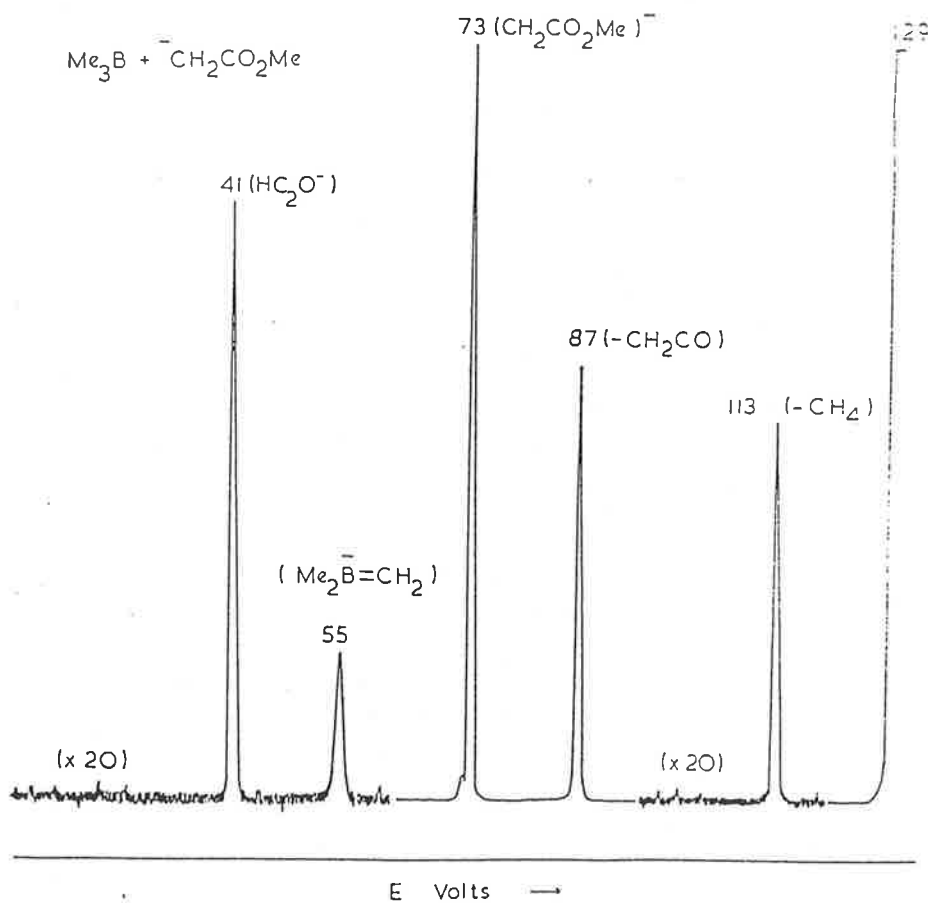
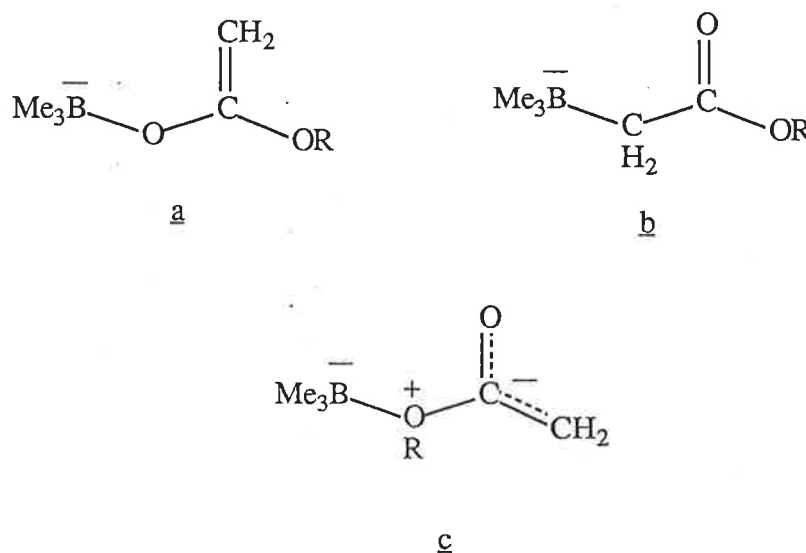


Figure 4.6: Collisional activation mass spectrum of the adduct(s) formed between the reaction of trimethylborane(^{11}B) and the methyl acetate enolate anion.

4.6.2 Enolates from Alkyl Acetates

The collisional activation mass spectrum of the adduct derived from the reaction of trimethylborane and deprotonated methyl acetate is shown in *Figure 4.6*. The spectra of deuterium labelled derivatives of this system are listed in *Table 4.8*, along with the spectra of the adducts of Me_3B and other deprotonated alkyl acetates. The spectra show losses of CH_4 , CH_2CO , and Me_3B and formation of the anions $\text{Me}_2\text{B}^-\text{CH}_2$ and HC_2O^- .

Ester enolates may act as ambident nucleophiles and hence produce more than one adduct on reaction with Me_3B ; however in addition to the possible formation of the two adducts a and b (*scheme 4.14*), there is also the possibility of a third adduct c being formed. The possible formation of these isomeric parent ions makes the interpretation of some fragmentations difficult.

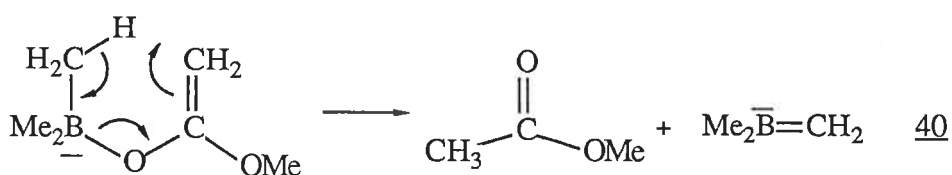
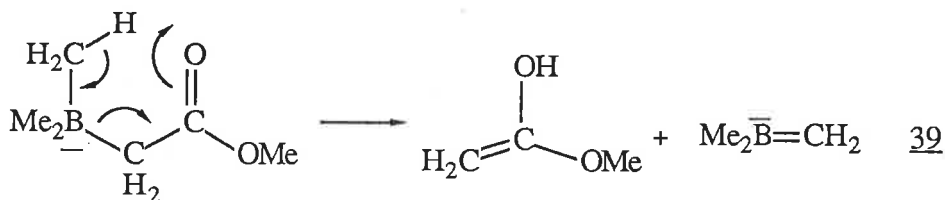
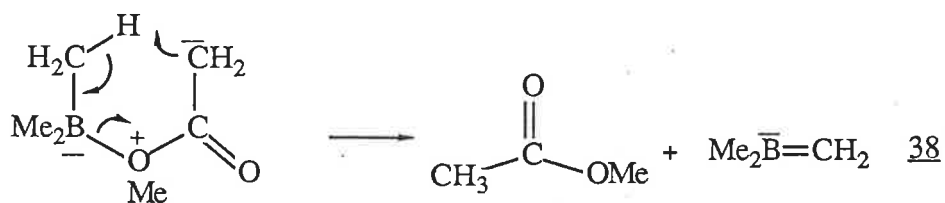


Scheme 4.14

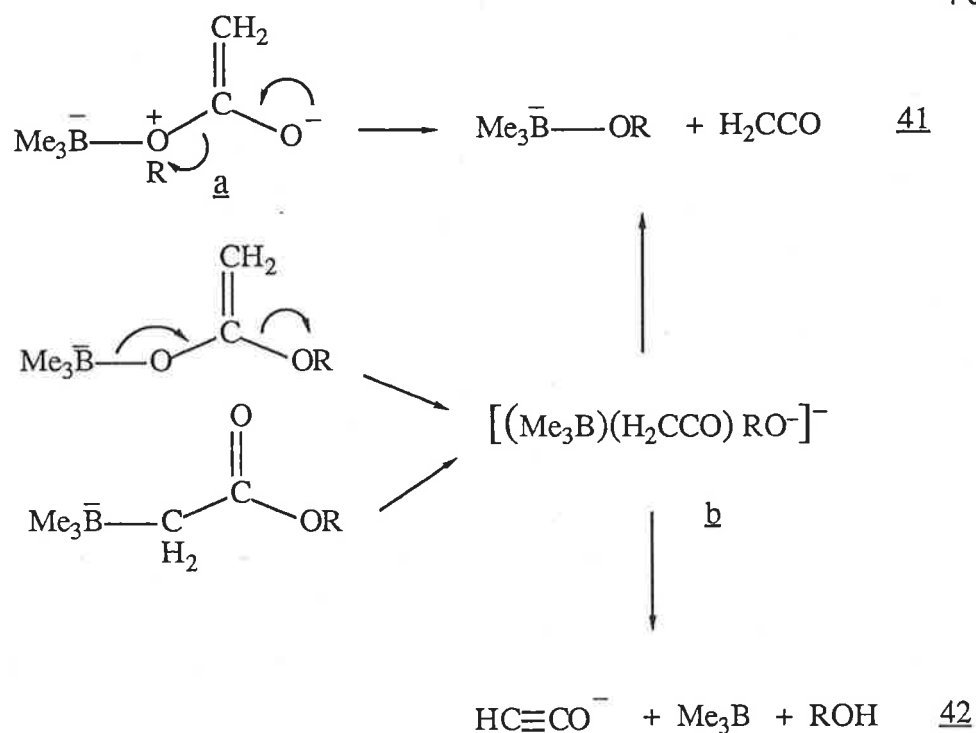
Table 4.8: Collisional Activation Spectra of Adducts Formed between Me₃¹¹B and Alkyl Acetate Enolate Anions.

Substrate	Reacting ion ≡ Nu	Loss of										Formation of			
		H ⁺	D ⁺	CH ₄	CH ₃ D	CD ₃ H	CD ₄	CH ₂ CO	CD ₂ CO	NuH	NuD	Me ₃ B	(CD ₃) ₃ B	HC ₂ O ⁻	DC ₂ O ⁻
Me ₃ B	⁻ CD ₂ CO ₂ CD ₃	2		1	1.5				62	1		100			2
Me ₃ B	⁻ CD ₂ CO ₂ Me	2		1	1.5				60	1		100			2
Me ₃ B	⁻ CD ₂ CO ₂ CD ₃	3		3				68		1		100		3	
(CD ₃) ₃ B	⁻ CD ₂ CO ₂ Me		1			2.5	1	78			1		100	2	
Me ₃ B	⁻ CD ₂ CO ₂ Et	5		3				28		0.5		100		3	
Me ₃ B	⁻ CD ₂ CO ₂ Pr	3		2				15		0.5		100		6	
Me ₃ B	⁻ CD ₂ CO ₂ isoPr	4		5				7		0.2		100		7	
Me ₃ B	⁻ CD ₂ CO ₂ Bu	1		2				8		0.3		100		5	
Me ₃ B	⁻ CD ₂ CO ₂ tert Bu	1		3				3		0.1		100		4	
Me ₃ B	⁻ CD ₂ CO ₂ CH ₂ Ph	1		2				9		0.3		100		1	

The losses of CH_4 and Me_3B are directly comparable to the analogous reactions occurring in the aldehyde enolate systems (*schemes 4.12 and 4.13, pages 103,104*). The formation of $\text{Me}_2\bar{\text{B}}\text{CH}_2$ may occur through an intermediate ion complex analogous to that in *equation 31 (scheme 4.12 page 103)*; however the reaction may also proceed through six centre transition states such as those outlined in *equations 38 to 40*. The data available does not allow us to distinguish between these mechanisms.



The pronounced loss of ketene and the formation of HC_2O^- are not observed in systems listed in *Table 4.6*. These fragmentations are observed for all the alkyl acetates studied (*Table 4.8*). The most plausible mechanisms for the loss of ketene are those illustrated in *Scheme 4.15*



Scheme 4.15

The abundance ratios for peaks arising from the loss of ketene are dependant upon the nature of the alkoxy group, i.e. $\text{MeO} > \text{EtO} > \text{PrO} > \text{iso PrO} \approx \text{BuO} > \text{tBuO}$; this order approximates the relative acidities of the analogous alcohols ROH ¹⁹³. This observation is not inconsistent with the formation and decomposition of a (Scheme 4.15), but the other possibilities cannot be excluded on available data.

Finally the formation of HC_2O^- (Figure 4.6 and Table 4.8) is not easily explained. There is no apparent correlation of the abundance of the peak corresponding to H_2CO^- with the "migratory aptitude" of RO (Table 4.8). However, a possible mechanism may involve the disolvated alkoxide intermediate b shown in equation 42.

Chapter 5

Conclusion

Proton abstraction from 3-ethylpentan-2-one yields two enolate anions, both of which may be identified by characteristic fragmentations. Double isotope fractionation experiments have been successfully employed to elucidate the stepwise mechanism for the loss of methane from deprotonated 3-ethylpentan-2-one. The questions raised about the fragmentations of 3,3-dimethylheptan-4-one have been answered, namely: i) the loss of C_2H_4 is the major collision induced dissociation of the 3,3-dimethylheptan-4-one enolate anion, the six centred mechanism proposed for this fragmentation is shown in *Scheme 2.11 (a) page 45*. However if there is a CD_3 group at position 1, a deuterium isotope effect discriminates against the reaction 2.11 (a) such that a second reaction 2.11 (b) is observed. (ii) The enolate ion of 3,3-dimethylheptan-4-one cannot eliminate CH_4 by a standard process (see *equation 7 page 28*), instead three alternative losses of methane are observed (*equations 11 to 13 page 47*).

The study of the collision induced dissociation of some aromatic anions has answered the questions raised in the introduction of chapter 3, namely: i) the characteristic fragmentation of $Ph\bar{C}Et_2$ is β cleavage to the anion site to form $\{Me^- [Ph(Et)C=CH_2]\}$ which then undergoes a number of subsequent reactions including deprotonation and elimination, ii) phenyl substituted benzyl anions eliminate C_4H_4 ; Ph_3C^- , in addition also loses C_6H_6 . iii) examples have been discovered where fragmentation of aromatic systems occur with the hydrogen skeleton of the ion remaining intact, e.g. losses of

C_4H_4 and C_6H_4 from Ph_3C^- . In contrast there are slow processes which involve both inter-ring H transfer and intra-ring H scrambling, e.g. loss of C_6H_6 from Ph_3C^- .

Deuterium labelling has shown that the non decomposing adduct formed from the reaction of Me_2BOR and RO^- ($R = Me, Et$) in the gas phase is likely to have a tetrahedral geometry. The collision induced fragmentations of this ion may be explained through the intermediacy of ion complexes. An interesting hydride transfer from the alkoxide to the borane occurs in these systems. This is illustrated in *equation 12 (page 81)*; this is the first time this type of reaction has been observed in gas phase boron chemistry.

The reaction of alkoxides of the type $XCH_2CH_2O^-$ with Me_3B ($X = Me_2N, MeS, MeO, F$ and HO) produces non decomposing adducts in the source of the mass spectrometer, it has been suggested that this reaction may form two isomeric adducts, viz: $Me_3\bar{B}OCH_2CH_2X$ and $Me_3\bar{B}XCH_2CH_2O^-$. Collisional activation of these adducts leads to some novel rearrangements; it has been suggested that some of these fragmentations occur through "remote" fragmentation mechanisms (*scheme 4.9, 4.10 and 4.11, pages 95, 97, 98 respectively*).

Chapter 6

Experimental

9.1 General

Collisional activation (CA) mass spectra were recorded on a VG ZAB 2HF mass spectrometer operating in the chemical ionization mode. All slits were fully open to obtain maximum sensitivity and to minimize energy resolution effects¹⁵¹. The chemical ionization slit was used in the ion source; ionizing energy was 100 eV (tungsten filament), ion source temperature 150°C, accelerating voltage -8 kV. Anions of compounds and their labelled derivatives were generated by H⁺ abstraction with HO⁻ (or H⁻ or O^{-•}), D⁺ abstraction with DO⁻ (or D⁻ or O^{-•}), or from the complexing with alkoxides (RO⁻). Reactant ions were generated from H₂O, D₂O or ROH introduced through the septum inlet. Solid samples were introduced via a heated direct inlet probe, gases and low boiling point liquids (< 30°) were introduced through a gas inlet, and all other liquid samples were introduced through the heated septum inlet. The indicated source ion gauge pressure (of reactant gas) was typically 5×10^{-6} Torr, the pressure of the substrate was 2×10^{-6} Torr and the estimated total pressure within the ion source was 10^{-2} Torr. The pressure of He in the second field free collision cell was 2×10^{-7} Torr, measured by an ion gauge situated between the electric sector and the second collision cell. This produced a decrease in the main beam of c.a. 10% and corresponds to essentially single collision conditions¹⁵². The same pressure was used in the first collision cell for linked scan experiments. CA mass spectra were measured with He in the second cell and by scanning the electric sector. CA linked scan mass spectra were measured with He in the

first collision cell and by simultaneously scanning ($E/B = \text{constant}$) the magnetic and electric sectors.

Isotope effects listed in the text were determined by comparing the peak areas of the appropriate dissociations in each spectrum: listed values are a mean of ten individual measurements. Peak widths at half height are also a mean of ten individual measurements.

Routine positive ion mass spectra were recorded with an AEI MS 3074 double sector mass spectrometer operating at an electron energy of 70 eV. The samples were introduced into the ion source by a direct insertion probe. Infrared spectra were recorded on a Jasco A-102 infrared spectrophotometer as a nujol mull or as a liquid film. The 1602 cm^{-1} peak of polystyrene was used as a standard. Proton nuclear magnetic resonance spectra were recorded on either a Jeol PMX-60 spectrometer, a Varian T-60 operating at 60 MHz, or a Bruker WP-80 spectrometer operating at 80 MHz. All n.m.r. spectra were obtained in deuteriochloroform using tetramethylsilane as an internal standard. Data are given in the following order; chemical shift (δ) in p.p.m., relative intensity indicating the number of protons, and multiplicity. Abbreviations s=singlet; d=doublet; t=triplet; q=quartet; m=multiplet; b=broad.

Melting points were determined using a Kofler hot-stage melting point apparatus and are uncorrected. All solvents were of analytical grade or were purified according to standard procedures¹⁵³ before use. Petroleum ether refers to petroleum ether boiling point in the range 60-70°C. Solvent removed *in vacuo* refers to removal of solvent using a Buchi Rotavap operating at water aspirator pressure.

9.2 Labelled Compounds.

The identity and incorporation of labelled compounds was routinely checked by positive ion mass spectrometry and proton n.m.r.. The following isotopically labelled compounds were commercially available and used without further purification: deuterium gas, deuterium oxide (> 99% atom, AINSE), iodomethane-d₃ (>99% atom, Aldrich), bromobenzene-d₅ (>99% atom, Aldrich), methanol-d₁ (>99% atom, Aldrich), methanol-d₄ (>99% atom, Aldrich), acetic acid-d₄ (> 99% atom, Service des molécule Marquées France), lithium aluminium hydride-d₄ (>98% atom, Aldrich), ethanol-d₆ (>99% atom, Merck, Sharp and Dohme.), 1-iodoethane-1-¹³C (98% atom), 1-iodoethane-2-¹³C (98% atom), benzoic acid-*carboxy*-¹³C (60% atom).

The following labelled compounds were prepared by standard methods:

ethan-1-ol-2,2,2-d₃¹⁵⁴, ethan-1-ol-1,1-d₂¹⁵⁵, 1-iodoethane-1,1-d₂¹⁵⁶,
 1-iodoethane-2,2,2-d₃¹⁵⁶, 1-iodoethane-1,1,2,2,2-d₅¹⁵⁶,
 bromobenzene-2,4,6-d₃¹⁵⁷, acetaldehyde-d₄¹⁵⁸, acetaldehyde-2,2,2-d₃¹⁵⁹,
 methyl acetate-1,1,1-d₃¹⁶⁰, and methyl-d₃ acetate¹⁶¹. These compounds were distilled before use.

9.3 Synthesis of Compounds Described in Chapter 2.

3-Ethylpentan-2-one

(i) Ethyl α -ethylacetoacetate

Potassium t-butoxide (11.2 g, 0.1 mol) was dissolved in anhydrous *tert*-butanol (100ml). Ethyl acetoacetate (13g, 0.1mol) was added dropwise

over a period of 10 min., and the solution allowed to stir for a further 15 min at 25°C. Iodoethane (0.1 mol, 8 ml) was added dropwise over 10 min., and the mixture heated under reflux for 3 hours. The *tert*-butanol was distilled off, water (50 ml) added, and the solution extracted with diethyl ether (2 x 40 ml). The combined organic phases were washed with water (25 ml), aqueous sodium chloride (saturated, 25 ml) and dried (Na_2SO_4). The solvent was removed *in vacuo* and the crude product distilled to yield ethyl α -ethylacetoacetate. b.p. 95°C/18 mm Hg (Lit¹⁶² :189°/743 mm Hg), [12.1 g, 76%],

$^1\text{H NMR}$: δ 4.2, 2H, s; 3.4, 1H, t; 2.15 3H, t; 1.95, 2H, m; 1.35, 3H, t; 0.95 3H, t.

(ii) *Ethyl α,α -diethylacetoacetate*

Potassium t-butoxide (0.72 g, 6.4 mmol) was dissolved in anhydrous *tert*-butanol (8 ml), ethyl α -ethylacetoacetate (1 g, 6.4 mmol) was added dropwise over a period of 10 min., and the solution allowed to stir for 15 min at 25°C. Iodoethane (6.4 mmol, 0.5 ml) was added dropwise over 10 min., and the mixture was heated under reflux for 3 hours. The *tert*-butanol was distilled off, water (30 ml) added, and the solution extracted with diethyl ether (3 x 12 ml). The organic extract was washed with water (20 ml), aqueous sodium chloride (saturated, 20 ml) and dried (Na_2SO_4). The solvent was removed *in vacuo* to yield crude ethyl α,α -diethylacetoacetate which was used without further purification.

(iii) *3-Ethylpentan-2-one*

Sodium hydroxide (0.9 g), methanol (2 ml) and water (8 ml) was added to the crude ethyl α,α -diethylacetoacetate (see (ii) above), and the mixture was

heated under reflux for 6 hours. Aqueous sodium chloride (saturated, 25 ml) was added and the solution extracted with diethyl ether (3 x 10 ml). The combined organic phases were washed with water (25 ml), aqueous sodium chloride (saturated, 25 ml) and dried (Na_2SO_4). Pure 3-ethylpentan-2-one was collected by distillation b.p. 138-140° (Lit¹⁶³: 135-139°), [0.6g, 82%].

(3-Ethyl-1,1-d₂)pentan-2-one (3-Ethyl-2,2,2-d₃)pentan-2-one
 (3-Ethyl-1-¹³C)pentan-2-one (3-Ethyl-1,1,2,2,2-d₅)pentan-2-one
 (3-Ethyl-2-¹³C)pentan-2-one-5-¹³C (3-Ethyl-2-¹³C)pentan-2-one
 (3-Ethyl-2,2,2-d₃)pentan-2-one-5,5,5-d₃

These compounds were prepared by the method used to prepare 3-ethylpentan-2-one, using the appropriate labelled iodoethanes. Yields were 83%, 85%, 92%, 91%, 92%, 80%, 81% respectively. Deuterium incorporation was greater than 98%, carbon-13 incorporation was 98%.

3,3-Dimethylheptan-4-one

(i) 3-chloro-3-methylbutane

This was prepared from 3-methylbutan-3-ol by a standard method¹⁶⁴ in 70 % yield.

(ii) 3,3-Dimethylpentan-2-one

This was prepared by modifications of the methods of Whitmore and Ansell¹⁶⁵.

A solution of the Grignard reagent prepared from 3-chloro-3-methylbutane (42.6 g) and magnesium (9.75 g) in anhydrous diethyl ether (100 ml) was added dropwise, with stirring over a 5 hour period, to a solution of acetic

anhydride (40.8 g) in anhydrous diethyl ether (75 ml) maintained at -78°C under an atmosphere of nitrogen. The mixture was allowed to warm to 20°C , aqueous ammonium chloride (saturated, 200 ml) was added, the organic phase was separated and the extracted with diethyl ether (2 x 100 ml). The combined organic extract was washed with aqueous sodium hydroxide (3 x 50 ml), aqueous sodium chloride (saturated, 50 ml), dried (Na_2SO_4) and fractionated. The fraction of b.p. $125\text{-}132^{\circ}/760$ mm (15.5 g) was redistilled ($70\text{-}72^{\circ}/98$ mm Hg) (Lit¹⁶⁶: 120°) to give 3,3-dimethylpentan-2-one as a colourless liquid (12.3 g, 27 %).

i.r. (film), ν , 2950 (C—H), 1705 (CO),

$^1\text{H NMR}$: δ , 2.1, 3H, s; 1.5, 2H, q; 1.15, 6H, s; 1.8, 3H, t.

(iii) *N,N*-Dimethylhydrazone of 3,3-dimethylpentan-4-one.

This was prepared by a modification of the method of Wiley and Irick¹⁶⁷.

A solution of 3,3-dimethylpentan-4-one (4.56 g) and *N,N*-dimethylhydrazine (3.8 ml) was heated under reflux for 4.5 hours under an atmosphere of nitrogen. The mixture was allowed to cool to 20°C , sodium hydroxide (2 g) was added, the organic phase was decanted and fractionated. Crude hydrazone (4.1 g) was obtained (b.p. $64\text{-}78^{\circ}/60$ mm).

$^1\text{H NMR}$: δ , 2.3, 6H, s; 1.8, 3H, s; 1.3 2H, q; 1.8, 3H, t.

(iv) *N,N*-Dimethylhydrazone of 3,3-dimethylheptan-4-one

This method was prepared by a modification of the method of Corey and Enders¹⁶⁸.

n-Butyl lithium in hexane (1.03 ml, 1.6 M, 1.65 mmol) was added with stirring

to a solution of diisopropylamine (167 mg) in anhydrous tetrahydrofuran (5 ml) at 0°, under nitrogen. The solution was allowed to stir for 15 min., and crude hydrazone (234 mg, see (iii) above) in anhydrous tetrahydrofuran (1.5 ml) was added, the mixture was stirred at 0° for 2 hours, then cooled to -78°. Iodoethane (260 mg) was added, the mixture stirred at -78° for 1.5 hours, allowed to warm to 20°, and poured into water (25 ml). The mixture was extracted with dichloromethane (3 x 15 ml), and the organic extract washed with water (2 x 10 ml), aqueous sodium chloride (saturated, 15 ml) and dried (Na₂SO₄). Removal of the solvent gave crude hydrazone (270 mg, 98%).

(v) 3,3-Dimethylheptan-4-one.

A mixture of hydrazone (270 mg, see (iv) above), aqueous hydrogen chloride (2N, 25 ml) and diethyl ether (25 ml) was allowed to stir at 20° for 3.5 hours. The organic phase was separated, the aqueous phase extracted with diethyl ether (2 x 10 ml), and the organic extract washed with water (15 ml), aqueous sodium chloride (saturated, 15 ml) and dried (K₂CO₃). Removal of the solvent followed by distillation of the remaining oil in a glass T tube at 120°/50 mm Hg gave 3,3-dimethylheptan-4-one (194 mg, 94 % yield) (Lit¹⁶⁹: 83-84°/10 mm Hg).

¹H NMR: δ, 2.0, 2H, t; 1.3, 4H, b; 1.0, 6H, s; 0.9, 3H, t, 0.85, 3H, t.

3,3-Dimethylheptan-4-one-6,6-d₂

This compound was prepared in a similar manner to that of 3,3-dimethylheptan-4-one, except that 1-iodoethane-1,1-d₂ was used instead of iodoethane in step (iii), b.p. 120-25°/50 mm Hg, [0.16 g, 64%], d₂=99%

3,3-Dimethylheptan-4-one-7,7,7-d₃

This compound was prepared in a similar manner to 3,3-dimethylheptan-4-one, except that 1-iodoethane-2,2,2-d₃ was used instead of iodoethane in step (iii), b.p. 120-25°/50 mm Hg, [0.15 g, 59%], d₃=99%

3,3-Dimethylheptan-4-one-2,2-d₂.*(i) 2-Bromo-2-methylhexan-3-one.*

Bromine (25 g) was added dropwise with stirring to a solution of 2-methylhexan-3-one (17.9 g), glacial acetic acid (100 ml) and water (20ml). The reaction temperature was increased to 80° over a period of 1 hour, and the reaction mixture allowed to stir at 80° for 20 min. The solution was allowed to cool to 20°, diluted with water (100 ml), sodium carbonate (10 g) added, and the mixture extracted with diethyl ether (3 x 50 ml). The ethereal extract was washed with water (50 ml), dried (Na₂SO₄), the solvent removed, and 2-bromo-2-methylhexan-3-one was obtained by distillation (b.p. 140-140°/100 mm Hg) (Lit¹⁷⁰ : 62-65°/13 mm Hg), [25.5 g, 85 %], d₂=99%

¹H NMR: δ, 2.6, 2H, t; 1.7, 6H, s; 1.1, 2H, q; 0.9, 3H, t.

(ii) 3,3-Dimethylheptan-4-one-2,2-d₂.

This was prepared by a modification of the method of Weiss¹⁷¹.

2-Bromo-2-methylhexan-3-one (1.2 g) was added dropwise to a stirred solution of lithium (0.91 g) in liquid ammonia (150 ml) under nitrogen. Iodoethane-1,1-d₂ (0.5 ml) in anhydrous diethyl ether (20 ml) was added, the solution was allowed to stir for 1 hour, then iodoethane-1,1-d₂ (0.5 ml) was

added and the solution allowed to stir at -33° for 12 hours. The ammonia was allowed to evaporate off as the solution warmed to 20° , ammonium chloride (2.0 g) was added, followed by water (20 ml) and diethyl ether (20 ml). The layers were separated and the aqueous layer extracted with diethyl ether (2 x 20 ml). The organic extract was washed with water (15 ml), aqueous sodium chloride (saturated, 20 ml) and dried (Na_2SO_4). Distillation yielded 3,3-dimethylheptan-4-one-2,2- d_2 (0.65 g, 90 %) b.p. $125-30^{\circ}/50$ mm, $d_2=99\%$.

3,3-Dimethylheptan-1,1,1- d_3 -4-one.

This was prepared in 92% yield in the same manner as 3,3-dimethylheptan-4-one-2,2- d_2 except that 1-iodoethane-2,2,2- d_3 was used instead of 1-iodoethane-1,1- d_2 , $d_3=98\%$.

3,3-Dimethylheptan-4-one-1,1,1,2,2- d_5 .

This was prepared in 89% yield in the same manner as 3,3-dimethylheptan-4-one-2,2- d_2 except that 1-iodoethane-1,1,2,2,2- d_5 was used instead of 1-iodoethane-1,1- d_2 , $d_5=98\%$.

9.4 Synthesis of Compounds Described in Chapter 3.

3-Phenylpentane-1,1,1- d_3

(i) 3-Phenylpentan-3-ol-1,1,1- d_3

1-Iodoethane-2,2,2- d_3 (1 g, 6.3 mmol) in anhydrous diethyl ether (2 ml) was

added dropwise with stirring to a mixture of magnesium (0.15 g, 6.3 mmol) in anhydrous diethyl ether (4 ml) at 20° under an atmosphere of nitrogen, and the mixture was allowed to stir for 20 min.. Propiophenone (0.84 g, 6.3 mmol) in anhydrous diethyl ether (2 ml) was added, the mixture was heated under reflux for 3 hours, and then allowed to cool to 20°C. Water (1 ml) was added, followed by concentrated sulphuric acid (15 ml), and the solution stirred for 30 min.. The solution was extracted with diethyl ether (3 x 10 ml), the combined organic extract was washed with aqueous sodium hydrogen carbonate (saturated, 2 x 20 ml), water (20 ml), aqueous sodium chloride (saturated, 20 ml) and dried (Na_2SO_4). The solvent was removed by distillation to yield a pale yellow oil (0.98 g).

(ii) 3-Phenylpentane-1,1,1-d₃

The crude product (0.98 g) from (i) above was dissolved in glacial acetic acid (10 ml) containing concentrated sulphuric acid (1 drop). 5 % Palladium on charcoal (50 mg) was added and the mixture stirred under an atmosphere of hydrogen for 6 hours. The mixture was filtered through celite, the celite washed with diethyl ether (30 ml), the combined organic extract was neutralized with aqueous sodium hydroxide (50 %, 15 ml), washed with water (20 ml), aqueous sodium chloride (saturated, 20 ml) and dried (Na_2SO_4).

3-Phenylpentane-1,1,1-d₃ was collected by distillation, b.p. 83-85°/22 mm Hg (Lit¹⁷²: 180°), (0.85 g, 88%), d₃=99%.

¹H NMR: δ , 7.1, 5H, s; 2.3, 1H, q; 1.8, 3H, q; 0.8, 4H, t.

(3-Phenyl-d₅)pentane*(i) (3-Phenyl-d₅)pentan-3-ol*

Bromobenzene-d₅ (0.96 g, 4.6 mmol) in anhydrous diethyl ether (2 ml) was added with stirring to a mixture of magnesium (0.11 g, 4.6 mmol) in anhydrous diethyl ether (5 ml) under an atmosphere of nitrogen, and the mixture was allowed to stir at 20° for 20 min.. Pentan-3-one (0.4 g, 4.6 mmol) in anhydrous diethyl ether (2 ml) was added, the mixture was heated under reflux for 1.5 hours, then allowed to cool to 20°C. Water (1 ml) was added, followed by concentrated sulphuric acid (15 ml), and the solution stirred for 30 min.. The solution was extracted with diethyl ether (3 x 10 ml), the organic extract was washed with aqueous sodium hydrogen carbonate (saturated, 2 x 20 ml), water (20 ml), aqueous sodium chloride (saturated, 20 ml) and dried (Na₂SO₄). The solvent was removed by distillation to yield a pale yellow oil (0.69 g).

(ii) (3-Phenyl-d₅)pentane

The crude product (0.69 g) from (i) above was dissolved in glacial acetic acid (10 ml) with concentrated sulphuric acid (1 drop). 5 % Palladium on charcoal (50 mg) was added and the mixture stirred under an atmosphere of hydrogen for 6 hours. The mixture was filtered through celite, the celite washed with diethyl ether (30 ml), the combined organic extract was neutralized with aqueous sodium hydroxide (50 %, 15 ml), washed with water (20 ml), aqueous sodium chloride (saturated, 20 ml) and dried (Na₂SO₄).

(3-Phenyl-d₅)pentane was collected by distillation, b.p. 83-85°/22 mm Hg, (0.58 g, 85 %), d₅=99%

¹H NMR: δ, 2.5, 1H, m; 1.9, 4H, m; 0.9, 6H, t.

Diphenylmethane

(i) Diphenylmethanol

Bromobenzene (0.45 ml, 0.67 g, 4.1 mmol) in anhydrous diethyl ether (2 ml) was added dropwise to a rapidly stirred mixture of magnesium (4.1 mmol, 0.1 g), iodine (1 crystal) and anhydrous diethyl ether (2 ml) at 20° under an atmosphere of nitrogen. The solution was allowed to stir for 30 min., and benzaldehyde (0.43 g, 0.42 ml, 4.1 mmol) in anhydrous diethyl ether (2 ml) was added dropwise over a period of 10 min.. The mixture was heated under reflux for 2 hours, and allowed to cool to 20°. Water (0.5 ml), aqueous sulphuric acid (10%, 5 ml), water (15 ml) was added, the organic layer was separated and the aqueous layer extracted with diethyl ether (3 x 10 ml). The combined organic extract was washed with aqueous sodium hydrogen carbonate (saturated, 2 x 20 ml), water (20 ml), aqueous sodium chloride (saturated, 20 ml) and dried (Na₂SO₄). The solvent was removed *in vacuo* to yield a pale yellow oil. Recrystallization (petroleum ether) of the oil gave pure diphenylmethanol, (0.66 g, 89%), m.p. = 69-70° (Lit¹⁷³ = 68°) .

(ii) Diphenylmethane

A mixture of diphenylmethanol (0.66 g, 3.5 mmol), palladium on charcoal (5%, 50 mg) and ethanol (15 ml) was stirred for 4 hours at 20°C under an atmosphere of hydrogen (in a standard hydrogenation apparatus). The

solution was filtered through celite and the solvent removed *in vacuo*. Pure diphenylmethane (0.53 g, 91%) was collected by sublimation 80-90°/10 mm Hg (lit¹⁷⁴ 261-262°), m.p. 24-25° (lit¹⁷⁵ 24-25°).

¹H NMR: δ , 7.0, 10H, s; 3.8, 2H, s.

(Phenyl-2,4,6-d₃)phenylmethane

This compound was prepared by the the reaction of phenyl-2,4,6-d₃ magnesium bromide with benzaldehyde followed by hydrogenation using the same procedure used for the preparation of diphenylmethane, [0.95 g, 63 %], b.p. 80-90°/10 mm Hg, m.p. 24-25°, d₃ = 98%.

(Phenyl-d₅)phenylmethane

This compound was prepared by the the reaction of phenyl-d₅ magnesium bromide with benzaldehyde followed by hydrogenation in a similar manner to that used for the preparation of diphenylmethane [1.13 g, 73 %], b.p. 80-90°/10 mm Hg, m.p. 24-25°, d₅ = 99%.

Diphenylmethane-1-¹³C

A mixture of diphenylmethanol-1-¹³C (25 mg, 0.14 mmol, available from a previous study), palladium on charcoal (5%, 10 mg) and ethanol (5 ml) was stirred for 6 hours at 20°C under an atmosphere of hydrogen (in a standard hydrogenation apparatus). The solution was filtered through celite and the solvent removed *in vacuo*. Diphenylmethane-1-¹³C (13 mg, 55%) was collected by sublimation (80-90°/10 mm Hg), m.p. 24-25°, ¹³C = 60.5%.

3-Phenylpentane-2,2-d₂

Li₂CuCl₄ in anhydrous tetrahydrofuran (0.5 ml, 0.1 M) was added with stirring to a solution of 1-bromo-1-phenylpropane (0.98 g, 4.9 mmol) and ethyl-1,1-d₂-magnesium iodide in anhydrous tetrahydrofuran (4.9 ml, 1M, 4.9 mmol) at 0° under an atmosphere of nitrogen. The solution was allowed to stir for 3 hours, and then warmed to 20°. Aqueous hydrogen chloride (10%, 20 ml) was added, the organic layer was separated and the aqueous layer extracted with diethyl ether (3 x 15 ml). The combined organic phases were washed with aqueous sodium hydrogen carbonate (saturated, 20 ml), water (20 ml), aqueous sodium chloride (saturated, 20 ml) and dried (Na₂SO₄). Pure 3-phenylpentane-2,2-d₂ was collected by distillation, b.p. 83-5°/20 mm Hg, [0.34 g, 46%], d₂=98%.

Triphenylmethane-¹³C

(i) Methyl benzoate-carboxy-¹³C

Diazald (1.5 g) was added portionwise at 20° to a two phase solution of benzoic acid-carboxy-¹³C (3 mmol, 0.376 g) in diethyl ether (6 ml) and aqueous sodium hydroxide (50%, 6 ml) until a faint yellow colour remained. The solution was allowed to stir at 20° for 2 hours, and the product extracted with diethyl ether (3 x 20 ml). The excess solvent was removed *in vacuo*, and distillation gave methyl benzoate-carboxy-¹³C, [0.38 g, 94 %], b.p. 90-93°/20 mm Hg (Lit¹⁷⁶ : 198-200°).

(ii) Triphenylmethanol-1-¹³C

Bromobenzene (0.62 g, 4 mmol) in anhydrous diethyl ether (2 ml) was added

dropwise to a rapidly stirred mixture of magnesium (4 mmol, 0.1 g) and iodine (1 crystal) in anhydrous diethyl ether (2 ml) under an atmosphere of nitrogen. The solution was allowed to stir for 30 min., methyl benzoate-*carboxy*- ^{13}C (0.2 g, 1.5 mmol) in anhydrous diethyl ether (5 ml) was added, and the mixture heated under reflux for 12 hours. Aqueous hydrogen chloride (10%, 20 ml) was added, the organic phase was separated and the aqueous phase extracted with diethyl ether (3 x 15 ml). The combined organic extract was washed with aqueous sodium hydrogen carbonate (saturated, 20 ml), water (20 ml), aqueous sodium chloride (saturated, 20 ml) and dried (Na_2SO_4). The solvent was removed *in vacuo* and the residue recrystallized from ethanol to give triphenylmethanol- ^{13}C (0.38 g, 97%), m.p = 157-160°C (Lit¹⁷⁷=164-165°), ^{13}C = 60%.

(iii) *Triphenylmethane-1- ^{13}C*

A mixture of triphenylmethanol- ^{13}C (0.3 g, 1.1 mmol) and sodium borohydride (0.7g, 20 mmol) was added portionwise with rapid stirring to trifluoroacetic acid (10 ml) at 0° under an atmosphere of nitrogen, the mixture was allowed to stir at 20° for 1 hour, and the trifluoroacetic acid was removed *in vacuo*. Aqueous sodium hydrogen carbonate (saturated, 30 ml) was added to the residue, and the solution extracted with diethyl ether (3 x 25 ml), the organic extract was washed with water (30 ml), aqueous sodium chloride (saturated, 30 ml) and dried (Na_2SO_4). The solvent was removed *in vacuo* and the crude product recrystallized from ethanol to give triphenylmethane-1- ^{13}C (0.2 g, 71%), m.p = 91-93° (Lit¹⁷⁸: 92°).

Tri(phenyl-2,4,6-d₃)methane*(i) Tri(phenyl-2,4,6-d₃)methanol*

Bromobenzene-2,4,6-d₃ (0.96 ml, 9 mmol) in anhydrous diethyl ether (2 ml) was added dropwise at 20° with stirring to a mixture of magnesium (9 mmol, 0.2 g) and iodine (1 crystal) in anhydrous diethyl ether (10 ml) at 20° under an atmosphere of nitrogen. The solution was allowed to stir for 30 min., and diethyl carbonate (0.36 ml, 3 mmol) in anhydrous diethyl ether (5 ml) was added dropwise over a period of 10 min.. The mixture was heated under reflux for 12 hours, and then allowed to cool to 20°. Aqueous hydrogen chloride (10%, 20 ml) was added, the organic layer was separated and the aqueous layer extracted with diethyl ether (3 x 15 ml). The combined organic extracts were washed with aqueous sodium hydrogen carbonate (saturated, 20 ml), water (20 ml), aqueous sodium chloride (saturated, 20 ml) and dried (Na₂SO₄). The solvent was removed *in vacuo* to give crude tri(phenyl-2,4,6-d₃)methanol [0.71 g], which was recrystallized from ethanol, m.p. = 161-63°, [0.62 g, 76%].

(ii) Tri(phenyl-2,4,6-d₃)methane

Tri(phenyl-2,4,6-d₃)methanol was reduced with sodium borohydride and trifluoroacetic acid in a similar manner to that described for the reduction of triphenylmethanol-1-¹³C to give tri(phenyl-2,4,6-d₃)methane, m.p. 93-95° [0.39 g, 85%], d₉ = 98%.

Tri(phenyl-d₅)methane

Tri(phenyl-d₅)methane was prepared by a similar procedure to that described for tri(phenyl-2,4,6-d₃)methane except that bromobenzene-d₅ was used instead of bromobenzene-2,4,6-d₃, m.p. = 91-92°, [0.2 g, 56%], d₁₅ = 97%.

(Phenyl-d₅)diphenylmethane

(i) (Phenyl-d₅)phenylmethanol

Bromobenzene-d₅ (0.32 ml, 3 mmol) in anhydrous diethyl ether (2 ml) was added dropwise with stirring to a mixture of magnesium (3 mmol, 0.07 g) and iodine (1 crystal) in anhydrous diethyl ether (6 ml) at 20° under an atmosphere of nitrogen. The solution was allowed to stir for 30 min., benzophenone (0.54 g, 3 mmol) in anhydrous diethyl ether (5 ml) added, and the mixture heated under reflux for 12 hours. Aqueous hydrogen chloride (10%, 20 ml) was added, the organic layer was separated and the aqueous layer extracted with diethyl ether (3 x 15 ml). The combined organic phases were washed with aqueous sodium hydrogen carbonate (saturated, 20 ml), water (20 ml), aqueous sodium chloride (saturated, 20 ml) and dried (Na₂SO₄). The solvent was removed *in vacuo* to give crude (phenyl-d₅)diphenylmethanol [0.7 g, 89%].

(ii) (Phenyl-d₅)diphenylmethane

(Phenyl-d₅)diphenylmethanol (from (i) above) was reduced with sodium borohydride and trifluoroacetic acid in a similar manner to that described for

the reduction of triphenylmethanol-1- ^{13}C to give (phenyl- d_5)diphenylmethane, m.p. = 91-92°, [0.56 g, 86%], $\text{d}_5 = 99\%$.

9.5 Synthesis of Compounds Described in Chapter 4.

2-Methoxyethan-1-ol-1,1- d_2

(i) Methyl 1-methoxyacetate

Methyl α -bromoacetate (20 ml, 0.15 mol) was added dropwise with stirring to a solution of sodium (3.45 g, 0.15 mol) in anhydrous methanol (100 ml). The solution was heated under reflux for 3 hours and methyl methoxyacetate was collected by distillation b.p. 129-130° (Lit¹⁷⁹: 129°), [10.6 g, 68%]

(ii) 2-Methoxyethan-1-ol-1,1- d_2

Methyl 1-methoxyacetate (5 mmol, 0.52g) was added dropwise at 20° to a rapidly stirred suspension of lithium aluminium deuteride (2.5 mmol, 0.12 g) in anhydrous diethyl ether (5 ml) under an atmosphere of nitrogen. The solution was heated under reflux for 1 hour, allowed to cool to 20° and aqueous sodium hydroxide (10%, 0.25 ml) was added to the suspension. The mixture was filtered, and the product collected by distillation, b.p. 124-125° (lit¹⁸⁰: 123.5-125°), [0.34 g, 88%], $\text{d}_2=99\%$.

2-(Methoxy- d_3)ethan-1-ol

A solution of sodium (0.16 g, 7.1 mmol), methanol- d_4 (0.25 g, 7.1 mmol), 2-chloroethan-1-ol (0.56 g, 0.71 mmol) and anhydrous tetrahydrofuran (5 ml) was placed in a sealed glass tube and heated at 80° for 1 hour. The reaction mixture was allowed to cool to 20°, filtered and the filtrate distilled to give

2-(methoxy-d₃)ethan-1-ol, b.p.=125-126°, [0.41 g, 74%], d₃=99%.

2-(Methylthio)ethan-1-ol

Potassium *tert*-butoxide (0.18g, 1.6 mmol) was added to a solution of 2-mercaptoethanol (0.11 ml, 1.6mmol, 0.13g) in anhydrous tetrahydrofuran (2 ml) and allowed to stir for 10 min. Iodomethane (0.1ml, 1.6 mmol) in anhydrous tetrahydrofuran (1 ml) was added, and the solution heated under reflux for one hour. The reaction mixture was filtered and the product collected by distillation, b.p. 169-171°C (Lit¹⁸¹: 68-70°/20 mm Hg); [0.13 g, 87%].

¹H NMR: δ, 3.9, 2H, t; 2.9, 2H, t; 4.8, 1H, s; 2.1, 3H, s.

2-(Methyl-d₃-thio)ethan-1-ol

This was prepared by the same method as 2-(methylthio)ethan-1-ol except iodomethane-d₃ was used instead of iodomethane, b.p. 169-171°C, [0.11g, 83%], d₃=98%.

2-(N,N-Dimethylamino-d₆)ethanol

A solution of ethanolamine (3.8 mmol, 0.23 g), triethylamine (1.6 ml, 11.5 mmol) and iodomethane-d₃ (0.5 ml, 1.14 g, 7.7 mmol) was heated under reflux for 3 hours, the reaction mixture was allowed to cool to 20° and filtered. The product was collected by distillation to yield 2-(N,N-dimethylamino-d₆)-ethanol b.p. 133-134° (Lit¹⁸² : 135°), [0.13 g, 37%], d₆=99%.

Bromodimethylborane

Tetramethyltin (5 ml, 6.45 g, 36.1 mmol) was added dropwise with stirring to tribromoborane (9.05 g, 36.1 mmol, 3.4 ml) at -50°C under an atmosphere of nitrogen, the reaction was allowed to stir for 1 hour, and then allowed to warm to 20°C . The reaction mixture was distilled at 170° and the distillate redistilled to yield bromodimethylborane (4.7 g, 39 %) b.p. $34-37^{\circ}$ (Lit¹⁸³ : $37-38^{\circ}$).

(Methyl- d_3)dimethylborane

Bromodimethylborane (7.86 mmol, 0.95 g) was added dropwise with stirring to a solution of methyl- d_3 magnesium iodide in anhydrous diethyl ether (1M, 8 ml, 7.86 mmol) at 0° under an atmosphere of nitrogen. The solution was allowed to stir for 30 min., and then heated under reflux for 10 min.. During this time (methyl- d_3)dimethylborane¹⁸⁴ distilled off, and was collected in a U tube cooled to -78° , [0.59 g, 85%], $\text{d}_3=99\%$.

Methoxydimethylborane

Anhydrous methanol (0.5 ml, 0.56 g, 15.5 mmol) was added dropwise with stirring to a solution of bromodimethylborane (15.5 mmol, 1.88 g) in anhydrous benzene (5 ml) under an atmosphere of nitrogen, and allowed to stir at 20° for 30 min.. Methoxydimethylborane was collected by distillation b.p. $34-38^{\circ}$ (Lit¹⁸⁵ : $34-36^{\circ}$), [0.86 g , 78%].

(Methoxy-d₃)dimethylborane

This was prepared in a similar manner to that of methoxydimethylborane except anhydrous methanol-d₄ was used instead of anhydrous methanol, b.p.= 35-37°, [0.45 g, 79%], d₃=99%.

3-Methoxypropan-1-ol*(i) Methyl 2-methoxypropanoate*

Methyl acrylate (19 g, 0.22 mol) was added dropwise with stirring at 0° to a solution of sodium (0.22 mol, 5.3 g) in anhydrous methanol (100 ml). The solution was allowed to stir for 1 hour at 0°, warmed to 20°, allowed to stir for a further 30 min., neutralized by the addition of carbon dioxide, filtered and the product collected by distillation, b.p. 141-143° (Lit¹⁸⁶:43-45°/13 mm Hg), [9.3 g, 36%].

(ii) 3-Methoxypropan-1-ol

Methyl 3-methoxypropanoate (8.5 mmol, 1 g) was added dropwise with stirring to a suspension of lithium aluminium hydride (0.09 g, 2.5 mmol) in anhydrous diethyl ether (5 ml) under an atmosphere of nitrogen. The solution was heated under reflux for 1 hour, allowed to cool to 20° and aqueous sodium hydroxide (10%, 0.25 ml) added to the suspension. The mixture was filtered, and the product collected by distillation, b.p. 151-152° (Lit¹⁸⁷ 148-149°), [0.7 g, 93%].

3-Methoxypropan-1-ol-1,1-d₂

This was prepared in a similar manner to that of 3-methoxypropanol except that lithium aluminium deuteride was used instead of lithium aluminium

hydride. b.p. 152-153° [0.71 g, 91%], $d_2 = 98\%$.

(3-Methoxy-d₃)propan-1-ol

3-Bromopropan-1-ol (2 g, 14.3 mmol) was added at 20° to a solution of sodium (0.33 g, 14.3 mmol) dissolved in methanol-d₄ (0.5 g, 14.3 mmol) and anhydrous tetrahydrofuran (3 ml). The reaction mixture was placed in a sealed glass tube and heated at 80° for 1 hour. The reaction mixture was filtered and the product collected by distillation. b.p. 152-153°, [0.97 g, 73 %], $d_3 = 99\%$.

4-Methoxybutan-1-ol

(i) 4-Bromobutan-1-ol

Aqueous hydrogen bromide (48%, 0.4 mol, 67 g) was added with stirring to a solution of tetrahydrofuran (100 ml) at 70°, heated under reflux for 2 hours, allowed to cool to 20°, neutralized with sodium carbonate (10 g), and filtered. The organic phase was separated, washed with water (2 x 30 ml), aqueous sodium chloride (saturated, 30 ml) and dried (Na₂SO₄). Vacuum distillation gave 4-bromobutan-1-ol, b.p. 64-67°/10 mm Hg (Lit¹⁸⁸ : 56-8°/3 mm Hg), [19.3 g, 32 %].

(ii) 4-Methoxybutan-1-ol

4-Bromobutan-1-ol (10 g, 65 mmol) was added at 20° with stirring to a solution of sodium (1.5 g, 65 mmol) dissolved in anhydrous methanol (100 ml). The reaction mixture was heated under reflux for 1 hour, allowed to cool to 20° and filtered. Vacuum distillation gave 4-methoxybutan-1-ol, b.p.

84-7°/10mm Hg (Lit¹⁸⁹ :63-64°/7 mm Hg), [4.6 g, 68%]

¹H NMR: δ , 3.4, 3H, s; 3.6, 6H, b; 1.8, 4H, b.

5-Methoxypentan-1-ol

5-Methoxypentan-1-ol was prepared in a similar manner to that of 4-methoxybutan-1-ol except that tetrahydropyran was used instead of tetrahydrofuran, b.p. 110-112°/16 mm Hg (Lit ¹⁸⁹ 102-104°/12 mm Hg), [2.4 g, 62%].

¹H NMR: δ , 3.9, 1H, d; 3.4, 3H, s; 3.6, 2H, t; 3.5, 2H, t; 1.5, 6H, b.

Alkylacetates

Tert-Butyl acetate was prepared from a standard reaction¹⁹⁰ of tert-butanol, acetylchloride and dimethylaniline. All other acetates were prepared from a standard reaction¹⁹¹ between acetylchloride and the appropriate alcohol.

Alkylacetate	Boiling Point (°C)	% Yield
n-Propyl	100-102 ¹⁹²	83
iso-Propyl	85-86 ¹⁹²	79
n-Butyl	124-6 ¹⁹²	83
tert-Butyl	96-8 ¹⁹²	36
Benzyl	93-4/10mm Hg ¹⁹²	52
Phenyl	195-196 ¹⁹²	45
Allyl	103-104 ¹⁹²	78

References

- (1) Aston, F.W., *Phil. Mag.*, 1919, 38, 707.
- (2) Dempster, A.J., *Phys Rev.*, 1918, 11, 316.
- (3) Brunee, C., *Spectra*, 1983, 9, 11.
- (4) Aplin, R.T., Budzikiewicz, H., Djerassi, C., *J. Amer. Chem. Soc.*, 1965, 87, 3180.
- (5) Wilson, J., *Mass Spec. Specialist Report.*, Chemical Soc. London 1971.
- (6) Melton, C.E., "*Mass Spectrometry of Negative Ions*", (Ed: McLafferty F.W.), Academic: New York 1971.
- (7) Stafford, G.C., *Envir. Hlth. Perspec.* 1980, 36, 85.
- (8) Bowie, J.H., *Mass Spec. Rev.*, 1984, 3, 161.
- (9) Jennings, K.R., *Phil. Trans. R. Soc. London A*, 1979, 293, 125.
- (10) Christophorou, L.G., *Envir Hlth. Perspec.*, 1980, 30, 3.
- (11) Large, R., Knof H., *Org. Mass Spectrom.*, 1976, 11, 582.
- (12) Gregor, I.K., Guilhaus M., *Mass Spec .Rev.* , 1984, 3 , 39.
- (13) von Ardenne, M., Steinfelder, K., Tummler, R., "*Electronenanlagerungs Massenspektrograhpic Organischen Substanzen*", Springer-Verlag: Berlin 1971.
- (14) Barber, M., Bordoli, R.S., Sedgwich, R.D., Tyler, A.N., *J. Chem. Soc. Chem. Comm.* 1981, 325.

- (15) Taylor, L.C.E. *Ind. Res. Dev.* 1981, 23, 124.
- (16) Tanaka, K., Mackay, G.I., Payzant, J.D., Bohme, D.K., *Can. J. Chem.*, 1976, 54, 1643.
- (17) von Ardenne, M., *Z. Angew. Phys.*, 1959, 11, 121.
- (18) McAllister, T., *J. Chem. Soc. Chem. Comm.*, 1972, 245.
- (19) Dougherty, R.C., Weisenberg, C.R., *J. Amer. Chem. Soc.*, 1968, 70, 6570.
- (20) Munson, M.S.B., Field, F.H., *J. Amer. Chem. Soc.*, 1966, 88, 2621.
- (21) Harrison, A.G., "*Chemical Ionization Mass Spectrometry*", 1983, CRC Press Inc.
- (22) Budzikiewicz, H., *Mass Spectrom Rev.*, 1986, 5, 345.
- (23) Schiff, H.I., Bohme, D.K., *Int. J. Mass Spec. Ion Phys.*, 1975, 16, 167.
- (24) Dawson, J.H.J., Kaandorp, A.M., Nibbering, N.M.M. *Org. Mass Spectrom.* 1977, 12, 330.
- (25) Faigl, J.F.G., Isolani, P.C., Riveros, J.M., *J. Amer. Chem. Soc.*, 1976, 98, 2049.
- (26) Westmane, J.B., Aludin, M.M., *Mass Spec. Rev.*, 1986, 5, 381.
- (27) Raftery, M.J., Bowie, J.H., *Int. J. Mass Spec. Ion Phys.*, in press.
- (28) Hunt, D.F., Giordani, A.B., Shabanowitz, J., Rhodes, C., *J. Org. Chem.*, 1982, 47, 738.

- (29) Caldwell, G., Bartmess, J.E., *Org. Mass Spectrom.*, 1982, 17, 456.
- (30) Field, F.H., Smit, A.L.C., *J. Amer. Chem. Soc.*, 1977, 99, 6471.
- (31) Hunt, D.F., Stafford, G.C., Crow, F.W., Russell, J.W., *Anal. Chem.*, 1976, 48, 2098.
- (32) Thomson, B., Davidson, W.B., Lovett, A.M., *Envir. Hlth. Persp.*, 1980, 36, 77.
- (33) Bruins, A.P., Harrison, A.J., Jennings, K.R., Mitchum, R.K., *Adv. Mass Spectrom.*, 1978, 1, 355.
- (34) Chantry, P.J., *J. Phys. Chem.*, 1969, 51, 3369.
- (35) Franklin J.R., Harland P.W., *Annu. Rev. Phys. Chem.*, 1974, 25, 2595.
- (36) Tedder, J.M., Vidaud, P.H., *J. Phys. D.*, 1980, 47, 1730.
- (37) Hunt, D.F., McEwen, C.N., Harvey, T.M., *Anal. Chem.*, 1975, 47, 1730.
- (38) Dzidic, I., Carroll, D.I., Stillwell, R.N., Horning, E.C., *Anal. Chem.*, 1975, 47, 1308.
- (39) Dougherty, R.C., *Biomed. Mass Spectrom.*, 1980, 7, 401.
- (40) Tannenbaum, H.P., Roberts, J.D., Dougherty, R.C., *Anal. Chem.*, 1975, 47, 49.
- (41) Ganguly, A.L., Cappuccino, N.F., Fujiwara, H.J., Bose, A.K., *J. Chem. Soc. Chem. Comm.*, 1978, 148.
- (42) Dougherty, R., Dalton, J., Biros, F.J., *Org. Mass. Spectrom.*, 1972, 6, 1171.

- (43) Parker, C.E., Yanaguchi, K., Harvan, D.J., Smith, R.W., Hass, J.R., *J. Chromatogr.*, 1985, 319, 273.
- (44) Bose, A.K., Fujiwara, H., Pramanik, B.N., *Tetrahedron Lett.*, 1979, 4017.
- (45) Hunt, D.F., Shabanowitz, J., Giordani, A.B., *Anal. Chem.*, 1980, 52, 386.
- (46) Hunt, D.F., McEwen, C.N., Harvey, T.M., *Anal. Chem.*, 1978, 47, 1730.
- (47) Levonowich, P.E., Tannenbaum, H.P., Dougherty R.C., *J. Chem. Soc. Chem. Comm.*, 1975, 597.
- (48) Bowie, J.H., *Mass Spec. Rev.*, 1984, 3, 1.
- (49) Roy, T.A., Field, F.H., Lin, Y.Y., Smith, L.C., *Anal. Chem.*, 1978, 51, 272.
- (50) Dzidic, I., Carrol, D.I., Stilwell, R.N., Horning, E.C., *Anal. Chem.*, 1975, 47, 1308.
- (51) Hunt, D.F., Stafford, G.C., Crow, F.W., Russel, A.W., *Anal. Chem.*, 1976, 48, 2098.
- (52) Hunt, D.F., Crow, F.W., *Anal. Chem.*, 1978, 50, 1761.
- (53) Schlunegger, U.P. "Advanced Mass Spectrometry", (Ed. Crompton, T.R.), Pergamamon Press: New York.
- (54) McLafferty, F.W., *Phil. Trans. R. Soc. Lond.*, 1979, 293, 93.

- (55) McLafferty, F.W., Kornfield, K., Hadden, W.F., Levsen, K., Sakai, I., Brente, P.F., Tsai, S., Schuddenamage, D.R., *J. Amer. Chem. Soc.*, 1973, 95, 3886.
- (56) McLafferty, F.W., Todd, P.J., McGilvory, D.C., Baldwin, M.A., *J. Amer. Chem. Soc.*, 1980, 102, 3360.
- (57) Jennings, K.R., *Int. J. Mass Spectrom. Ion Phys.*, 1968, 1, 227.
- (58) Rosenstock, H.M., Krauss, M., *Adv. Mass Spectrom.*, 1963, 2, 251.
- (59) Bradley, C.V., Howe, I., Beynon, J.H., *J. Chem. Soc. Chem. Comm.*, 1980, 562.
- (60) Cooks, R.G., Beynon, J.H. Caprioli, R.M. Lester, G., "Metastable Ions", Elsevier: Amsterdam 1973.
- (61) Szulesko, J.E., Bowie, J.H., Howe, I., Beynon, J.H., *Int. J. Mass Spec. Ion Phys.*, 1980, 34, 99.
- (62) Bowie, J.H., Ho, A.C., *Aust. J. Chem.*, 1977, 30, 675.
- (63) Bowie, J.H., Blumenthal, T., *J. Amer. Chem. Soc.*, 1975, 93, 2959.
- (64) Holmes, J.L. Terlouw, J.K., *Org. Mass Spectrom.*, 1980, 15, 383.
- (65) Cooks, R.G., Beynon, J.H., *J. Chem. Educ.*, 1974, 51, 437.
- (66) Bowie, J.H., Hart, S.G., Blumenthal, T., *Int. J. Mass Spec. Ion Phys.*, 1976, 22, 7.
- (67) Cooks, R.G., Beynon, J.H., "Int. Sci. Phys. Rev. Ser. Two", 1975, 5, 159, (ed: Maccoll A.) Butterworth: London.
- (68) Brenton, A.G., Beynon, J.H., *Eur. Spectrosc. News.*, 1980, 29, 39.

- (69) Weston, A.F., Jennings, K.R., Evans, S., Elliott, R.M., *Int. J. Mass Spec. Ion Phys.*, 1976, 20, 317.
- (70) Boyd, R.K., Beynon, J.H., *Org. Mass Spectrom.*, 1973, 12, 163.
- (71) Westheimer, F.H., *Chem. Rev.*, 1963, 61, 265.
- (72) Melander, L.C.S., "*Reaction Rates of Isotopic Molecules*", Ronald Press Co.: New York, 1979.
- (73) Shiner, V.J., "*Isotopes and Chemical Principles*", (Ed: Rock, P.A.), American Chemical Society: Washington, 1975.
- (74) Born, M., Oppenheimer, J.R., *Annal. der Physik.*, 1927, 84, 457.
- (75) Davidson, N. in "*Statistical Mechanics*", McGraw-Hill: New York 1962.
- (76) Derrick, P.J., *Mass Spec. Rev.*, 1983, 2, 285.
- (77) Allison, C.E., Stringer, M.B., Bowie, J.H., Derrick, P.J., *J. Amer. Chem. Soc.*, in press.
- (78) Westheimer, F.H., *Chem. Rev.*, 1961, 3, 131.
- (79) "*Gas Phase Ion Chemistry*", Vol. 1 and 2, Bowers, M.T., Ed., Academic: New York 1979.
- (80) Bowie, J.H., *Advances in Mass Spectrometry*, 1986, 553; Kebarle, P., Chowdhury, S., *Chem. Rev.*, 1987, 87, 513.
- (81) Oehme, M., "*Negative Ion Chemical Ionization Mass Spectrometry*", In: "*Mass Spectrometry of Large Molecules*", Facchetti, S., Ed., Elsevier : Amsterdam 1983.

- (82) Jennings, K.R. in "*Mass Spectrometry*", Chem. Soc. Spec. Report, ed. Johnstone, R.A.W., 1979, 5, 203.
- (83) Moylan, C.R., Janinski, J.M., Brauman, J.I., *Chem. Phys. Lett.*, 1983, 1, 98.
- (84) Foster, R.F., Tumas, W., Brauman, J.I., *J. Chem. Phys.*, 1983, 79, 4644.
- (85) Tumas, W., Foster, R.F., Pellerite, M.J., Brauman, J.I., *J. Amer. Chem. Soc.*, 1984, 105, 7465.
- (86) Tumas, W., Foster, R.F., Brauman, J.I., *J. Amer. Chem. Soc.*, 1984, 109, 4053.
- (87) Hayes, R.N., Sheldon, J.C., Bowie, J.H., Lewis, D.E., *Aust. J. Chem.*, 1985, 38, 1197.
- (88) Raftery, M.J., Bowie, J.H., *Int. J. Mass Spec. Ion Phys.*, 1987, 79, 267.
- (89) Hunt, D.F., Shabanowitz, J., Giordani, A.G., *Anal. Chem.*, 1980, 52, 386.
- (90) Sheldon, J.C., Currie, G.J., Lahnstein, J., Hayes, R.N., Bowie, J.H., *Nouv. J. Chim.*, 1985, 9, 205.
- (91) Stringer, M.B., Bowie, J.H., Holmes, J.L., *J. Amer. Chem. Soc.*, 1986, 108, 3888.
- (92) Stringer, M.B., Underwood, D.J., Bowie, J.H., Holmes, J.L., Mommers, A.A., Szulejko, S.E., *Can. J. Chem.* 1986, 64, 764.
- (93) Hayes, R.N., Sheldon, J.C., Bowie, J.H., Lewis, D.E., *J. Chem. Soc. Chem. Soc. Chem. Comm.*, 1984, 143.

- (94) Belasko, J.G., Albery, W.J., Knowles, J.R., *J. Amer. Chem. Soc.*, 1983, 105, 2475.
- (95) Sheldon, J.C., personal communication, Ab initio calculations on the deprotonation of ketene shows the product ion to be $\text{HC}=\text{CO}^-$, with bond lengths $\text{HC} = 1.05 \text{ \AA}$, $\text{C}=\text{C} = 1.22 \text{ \AA}$ and $\text{CO} = 1.25 \text{ \AA}$ (6-31G)
- (96) Froelicher, S.W., Lee, R.E., Squires, R.R., Freiser, B.S., *Org. Mass Spectrom.*, 1985, 20, 4.
- (97) Bowie, J.H., Stringer, M.B., Currie, G.J., *J. Chem. Soc. Perkin Trans. II*, 1986, 1821.
- (98) Eichinger, P.C.H., Bowie, J.H., *Org. Mass Spectrom.*, in press.
- (99) Bentley, T.W., *Mass Spectrometry Specialist Reports*, Chemical Society (London), 1979, 5, 81.
- (100) McLafferty, F.W., Bockhoff, F.M., *J. Amer. Chem. Soc.*, 1979, 101, 1783.
- (101) Beynon, J.H., Caprioli, R.M., Perry, W.O., Baitinger, W.E., *J. Amer. Chem. Soc.*, 1972, 94, 6828.
- (102) Rosenstock, H.M., Dannacher, J., Liebman, J.F., *Radiat. Phys. Chem.*, 1982, 20, 7.
- (103) Dickinson, R.J., Williams, D.H., *J. Chem. Soc. Perkin Trans. II*, 1972, 1362.
- (104) Kluff, E., Nibbering, N.M.M., *Int. J. Mass Spec. Ion Proc.*, in press.
- (105) Depuy, C.H., Bierbaum, V.M., *Accts. Chem. Res.*, 1981, 14, 146.
- (106) Wight, C.A., Beachamp, J.L., *J. Amer. Chem. Soc.*, 1981, 103, 6499.

- (107) White, R.L., Wilkins, C.L., Heitkamp, J.J., Staley, S.H., *J. Amer. Chem. Soc.*, 1983, 105, 4868.
- (108) Bowie, J.H., Nussey, B., *J. Chem. Soc. Chem. Comm.*, 1970, 17.
- (109) Bowie, J.H., Nussey, B., *Org. Mass Spectrom.*, 1970, 3, 933.
- (110) Eichinger, P.C.H., Bowie, J.H., Blumenthal, T., *J. Org. Chem.*, 1987, 51, 5078.
- (111) Bowie, J.H., *Aust J. Chem.*, 1971, 24, 989.
- (112) Bowie, J.H., Janprosri, S., *Org. Mass Spectrom.*, 1976, 11, 1290.
- (113) Bowie, J.H., Stringer, M.B., *Org. Mass Spectrom.*, 1985, 20, 138.
- (114) Klass, G., Trenerry, V.C., Sheldon, J.C., Bowie, J.H., *Aust. J. Chem.*, 1981, 34, 519.
- (115) Bowie, J.H., Hayes, R.N., Raftery, M.J., Stringer, M.B., Currie, G.J., *Spectrosc. Int. J.*, 1987, 6, 277.
- (116) Buchanan, M.V., Wise, M.B., *Fuel*, 1987, 66, 954.
- (117) Hilpert, L.R., *Biomed. Envir. Mass Spec.*, 1987, 14, 383.
- (118) Wickramanayake, P.P., Siu, K.W.M., Berman, S.S., *Org. Mass Spectrom.*, 1986, 21, 279.
- (119) Buchanan, M.V., Olerich, G., *Org. Mass Spectrom.*, 1984, 19, 486.
- (120) Dehme, M., *Anal Chem.*, 1983, 55, 2290.
- (121) Iada, Y., Daishima, S., *Chem. Lett.*, 1983, 3, 273.

- (122) Lewis, E., Peach, M.E., *Org. Mass Spectrom.*, 1987, 17, 597.
- (123) Stringer, M.B., Bowie, J.H., Eichinger, P.C.H., Currie, G.J., *J. Chem. Soc. Perk. Trans. II*, 1987, 385.
- (124) Negishi, E., Idacavage, M.J., "*Organic reactions*" Vol. 33, John Wiley & Sons, Inc., New York, 1985.
- (125) Smith, K., "*Organometallic Compounds of Boron*", Chapman Hall Ltd., London 1985.
- (126) "*Organometallic Chemistry*", Specialist Per. Report, Royal Soc. Chem, London.
- (127) Pelter, A., Smith, K., "*Comprehensive Organic Chemistry*", 1979, Vol 3, 687, Ed. Benton, D.H.R. and Ollis, W.D., Pergammon Press: Oxford.
- (128) Milvitskaya, E.M., Pojarenko, M., *Russ. Chem. Rev.*, 1976, 45, 469.
- (129) Pasto, D.J., Hickman, J., *J. Amer. Chem. Soc.*, 1967, 89, 5608.
- (130) Pasto, D.J., Hickman, J., *J. Amer. Chem. Soc.*, 1968, 90, 4445.
- (131) Pasto, D.J., Chow, J., Arora, S.K., *Tetrahedron*, 1969, 25, 1559.
- (132) Henneberg, D., Damen, H., Koster, R., *Lieb. Ann. Chem.*, 1961, 52, 640.
- (133) Glockling, F., Strafford, R.G., *J. Chem. Soc. (A)*, 1971, 1761.
- (134) Pasto, D.J., Timony, P.E., *Org. Mass Spectrom.*, 1975, 10, 222.
- (135) Pasto, D.J., *J. Amer. Chem. Soc.*, 1975, 97, 136.

- (136) Herstad, O., Pressley, G.A. Jr., Stafford, F.E., *J. Phys. Chem.*, 1970, 74, 874.
- (137) Rosen, R., Enrione, R.E., *Inorg. Chim. Acta*, 1967, 1, 169.
- (138) Murphy, M.K., Beachamp, J.L., *J. Amer. Chem. Soc.*, 1976, 98, 1433.
- (139) Murphy, M.K., Beachamp, J.L., *Inorganic Chemistry*, 1977, 16, 2437.
- (140) Sullivan, S.A., Sandford, H., Beachamp, J.L., Ashe, A.J., *J. Amer. Chem. Soc.*, 1978, 100, 3737.
- (141) Hayes, R.N., Sheldon, J.C., Bowie, J.H., *Organometallics*, 1986, 5, 163.
- (142) van der Wel, H., Nibbering, N.M.M., Sheldon, J.C., Hayes, R.N., Bowie, J.H., *J. Amer. Chem. Soc.*, 1987, 109, 5823.
- (143) O'Hair, R.A., Sheldon, J.C., Bowie, J.H., *J. Chem. Soc. Dalton Trans.*, 1988, in press.
- (144) Depuy, C.H., Damrauer, R., Bowie, J.H., Sheldon, *Acc. Chem. Res.*, 1987, 20, 227.
- (145) Frisch, M., Binkley, J.S., Schlegel, H.B., Raghavachari, K., Martin, R., Stewart, J.J.P., Bobrowicz, F., DeFress, D., Seeger, R., Whiteside, R., Fox, D., Fluder, E., Pople, J.A., "Gaussian 86. Release C", Carnegie Mellon University.
- (146) Schlegel, H.B., *J. Chem. Phys.*, 1986, 84, 4530; Sosa, C., Schelegel, H.B., *Int. J. Quantum Chem.*, 1986, 29, 1001.
- (147) Sheldon, J.C., Hayes, R.N., Bowie, J.H., unpublished results.

- (148) Aurelle, H., Treilhou, M., Prome, D., Savagnac, A., Prome, J.C., *Rapid Comm. Mass Spec.*, 1987, 1, 65.
- (149) Tomer, K.B., Gross, M.L., *Biomed. Envir. Mass Spect.*, 1988, 15, 89.
- (150) Jensend, N.J., Tomer, K.B., Gross, M.L., Lyon, P.A., *ACS Symp. Ser 291 (Desorption Mass Spect.)*, 1985, 194.
- (151) Terlouw, J.K., Burgers, P.C., Hommes, H., *Org. Mass Spectrom.*, 1979, 14, 387.
- (152) Todd, P.J., McLafferty, F.W., *Int. J. Mass Spec. Ion Phys.*, 1981, 38, 371.
- (153) Perrin, D.D., Armarego, W.L.F., Perrin, D.R., "*Purification of Laboratory Chemicals*", 1980, Pergamon Press, Oxford.
- (154) Nystrom, R.F., Brown, W.G., *J. Amer. Chem. Soc.*, 1947, 69, 1197.
- (155) Trzupsek, L.S., Stredonsky, E.R., Whitesides, G.M., *J. Org. Chem.*, 1972, 37, 3300.
- (156) Vogel, A.I., "*Practical Organic Chemistry*", 3rd Edn, p. 287 (Longmans: London 1956).
- (157) Best, A.P., Wilson, C.L., *J. Chem. Soc.*, 1946, 239.
- (158) Zanetti, J.E., Sickman, D.V., *J. Amer. Chem. Soc.*, 1936, 58, 2034.
- (159) Baldwin, J.E., Pudussey, R.G., *Chem. Commun.*, 1968, 7, 408.
- (160) Brown, W.G., Eberly, K., *J. Amer. Chem. Soc.*, 1940, 62, 113.
- (161) Corval, M., Piolet, C., *Bull. Soc. Chim. France*, 1954, 21, 234.

- (162) Hackman, R.H., *J. Chem. Soc.*, 1951, 2505.
- (163) Man, E.G., Swamer, F.W., Hauser, C.R., *J. Amer. Chem. Soc.*, 1951, 73, 901.
- (164) Vogel, A.I., "*Practical Organic Chemistry*", 3rd Edn, p. 276 (Longmans: London 1956).
- (165) Ansell, M.F., Davis, M.A., Hancock, J.W., Hickinbottom, W.J., Holton, P.G., Hyatt, A.A., *J. Chem. Soc.*, 1955, 2705.
- (166) Stiles, M., Mayer, R.P., *J. Amer. Chem. Soc.*, 1959, 81, 1497.
- (167) Wiley, R.H., Irick, G.J., *J. Org. Chem.*, 1959, 24, 1925.
- (168) Corey, E.J., Enders, D., *Tetrahedron Lett.*, 1976, 3.
- (169) Dubois, J.E., Lion, C., *C.R. Hebd. Seances Acad. Sci. Ser. C.*, 1975, 280, 217.
- (170) Rappe, C., Knutsson, L., *Acta Chem. Scand.*, 1967, 21(8), 2205.
- (171) Weis, M.J., Schaub, R.E., Allen, G.R., Poletto, J.F., Pidacks, C., Conrow, R.B., Coscia, C.J., *Tetrahedron*, 1964, 20, 357.
- (172) Levene, P.A., Marker, R.A., *J. Biol. Chem.*, 1935, 108, 409.
- (173) Marvel, C.S., Hansen, N.A., *Organic Synthesis*, Col. Vol. 1, 84.
- (174) Gazopoulus, I., *Chem. Abstracts*, 1934, 28, 1672.
- (175) Hartmann, W.W., Phillips, R., *Organic Synthesis*, 1934, 14, 34.
- (176) Vogel, A.I., "*Practical Organic Chemistry*", 4th Edn, p. 841 (Longmans: London 1978).

- (177) Morton, A.A., Stevens, J.R., *J. Amer. Chem. Soc.*, 1931, 53, 4030.
- (178) Norris, J.F., *Organic Synthesis*, Col. Vol. 1, 532.
- (179) Brehm, W.J., Levenson, T., *J. Amer. Chem. Soc.*, 1954, 76, 5389.
- (180) Petrov, A.A., *Chem. Abst.*, 1941, 35, 3603.
- (181) Sumiki, Y., Yamamoto, K., Takeda, K., *Chem. Abst.*, 1953, 47, 3505.
- (182) Knorr, L., Matthes, H., *Ber.*, 1901, 34, 3482.
- (183) Noth, H., Vahrenkamp, H., *J. Organomet. Chem.*, 1968, 21, 389.
- (184) Brown, H.C., *J. Amer. Chem. Soc.*, 1945, 67, 374.
- (185) Wilberg, E., Kruerke, U., *Z. Naturforsch., B: Anorg. Chem., Org. Chem., Biochem., Biophys., Biol.*, 1953, 8B, 608.
- (186) Sorm, F., Smrt, J., *Chem. Abs.*, 1955, 49, 175.
- (187) Smith, L.I., Sprang, J.A., *J. Amer. Chem. Soc.*, 1943, 65, 1276.
- (188) Krueerke, U., Wittouck, E., *Chem. Ber.*, 1962, 95, 174.
- (189) Palomaa, M.H., Jansson, R., *Ber.*, 1931, 64B, 1606.
- (190) Vogel, A.I., "*Practical Organic Chemistry*", 3rd Edn, p.389 (Longmans: London 1956).
- (191) Vogel, A.I., "*Practical Organic Chemistry*", 3rd Edn, p. 383 (Longmans: London 1956).
- (192) "*Dictionary of Organic Compounds*", 4th Edn, Vol. 1-5, Eds Pollock, J.R.A. and Stevens, R., Eyre & Spottiswoode : London.

(193) Brauman, J.I., Blair, L.K., *J. Amer. Chem. Soc.*, 1968, 90, 6561.

Publications

Bowie, J.H., Stringer, M.B., Currie, G.J., *J. Chem. Soc. Perkin Trans. II*, 1986, 1821.

Currie, G.J., Stringer, M.B., Bowie, J.H., *Aust. J. Chem.*, 1987, 40, 1365.

Currie, G.J., Bowie, J.H., Massy-Westropp, R.A., Adams, G.W., *J. Chem. Soc. Perkin Trans. II*, 1988, 403.

Bowie, J. H., Stringer, M. B. & Currie, G. J. (1986). Carbanion rearrangements. Collision-induced dissociations of enolate ions derived from 3-ethylpentan-2-one. *Journal of the Chemical Society, Perkin Transactions 2*, 11, 1821-1825.

NOTE:

This publication is included in the print copy of the thesis held in the University of Adelaide Library.

It is also available online to authorised users at:

<http://dx.doi.org/10.1039/P29860001821>